Synthesis, Characterisation and Applications of Novel Ionic Liquids

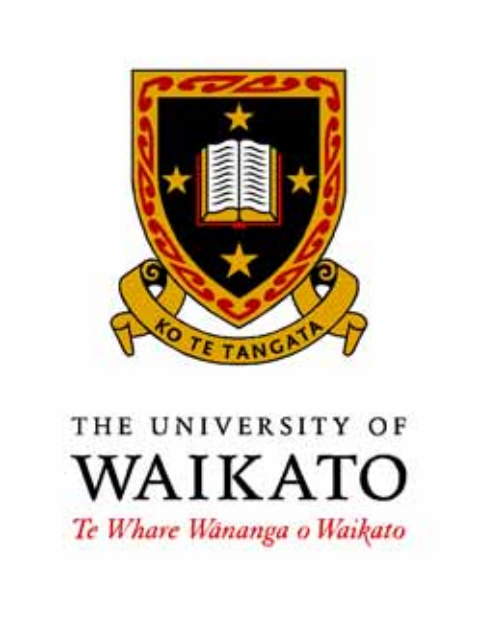

A thesis
submitted in partial fulfilment
of the requirements for the degree of

Master of Philosophy in Chemistry

at the
University of Waikato
by

Lucia (Li) Ying

University of Waikato
March 2006

Abstract

A series of novel phosphinate-based ionic liquids have been synthesised using various organic phosphorus acids, such as mono-*n*-octylphosphinic acid (octylPO_2H_2), mono-*n*-hexylphosphinic acid (hexylPO_2H_2), di-*n*-octylphosphinic acid ((octyl)$_2PO_2H$), di-*n*-hexylphosphinic acid ((hexyl)$_2PO_2H$) and bis(2,4,4-trimethylpentyl)phosphinic acid ((TMP)$_2PO_2H$), by reaction with tetrabutylphosphonium hydroxide (Bu_4POH), tetrabutylammonium hydroxide (Bu_4NOH), pyridine (py) and triethylamine (Et_3N). Reactions simply involve neutralizing the organophosphorus acids with bases. The only byproduct, water, and excess amine, py/Et_3N can be easily removed under vacuum (Chapter 2).

Some of the physical and chemical properties of these ionic liquids have been characterized by NMR, ES-MS, TGA, UV-Visible spectroscopy etc. The formed tetraalkylphosphonium/tetraalkylammonium phosphinate ionic liquids are viscous, hygroscopic liquids, but are more thermally stable than trialkylammonium and pyridinium analogues. For example, for the most stable ionic liquid, [Bu_4P][(octyl)$_2PO_2$], its onset temperature of decomposition in thermal gravimetric analysis (TGA) is 358 °C (Chapter 2).

One of the applications of these novel phosphinate-based ionic liquids has been investigated. Au(0), Rh(0) and Ir(0) nanoparticles have been prepared in some of these phosphinate-based ionic liquids as a media and (or) reducing agents and have been characterized by SEM, TEM, Zetasizer, UV-Visible spectroscopy and IR spectroscopy. In general, the average particles size of Au(0), and Ir(0) were *ca*. 25 nm, but some of the particles average size formed was less than 2 nm, such as Rh(0) and Ir(0) nanoparticles formed in [Bu_4P][(octyl)$_2PO_2$] or [Bu_4P][(TMP)$_2PO_2$]. Generally, these phosphinate-based ionic liquids are good media to prevent nanoparticle aggregation (Chapter 3).

Acknowledgements

I would like to acknowledge a number of people who have provided valuable assistance to me during my study.

Firstly, special thanks go to my supervisors for their help and support. Thank you to Professor Bill Henderson for his enthusiasm, wisdom, research guidance, regular instruction and tireless and elaborate revision of my thesis. The patience, kindness and expertise of Professor Brian Nicholson are greatly appreciated. Thanks also to Dr. Michael Mucalo for his patience and guidance in teaching me physical chemistry, particularly IR spectroscopy and Zetasizer.

Many thanks to all the technicians, especially Pat Gread for ES-MS, Jannine Sims for UV-Visible, and Annie Barker for DSC, and Ralph Thomson for NMR. The kindness and understanding of the Chemistry secretary, Jacqueline Mackenzie, is also greatly appreciated. Additional thanks go to Narendra Jai Prasad for help in checking my thesis, Nick Lloyd for his daily help in the laboratory, Carol Goss, Mahima Senanayake, Jessica Zhu, Kelly Kilpin and others for their friendship and support.

I wish to acknowledge the Science Librarian, Cheryl Ward, for her kindness and patience in teaching me how to use the library resources effectively.

Special mention should be made of Kevin McGhee for his willingness in proofreading the many drafts of my thesis.

Last but not least, I would like to thank my family – my husband, Shunping Liu, for his financial support, my parents and son, Jack Liu, for their encouragement and understanding.

To all of you, your support has enabled me to complete this course – many thanks!

Table of Contents

Chapter Two. Synthesis and characterisation of phosphinate-based ionic liquids 34

Chapter Three. Application of ionic liquids: Synthesis of transition metal nanoparticles in phosphinate-based ionic liquids 76

List of Tables

List of Figures

List of Schemes

List of Equations

Abbreviations

ACAC	-	acetylacetonate
BINAP	-	2,2'-bis(diphenylphosphanyl)-1,1'-binaphthyl
[BMIM]	-	1-butyl-3-methylimidazolium
BPC	-	N-*n*-butylpyridinium chloride
Bu	-	butyl
$camSO_3H$	-	D-camphor-10-sulfonic acid
[Cn-MIM]	-	1-*n*-alkyl-3-methylimidazolium
diop	-	4,5-bis[(diphenylphosphanyl)-methyl]-2,2-dimethyl-1,3-dioxolan-4,5-diol
DMF	-	N,N-dimethylformamide
[EMIM]	-	1-ethyl-3-methylimidazolium
Et	-	ethyl
Hex	-	hexyl
Me	-	methyl
MEIC	-	1-methyl-3-ethylimidazolium chloride
[MMIM]	-	1,3-dimethylimidazolium
NBD	-	norbornadiene
NMDPP	-	neomenthyldiphenylphosphine
Oct	-	octyl
[OMIM]	-	1-*n*-octyl-3-methylimidazolium
Ph	-	phenyl
[PMIM]	-	1-propyl-3-methylimidazolium
Pr	-	propyl (ie *n*-propyl)
^{i}Pr	-	isopropyl
py	-	pyridine
[RMIM]	-	dialkylimidazolium
THF	-	tetrahydrofuran
TsOH	-	*p*-toluenesulfonic acid
TPPTS	-	triphenylphosphinetrisulfonate, sodium salt
$(TMP)_2PO_2H$	-	bis(2,4,4-trimethylpentyl)phosphinic acid
Tf_2N	-	bis((trifluoromethyl)sulfonyl)imide

cat.	-	catalyst
cP	-	centipoise
DSC	-	differential scanning calorimeter
ee	-	enantiomeric excess
$E_{NR} = E_T(30)$	-	transition energies
ES-MS	-	electrospray mass spectrometry
IL	-	ionic liquid
IR spectroscopy	-	infrared
J	-	coupling constant in Hz (NMR)
M.P.	-	melting point
NMR	-	nuclear magnetic resonance
PCS	-	photon correlation spectroscopy
SEM	-	scanning electron microscopy
S	-	solid
sol.	-	solubility
TEM	-	transmission electron microscopy
TGA	-	thermal gravimetric analysis
TOF	-	turnover frequency (h^{-1})
T_{onset}	-	onset temperature of decomposition
TTO	-	total turnover
UV	-	ultraviolet
XAFS	-	X-ray absorption fine structure
ΔE	-	potential window
ν	-	stretching frequencies (cm^{-1}) (IR)
λ_{max}	-	visible absorption maximum
δ	-	chemical shift (ppm)

Chapter One

Ionic liquids ─ Phosphorus containing ionic liquids

1.1 Introduction of historical development

Ionic liquids are salts that melt below about 100 °C, often even lower than room temperature. There are many synonyms used for ionic liquids, such as room-temperature ionic liquids, non-aqueous ionic liquids, molten salts, and fused salts [1]. Molten salt was the term first used for ionic liquids when there was not much literature on low-melting salts. Nowadays the terms "ionic liquids" is more popularly used for those that are liquids at room temperature.

Ionic liquids have obtained increased attention in the past decade as an alternative good medium for organic synthesis [2] and in electrochemistry [3]. It is remarkable to think that since the first book [4] dedicated to room temperature ionic liquids in 2002, three other books have already appeared in a year. Figure 1.1 shows the growth in publications on ionic liquids up to 2005.

Ionic liquids have excellent solvent properties for most organic and inorganic compounds. They have high thermal stability, no measurable vapour pressure and are non-flammable. Optimization of compound characteristics is readily achieved from a broad choice of anion and cation combination, so ionic liquids are sometimes called tailor-made [5] solvents. Their physical and chemical properties can be tuned and tailored for different purposes.

Ionic liquids are not new, and their initial development goes back to 1914. Generally, the history of ionic liquids began with the first report of the synthesis

of ethylammonium nitrate ([$EtNH_3$][NO_3]) in 1914 [6] which has a melting point of 12 °C. In 1948, Hurley and Wier developed ionic liquids with chloroaluminate ions [7]. The system was rediscovered by Osteryoung and Wilkes [8] who prepared room-temperature liquid chloroaluminate melts, concentrating on electrochemical applications.

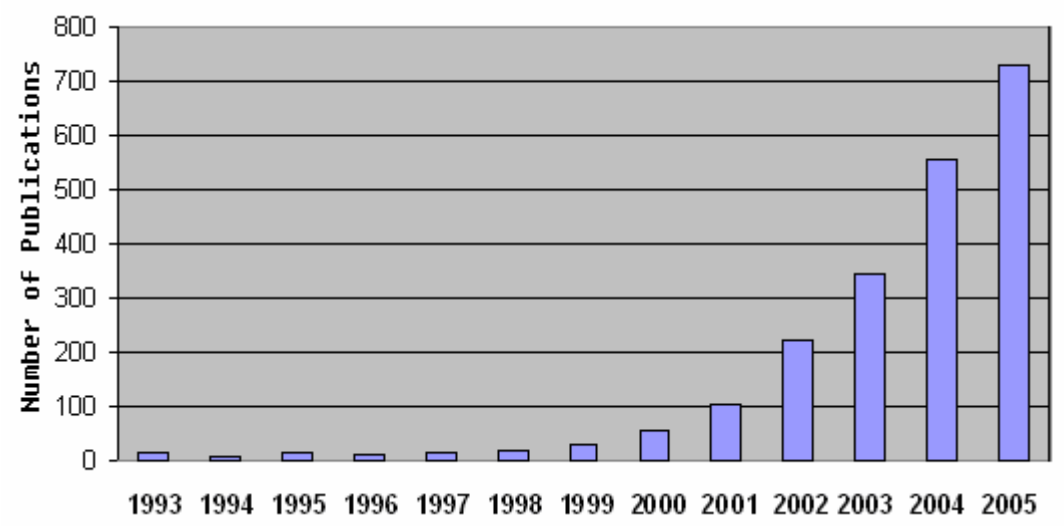

Figure 1.1: Publications containing the phrase "ionic liquid" in the title, abstract, or keywords, determined by ISI Web of Science, as a function of time (2005 data until Oct 22nd)

A liquid salt, tetra-*n*-hexylammonium benzoate, was used as a solvent for kinetic and electrochemical investigations by Swain *et al*. as early as 1967 [9]. Though the liquid salt was a hemihydrate at room temperature, the ionization strength of the ionic medium was quantitatively investigated, so this work had a pioneering significance.

In the early 1980s chloroaluminate melts, such as aluminum chloride-N-*n*-butylpyridinium chloride ($AlCl_3$-BPC) and aluminium chloride-1-methyl-3-ethylimidazolium chloride ($AlCl_3$-MEIC) were used as nonaqueous, polar solvents to investigate transition metal complexes by the Seddon and Hussey group. Their investigation first involved the electrochemical aspects of the transition metal complexes [10], followed by spectroscopic and coordination chemistry experiments [11].

Ionic liquids were reported as new reaction media and sometimes as catalysts for organic synthesis at the end of the 1980s. The imidazolium chloroaluminate room-temperature molten salts proved to be a good medium and a catalyst for Friedel-Crafts alkylations and acylations [12]. Phosphonium halide melts were successfully used in nucleophilic aromatic substitution reactions [13].

The first time when ionic liquids were reported as solvents for homogeneous transition metal catalysts were in 1990 by Chauvin *et al*. and Wilkes *et al*. Chauvin's group investigated the catalytic dimerization of propene by nickel complexes in chloroaluminate molten salts [14], while the Wilkes group studied ethylene polymerization *via* Ziegler-Natta catalysis also in a chloroaluminate molten salt [15].

After the Wilkes group's work based on preparation and characterization of the air- and water-stable low melting ionic liquid systems, such as 1-ethyl-3-methylimidazolium tetrafluoroborate ([EMIM][BF_4]) [16], the concept of ionic liquids had a substantial boost. This ionic liquid system has a greater range of applications, especially for transition metal catalysis, in contrast to chloroaluminate ionic liquids. An example is in the rhodium-catalyzed hydroformylation of alkenes [17]. Based on Wilkes' work, it became clearly apparent that ionic liquids were not only limited to chloroaluminate melts but it was a whole range of cation/anion combinations which could form low-melting salts [18].

Now, recent publications are mostly interested in the synthesis of new ionic liquids [19], such as thiazolium-ion based ionic liquids, 1-ethyl-3-methylimidazolium fluoride ionic liquid and N,N'-dialkylimidazolium tetrachloroaurate salts etc, with detailed and systematically investigated physical and chemical properties [20] using a wide variety of techniques, including NMR and IR spectroscopies, DSC (differential scanning calorimetry), X-ray and XAFS (X-ray absorption fine structure) etc. Further applications of new ionic liquids as solvents and catalysts were also investigated [21].

1.2 Synthesis and purification of ionic liquids

1.2.1 Introduction

The first ionic liquid, ethylammonium nitrate [6] was synthesised by the addition of concentrated nitric acid to ethylamine, and after removal of water, it give the pure salt which was liquid at room temperature. It is the simplest method for the formation of ionic liquids; to protonate suitable starting materials such as amines and phosphines. The method can only be used for a small range of salts; furthermore, the decomposition of these ionic liquids could happen through deprotonation, so it has severely limited the application of such ionic liquids. Thus synthesis of some ionic liquids generally requires more complex methods. The most widely used cations and anions are shown in Figure 1.2 [22].

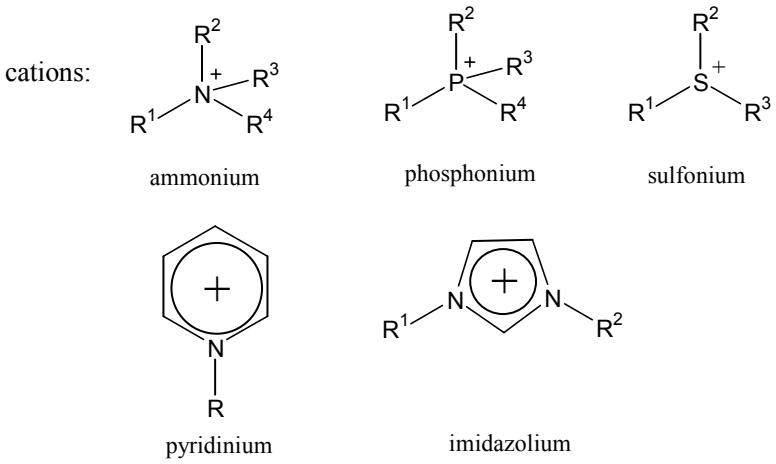

anions: BF_4^-, PF_6^-, SbF_6^-, NO_3^-, $CF_3SO_3^-$, $(CF_3SO_3)_2N^-$, $ArSO_3^-$, $CF_3CO_2^-$, $CH_3CO_2^-$, $Al_2Cl_7^-$

Figure 1.2: Important types of cations and anions used in ionic liquids [22]

Scheme 1.1 shows the synthesis paths of the preparation of ionic liquids [18]. In some cases only the first step is required, such as the synthesis of ethylammonium nitrate. However, in many cases, it is not possible to form the desired anion directly by the quaternization reaction, so a further step needs to be followed. It can be split into two parts: the formation of the desired cation, followed by the exchange, where it is necessary, to form the desired product.

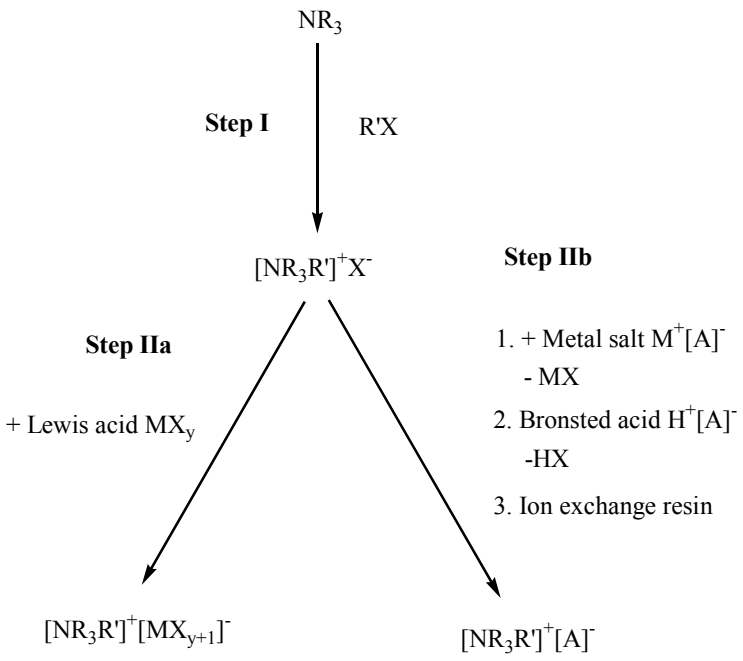

Scheme 1.1: Typical synthesis paths for the preparation of ammonium ionic liquids [18]

1.2.2 Quaternization reactions

Cations can be formed by reaction of an amine or phosphine with an acid (protonation) or with a haloalkane (alkylation). The protonation reaction is used to form salts, such as ethylammonium nitrate which is formed by adding nitric acid to a cooled aqueous solution of ethylamine [23]. A slight excess of amine remains and it can be removed, along with the water, by heating it to 60 °C in a vacuum. The preparation of all salts of this type can use the same process, but there could be a possibility of contamination by residual amine when a higher molecular weight amine is employed. Low melting point, liquid crystalline, long alkyl chain-

substituted 1-alkylimidazolium chloride, nitrate, and tetrafluoroborate salts have been synthesised using the similar method to the one above [24]. A slight excess of acids were used for these preparations.

The alkylation process has several advantages such as a great amount of cheap haloalkanes are available, the substitution reactions generally take place smoothly and the formed halide salts can easily be converted to salts with other anions. The quaternization reaction of amines and phosphines with haloalkanes has been known for many years, but it has just recently been used for the synthesis of ionic liquids. The reaction can be done with chloroalkanes, bromoalkanes and iodoalkanes. From Cl to Br to I, the reaction conditions required are more gentle, due to more facile nucleophilic substitution reactions. In general, the quaternization reaction is a very simple method for formation of stable cations. A general method for the preparation of 1-methylimidazolium salt is to mix the imidazole and haloalkane, and then heat under vacuum. The halide salts are generally solids at room temperature. Generally, the reaction mixture should be kept free of moisture, because the products are often extremely hygroscopic. The reaction can be carried out without using a solvent, as the reagents are generally liquids and mutually miscible, while the formed halide salt products are immiscible in the starting materials [25]. Even though no particular advantage appears, a solvent was often used, such as, alkyl halide itself [8c], 1,1,1-trichloroethane [19a], ethyl ethanoate [26] and toluene [27]. The solvent could be removed by decantation after reaction was complete. It is also necessary to remove all excess solvent and starting material under vacuum with heating. The most common starting material is 1-methylimidazole which forms the majority of cations using this route. The 1-alkylimidazoles are easily prepared as shown in Scheme 1.2 [25]. Additional, a wider range of C-substituted imidazoles, which are commercially available, also combine with these (NaOEt and RBr) to form a lot of possible starting materials.

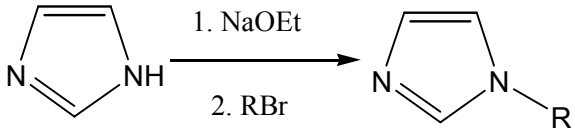

Scheme 1.2: Synthesis of alkylimidazoles [25]

Quaternization reactions have also been used between 1-alkylimidazoles and methyl triflate [19a], and triphenylphosphine and octyl tosylate [28] to directly prepare ionic liquids. These are alkylating agents containing a good leaving group. Scheme 1.3 shows the syntheses of the phosphonium tosylates by reaction of the tosylate esters (1) with the appropriate tertiary phosphine (2).

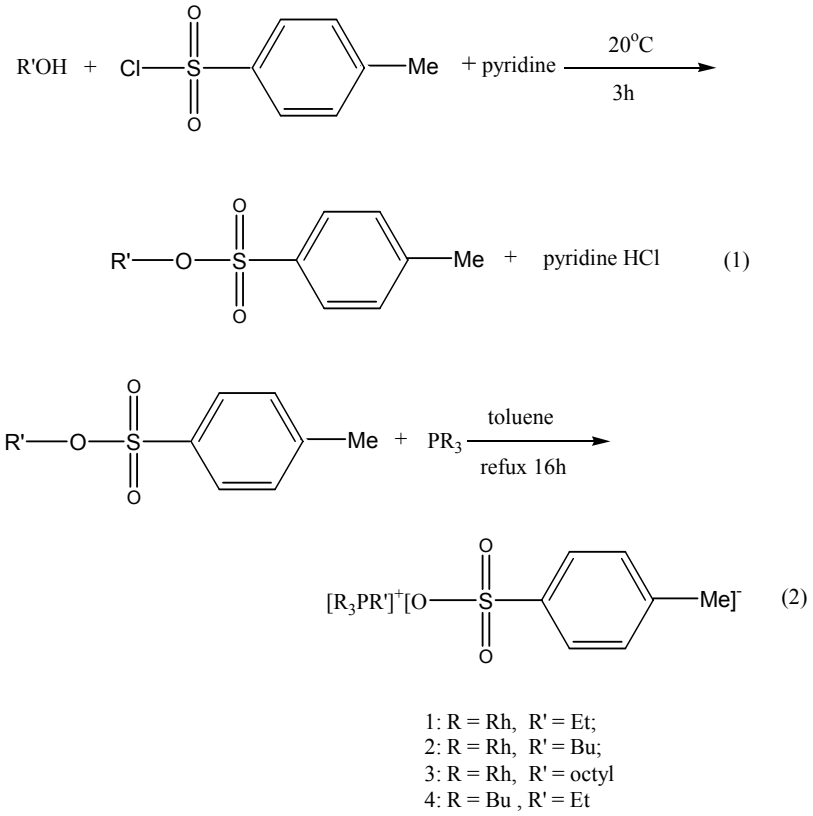

Scheme 1.3: The synthesis of phosphonium tosylate salts [28]

1.2.3 Anion-exchange reactions

The anion-exchange reactions of ionic liquids can be divided into two different types: treating halide salts with Lewis acids directly and the synthesis of ionic liquids by anion metathesis.

1.2.3.1 Lewis acid-based ionic liquids

The treatment of halide salts with Lewis acids (most notably $AlCl_3$) to form ionic liquids dominated the early years of this area of chemistry. In 1951 Hurley and Wier reported the formation of a salt that was liquid at room temperature, based on the combination of ethylpyridinium bromide with $AlCl_3$ in 1:2 molar proportions [7b]. Recently, the technology of room temperature chloroaluminate melts based on 1-alkylpyridinium [8a] [8b] and 1,3-dialkylimidazolium ($[RMIM]^+$, R = methyl; ethyl; propyl; butyl) [8c] have been developed by Osteryoung and Wilkes groups. An example of the reaction between 1-methyl-3-ethylimidazolium chloride ([EMIM]Cl) and $AlCl_3$ is shown in Equation 1.1. When the moles of [EMIM]Cl > $AlCl_3$, only equilibrium (a) was present, and a basic ionic liquid was formed. On the other hand, when the moles of $AlCl_3$ > [EMIM]Cl, the ionic liquid was acidic and equilibria (b) and (c) dominate [29].

$$[EMIM]^+Cl^- + AlCl_3 \rightleftharpoons [EMIM]^+[AlCl_4]^- \quad (a)$$

$$[EMIM]^+[AlCl_4]^- + AlCl_3 \rightleftharpoons [EMIM]^+[Al_2Cl_7]^- \quad (b)$$

$$[EMIM]^+[Al_2Cl_7]^- + AlCl_3 \rightleftharpoons [EMIM]^+[Al_3Cl_{10}]^- \quad (c)$$

Equation 1.1: A series of equilibria of the reaction between [EMIM] and $AlCl_3$ [29]

Chloroaluminates are well known but not the only ionic liquids that can be synthesised by the reaction of a halide with a Lewis acid. Others such as BCl_3 [30], CuCl [31] and $SnCl_2$ [32] have also been described, and further examples are

shown in Table 1.1. The most common method for synthesis of such liquids was simply mixing the Lewis acid and the halide salt; the ionic liquid formed on contact of the two materials, in a (generally) exothermic reaction [25].

Table 1.1: Examples of ionic liquids that can be generated by the reaction of a halide with a Lewis acid

Ionic liquid	Established anion	Reference
[cation]Cl/$AlEtCl_2$	$AlEtCl_3^-$, $Al_2Et_2Cl_5^-$	[33]
[cation]Cl/BCl_3	Cl^-, BCl_4^-	[30]
[cation]Cl/$ZnCl_2$	$ZnCl_3^-$, $Zn_2Cl_5^-$, $Zn_3Cl_7^-$	[34] [35]
[cation]Cl/$SnCl_2$	$SnCl_3^-$, $Sn_2Cl_5^-$	[35]
[cation]Cl/$FeCl_3$($FeCl_2$)	$FeCl_4^-$($FeCl_3^-$), $Fe_2Cl_7^-$($FeCl_4^{2-}$)	[36]

1.2.3.2 Anion metathesis

The main aim of all anion exchange reactions is the formation of desired ionic liquids uncontaminated with unwanted cations and anions. Over the past few years, many anion exchange reactions have been reported for the preparation of ionic liquids (Scheme 1.1 step IIb). A series of novel air- and water-stable low melting salts based on the 1-ethyl-3-methylimidazolium cation ($[EMIM]^+$) were first reported by Wilkes and Zaworotko [16]. This synthesis involved a metathesis reaction between [EMIM]I with a range of silver salts such as $AgNO_3$, $AgNO_2$, $AgBF_4$, $Ag[CO_2CH_3]$, and Ag_2SO_4. The ionic liquids formed were pure and were obtained in high yields because the low solubility of silver iodide in solvent allowed easier isolation of the products from the ionic liquid by filtration [16]. The methods of preparation generally employed are similar, and representative examples are reviewed in Table 1.2. The low-melting salts have been prepared by anion-exchange reactions for many years, for example tetrahexylammonium benzoate, a liquid salt at 25 °C, was synthesised from tetrahexylammonium iodide, silver oxide and benzoic acid, and was reported in 1966 [37].

Table 1.2: Examples of ionic liquids prepared by anion metathesis

Ionic liquid	Reference
[cation][PF_6]	[20a] [26] [38]
[cation][BF_4]	[38]
[cation][$(CF_3SO_2)_2N$]	[19a]
[cation][CF_3SO_3]	[19a]
[cation][$AuCl_4$]	[19e]

[cation]: dialkylimidazolim cation

1.2.4 Purification of ionic liquids

The lack of any significant vapour pressure prevents the purification of most ionic liquids by distillation; on the contrary, any volatile impurity can be separated from an ionic liquid by distillation or vacuum. Generally, it is better to purify starting materials before use as this will allow using synthetic methods that generate fewer side products or allow their easy separation from the product [25]. The most common impurities are halide anions in ionic liquids formed by anion metathesis. The presence of such impurities can be extremely detrimental [39] and affect the performance of the ionic liquids, especially in applications involving transition metal-based catalysts [40], which can have decreased activity in the presence of halide ions. It is a particular problem for water-soluble ionic liquids, as water-immiscible salts can be readily purified by simply washing with water [25].

In the absence of any chromophore in the cation or anion, most ionic liquids should be colourless, but the salts often have a yellow hue. The amount of impurity causing this colouration is usually extremely small, and undetectable by NMR or CHN microanalysis. Traces of acetone present sometimes can cause discoloration during the quaternization step, so the best way is that all glassware used in this step should be kept free of acetone. The impurity present in the largest amount in most ionic liquids is water. The removal of water is generally achieved

by heating to at least 70 °C for several hours with stirring, until an acceptable low degree of water contamination is achieved [25].

1.3 Physicochemical properties of ionic liquids

1.3.1 Melting point

It is generally accepted that ionic liquids have relatively low melting points, usually below ambient [41]. Melting point is therefore the key criterion used to evaluate an ionic liquid [18]. The characteristic properties of ionic liquids depend on the composition of the anion and cation. The main factors that influence the melting points of the salts are charge, size and distribution of charge on the respective ions [42].

1.3.1.1 Effect of the anion

In ionic liquids, increasing anion size generally gives rise to reductions in the melting points of salts, because the Coulombic attraction contributions to the lattice energy of the crystal are reduced. An example of the variation in melting point of the [EMIM]X salts with different X anions is shown Table 1.3.

Table 1.3: Effect of the anion X on melting points of [EMIM]X salts

Anion [X]	Melting point (°C)	Reference
Cl^-	87	[8c]
Br^-	81	[43]
I^-	79-81	[43]
$[NO_3]^-$	38	[16]
$[NO_2]^-$	55	[16]
$[CF_3SO_3]^-$	-9	[19a]
$[CF_3CO_2]^-$	-14	[19a]

Complex anions can produce ionic liquids with reduced melting points through the formation of eutectic compositions, such as halide salts combined with the Lewis acid ($AlCl_3$) [8c] [44]. The molar ratio of the two reactants will affect the melting point of the resultant mixed salt system through equilibria. Figure 1.3 shows the solid-liquid phase diagram for the [EMIM]Cl-$AlCl_3$ system.

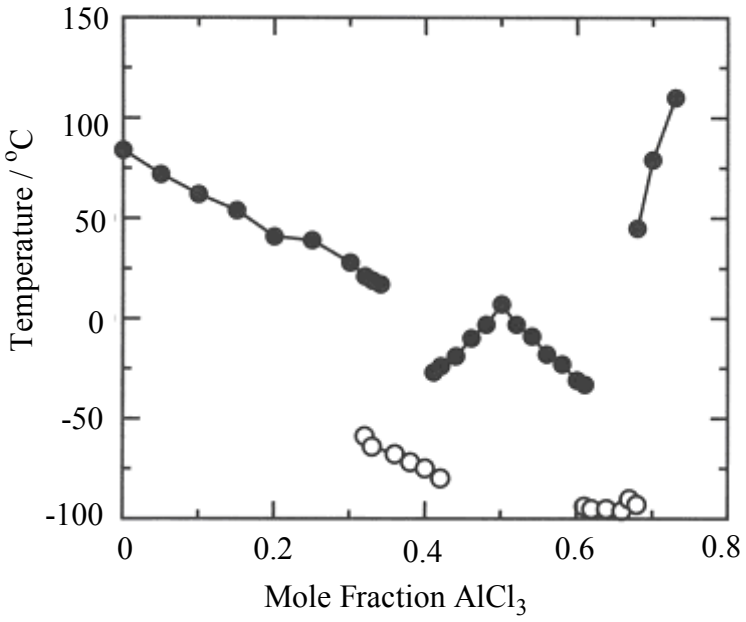

Figure 1.3: Phase diagram for [EMIM]Cl/$AlCl_3$: (○) melting and freezing points; (●) glass transition points [44]

The contribution of the anion and cation cannot be taken in isolation, because induced dipoles can cause increasing melting points through hydrogen bonding interactions, seen in the crystal structures of [EMIM]X (X= Cl, Br, I) salts [43].

1.3.1.2 Effect of cation

The melting points of ionic liquids are also influenced by the size and shape of the cation. Large ions generally tend to produce a decrease in melting points of the salts. With the increasing cation size, the melting points were lower; an example of tetraalkylammonium bromide salts is shown in Table 1.4 [42].

Table 1.4: Changes in melting points for tetraalkylammonium bromide salts with increasing size of alkyl substituents [42]

Cation	Melting Point (°C)
$[NMe_4]^+$	> 300
$[NEt_4]^+$	284
$[NBu_4]^+$	124-128
$[NHex_4]^+$	99-100
$[NOct_4]^+$	95-98

Symmetry of the ions can also influence the melting points of organic salts, increasing symmetry in the ions causing on increase in melting points through permitting more efficient ion-ion packing in the crystal. Oppositely, reduction in the symmetry of the cations brings a distortion from ideal close-packing of the ionic charges in the solid state lattice, a decrease in the lattice energy, and a decrease in the melting point. On moving from spherical or high-symmetry ions such as Na^+ or $[NMe_4]^+$ to lower-symmetry ions such as the imidazolium cation, the Coulombic charge distribution will tend to distort. Table 1.5 shows the effect of symmetry for a series of $[NR_4]X$ salts [45]. Room-temperature liquids are obtained for the salts $[N_{8543}]Br$, $[N_{7733}]Br$, $[N_{8651}]Br$ and $[N_{9641}][ClO_4]$ etc. whereas the salts containing cations with high symmetry such as $[N_{5555}][BPh_4]$ have much higher melting points.

Table 1.5: Effects of cation symmetry on the melting points (°C) of isomeric tetraalkylammonium salts ($[Nnmop]^+$ has four linear alkyl substituents, containing n = 5-17; m = 1-9; o = 1-6; and p = 1-5, n, m, o, and p a total of 20 carbons; L = liquid) [45]

Cation ($[Nnmop]^+$)	Br^-	$[ClO_4]^-$	$[BPh_4]^-$
5,5,5,5	101.3	117.7	203.0
6,5,5,4		83.4	
6,6,4,4		83.0	
8,4,4,4		67.3	
8,5,4,3	L		109.5
6,6,6,2		46.5	
7,7,3,3	L	45-58	138.8
8,6,3,3	L	L	110.2
7,7,5,1	L		104
8,6,5,1	L		91.0
9,5,5,1	L		85
9,6,4,1	L	L	65.0
11,3,3,3	67-68	65.5	
11,4,3,2	L		100
8,8,2,2		62	
9,8,2,1	L		93.0
13,3,3,1	71-72		
9,9,1,1	L	53-53	98.0
10,8,1,1	L	L	
14,2,2,2	170	152	
16,2,1,1	180	155	
17,1,1,1	210	205	

Substituent alkyl chain length influences the melting point of 1-alkyl-3-methylimidazolium tetrafluoroborate salts, as shown in Figure 1.4 [20c]. It is noticeable that increasing the substituent length initially decreases the melting point of the ionic liquid ($[C_n\text{-MIM}][BF_4]$). Compounds when n = 2-9 show a strong tendency to supercool, forming glasses. On lengthening the alkyl chain beyond a certain point (n > 9), the melting point of these salts start to increase

again with increasing chain length, because van der Waals interactions increase [42].

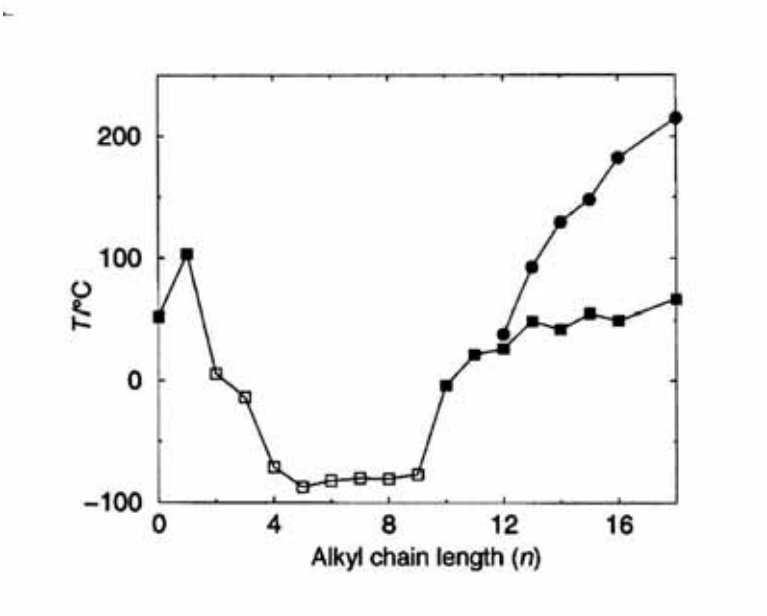

Figure 1.4: A phase diagram for 1-(C_nH_{2n+1})-3-methylimidazolium tetrafluoroborate ionic liquids and liquid crystals showing the melting (closed square), glass (open square) and clearing (circle) transitions [20c]

The degree of branching of the alkyl chain also influences the melting point. Table 1.6 shows data for a series of ionic liquids, in which the only difference is the degree of branching within the alkyl chain on the imidazolium nitrogen atom. With the degree of chain branching increasing, the melting points and enthalpy of fusion of the three isomers of 1-butyl-3-methylimidazolium hexafluorophosphate salts ([BMIM][PF_6]) [46] increase. The same result is observed for the two isomeric 1-propyl-3-methylimidazolium hexafluorophosphate salts ([PMIM][PF_6]) [47].

Table 1.6: Meting points and heats of fusion for isomeric [BMIM][PF_6] and [PMIM][PF_6]

N(1)-substitution	Melting point (°C)	ΔH_{fusion} (kJ mol^{-1})	Reference
n-butyl	6.4	31	[46]
sec-butyl	83.3	72	[46]
tert-butyl	159.7	83	[46]
n-propyl	40		[47]
isopropyl	102		[47]

The melting point of the phosphonium salt ($[R^1R^2R^3R^4P]^+X^-$) (R^1, R^2, R^3 and R^4 = $C_{1\text{-}20}$ hydrocarbyl group) would be lower when R group has a higher number of carbon atoms. However, branching also tends to result in a lower melting product. An α-branched or β-branched alkyl group is preferred to form a lower melting salt [40]. The same result was reported for phosphonium phosphinate salts by Robertson [48].

1.3.2 Viscosity and density of ionic liquids

1.3.2.1 Viscosity

In general, ionic liquids are more viscous than most common molecular solvents. The range of viscosities covers from 10 cP to over 500 cP. For comparison, the viscosities of water and glycerol at 25 °C are 1 and 934 cP respectively [49]. The viscosities of many ionic liquids strongly depend on temperature. For example the viscosity of [BMIM][PF_6] has an increase of 27% with a 5 degree change from 298 to 293 K [50]. Impurities in ionic liquids such as chloride and water dramatically influence the viscosities of ionic liquids. For example, an increase in residual chloride concentrations from 0.01 to 2 (mol kg^{-1}) in [C_4MIM][BF_4], increases viscosity from 154 to 600 (mPa s) at 20 °C [51]. In this work, the strong propensity of the non-haloaluminate alkylimidazolium ionic liquids to absorb water from laboratory air was observed, with one of the ionic liquids absorbing water up to 14 wt.%. Only 2 wt.% water (or other co-solvents) caused a reduction in the viscosity of [BMIM][BF_4] by more than 50% [51].

1.3.2.2 Density

The densities of ionic liquids vary from 1.12 g cm^{-3} for [(*n*-C_8H_{17})(C_4H_9)$_3$N][(CF_3SO_2)$_2$N] [52] to 2.4 g cm^{-3} for a 34-66 mole % [(CH_3)$_3$S]Br/$AlBr_3$ [53] ionic liquid. The densities of ionic liquids are least sensitive to variations in temperature [54]. In addition, the effect of impurities on density is much less than on the viscosity. For example, [BMIM][BF_4] containing 20 wt.% water results in only a 4% decrease in density [54].

1.3.3 Gas solubilities in ionic liquids

1.3.3.1 Water vapour

Many ionic liquids are extremely hygroscopic and it also is a good test of the strength of molecular interactions in these fluids. The water vapour solubility data for the three compounds [BMIM][PF_6], [OMIM][PF_6] and [OMIM][BF_4] at 25 °C are shown in Figure 1.5. The saturation pressure of these three compounds is just 0.031 bar [55]. The solubility of water vapour is much higher in the ionic liquid containing $[BF_4]^-$, which may be due to the greater charge density [56] or the presence of more space for the water molecules [57].

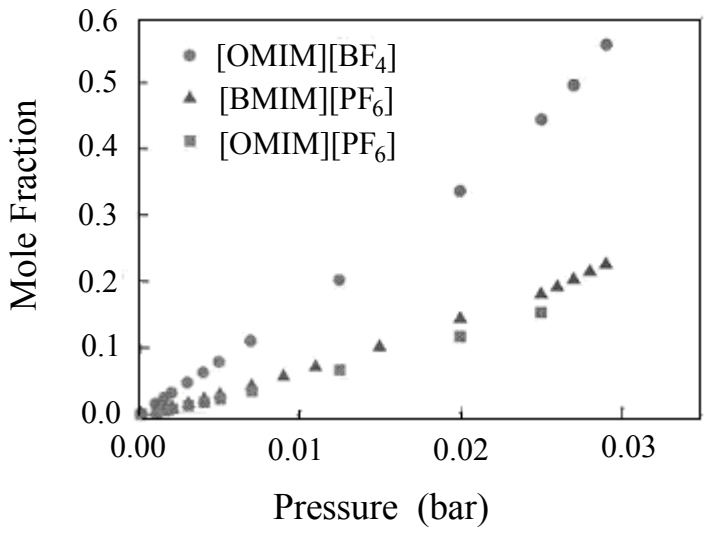

Figure 1.5: Solubility of water vapour in [BMIM][PF_6], [OMIM][PF_6] and [OMIM][BF_4] at 25 °C [58]

1.3.3.2 Other gases

The solubilities of CO_2, C_2H_6, C_2H_4, CH_4, O_2, Ar, H_2, N_2, and CO in [BMIM][PF_6] at temperatures of 10, 25 and 50 °C and pressure to 13 bar were investigated by Anthony *et al*. [59]. CO_2 has the highest solubility of all of the

gases tested, with the exception of water vapour, as can be seen from Table 1.7, which gives the Henry's Law constants of the various gases in [BMIM][PF_6] at 25 °C.

Table 1.7: Henry's Law Constants, H_1, for various gases in [BMIM][PF_6] at 25 °C [59]

Gas	*Henry's Law Constant (Bar)
CO_2	53.4 ± 0.3
C_2H_4	173 ± 17
C_2H_6	355 ± 36
CH_4	1690 ± 180
O_2	8000 ± 5400
Ar	8000 ± 3800
H_2	Non-detectable (>1500)
N_2	Non-detectable (>20000)
CO	Non-detectable (>20000)

*: $H_1(T,P) = \lim_{x_1 \to 0} \frac{f_1^L}{x_1} \approx \frac{P_1}{x_1}$, where $H_1(T,P)$ is the Henry's constant, x_1 is the mole fraction of gas dissolved in the liquid phase, f_1^L is the fugacity of vapour in the liquid phase, and P_1 is the pressure of the gas.

1.3.4 Polarity

Most current discussions of solvent effects are strongly related to the concept of solvent polarity. The most common measure of polarity is that of dielectric constant for most molecular liquids. However, direct measurement is not available for ionic liquids, because measurement needs a non-conducting medium [60]. Other methods such as chromatographic measurements [61], absorption spectra, fluorescence spectra [19a] [50] and organic reactions have been used to determine the polarities of solvents.

The phenomenon of solvatochromism arises when a solute is dissolved in different polar solvents; there appears to be an obvious change in position, intensity and shape of an UV absorption band. A bathochromic red shift with

increasing solvent polarity is called positive and a hypsochromic blue shift is called negative when the solvent polarity increases. Solvatochromic compounds are those solutes which undergo a change in the colour of the solution with a change in solvent polarity [62]. So, solvatochromic dyes can be used to measure the polarity of the medium in which they are dissolved [63]. Nile Red and Reichardt's dye are widely used as solvatochromic dyes for measuring solvent strength [62].

The solvatochromic probes using Reichardt's dye and Nile Red in [BMIM][PF_6] were investigated through absorbance by Fletcher *et al*. [64]. Reichardt's dye is the most common negative solvatochromic charge-transfer absorption probe used to measure the polarity, so for the more polar solvent the absorbance band will move down to a lower wavelength. Table 1.8 shows the absorption of Reichardt's betaine dye in common solvents and [BMIM][PF_6], and corresponding $E_T(30)$. The $E_T(30)$ polarity scale clearly indicates that [BMIM][PF_6] is less polar than methanol, ethylene glycol and water, and more polar than dichloromethane, acetonitrile and dimethyl sulfoxide.

Table 1.8: Intramolecular charge-transfer absorption maxima (λ_{max}) and corresponding $E_T(30)$ solvent polarity value for Reichardt's betaine dye dissolved in [BMIM][PF_6] and other solvents [64]

Solvent	λ_{max}/nm[a]	$E_T(30)$/kcal mol^{-1}[b]
Dichloromethane	700	40.8
Acetonitrile	630	45.4
Dimethyl sulfoxide	630	45.4
Ethanol	546	52.4
[BMIM][PF_6]	545	52.5
Methanol	515	55.1
Ethylene glycol	508	56.3
90 wt% glycerol in water	495	57.9
Water	453	63.1

[a]: Standard deviations associate with λ_{max} values are ± 2 nm. [b]: Calculated from equation ($E_T(30)$/kcal mol^{-1} = 28591/λ_{max}(nm), where λ_{max} is the wavelength of the maximum).

1.3.5. Electrochemical properties of ionic liquids

1.3.5.1 Electrochemical potential windows

The electrochemical stability of a solvent is a key criterion for selection for electrochemical studies [65]. It is shown through the range of voltages over which the solvent is electrochemically inert. This electrochemical potential "window" is dependent on the redox stability of the solvent. So the potential window of ionic liquids depends on the resistance of the cation to be reduced and anion to be oxidised.

Impurities, such as residual halide and water, can have a significant impact on the potential limits and the corresponding electrochemical window. For example, the potential window (ΔE) of dry [BMIM][BF_4] was 4.10 V, while for [BMIM][BF_4] containing 3 wt.% water, ΔE decreased to 1.95 V [66].

1.3.5.2 Ionic conductivity

The ionic conductivity of a solvent is one of the critical factors for any electrochemical application. Ionic liquids have good ionic conductivities, comparing well with the best nonaqueous solvent/electrolyte systems, but they are less conductive than concentrated aqueous electrolytes. Above room temperature, the conductivity of an ionic liquid often displays classical linear Arrhenius behaviour. The conductivity shows significant deviation from linear behaviour when the temperatures approach glass transition temperatures of the ionic liquid. The overall trend in conductivity of ionic liquids containing various cations follows the order: imidazolium $\geq$ sulfonium $>$ ammonium $\geq$ pyridinium. The correlation between the anion type or size and conductivity is relatively low. Ionic liquid conductivity has been found to strongly correlate with viscosity [67], and the addition of a variety of co-solvents can also increase the conductivity [68].

1.4 Phosphorus-containing ionic liquids

1.4.1 Phosphonium-based ionic liquids

Cytec, Fluka and Merck etc have recently commercialized a new promising class of the phosphonium-based ionic liquids. Figure 1.6 shows some anions that can be paired with tetraalkylphosphonium cations to produce ionic liquids.

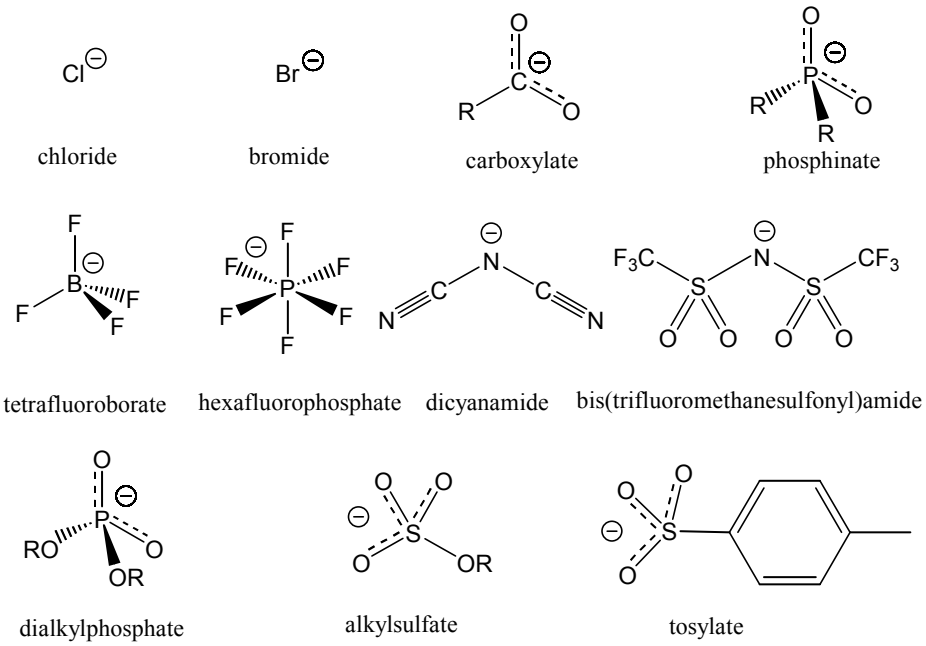

Figure 1.6: Anion structures for tetraalkylphosphonium ionic liquids [39]

In recent years, Wilkes *et al*. [69] reported new anions for making phosphonium ionic liquids, as shown in Figure 1.7.

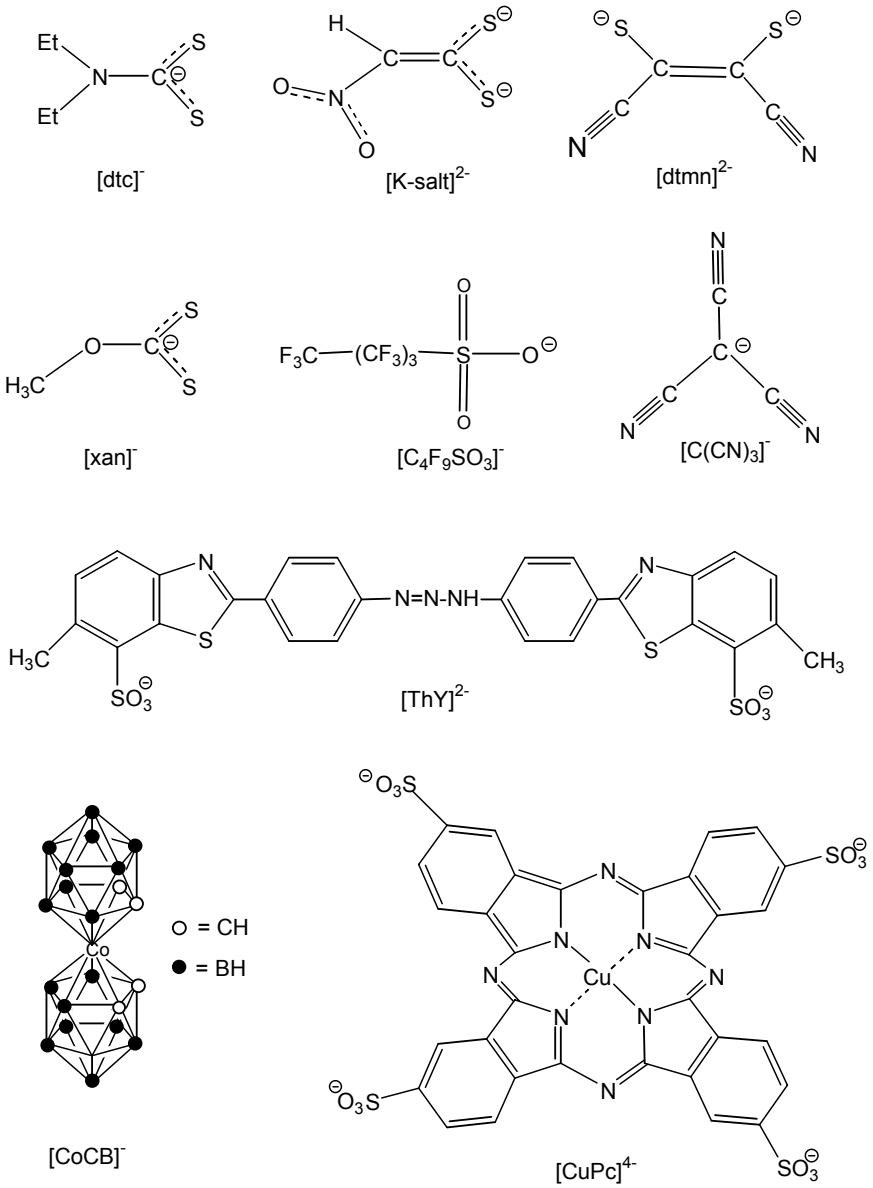

Figure 1.7: Anion structures for phosphonium ionic liquids used by Wilkes et al. [69]

1.4.1.1 Synthesis of phosphonium-based ionic liquids

Asymmetrical tetraalkylphosphonium halide ($[R'PR_3^+]X^-$) can synthesised by reaction of tertiary phosphines (PR_3) with haloalkanes (R'X, X= Cl, Br, I) (Equation 1.2) [70]. The pK_a for tertiary phosphines are lower than the corresponding amines and their larger radii and more polarizable lone pair makes them more nucleophilic, so the kinetics of salt formation are generally much faster than for amines [71] (as discussed in Section 1.2.2).

$$PR_3 + R'X \rightarrow [R'PR_3]^+X^-$$

Equation 1.2: Quaternization of phosphine to synthesise phosphonium salts [70]

Phosphonium ionic liquids can also be prepared by the anion exchange route (Equation 1.3 (a) or (b)), where R, R' = alkyl; X = halogen; M = alkali metal; A = anion (Figure 1.7). For example, $[(C_6H_{13})_3P(C_{14}H_{29})]^+Cl$ as a starting material can easily be used to prepare phosphonium ionic liquids [39]. The physical properties of phosphonium ionic liquids containing $[(C_6H_{13})_3P(C_{14}H_{29})]^+$ combined with different anions are shown in Table 1.9 [69]

$$[R'RP_3]^+X^- + MA \rightarrow [R'PR_3]^+A^- + MX \quad (a)$$

$$[R'RP_3]^+X^- + HA + MOH \rightarrow [R'PR_3]^+A^- + MA + H_2O \quad (b)$$

Equation 1.3: Metathesis methods to synthesise phosphonium ionic liquids

Table 1.9: Physical properties of $[(C_6H_{13})_3P(C_{14}H_{29})]_\chi[anion]^{\chi-}$ ionic liquids [69]

Anion[x]	T_g	T_{dec}[a] (°C)	Density[b] (g cm^{-3})	Viscosity[b] (cP)
$[dtc]^-$	-77	255	0.942	1470
$[xan]^-$	-70[d]	290	0.920	1480
$[K\text{-salt}]^{2-}$	-79	350	0.960	560
$[dtmn]^{2-}$	-71	360	0.942	4780
$[C_4F_9SO_3]^-$	-68	390	1.079	805
$[C(CN)_3]^-$	-65	415	0.901	320
$[CoCB]^-$	-71	420	1.00	3702
$[CuPc(SO_3)_4]^{4-}$	-45	400	e	e
$[ThY]^{2-}$	+65	395	e	e

[a:] T_{dec} is decomposition onset temperature.
[b:] Density and viscosity reported for room temperature (20 °C)
[e:] Viscosity too large to measure at room temperature.
[X]: Refer to Figure 1.7 for abbreviations.

Many of the physical and chemical properties of ionic liquids can be varied depending on the selection of suitable cations and anions. It is possible to

optimize an ionic reaction medium for a specific application by adjusting the relevant properties to some extent [18], so ionic liquids have been called "designer solvents" in some publications [72].

In a patent [73], phosphonium salts ($R^1R^2R^3R^4P^+X^-$) (R^1, R^2, R^3 and R^4 each independently represents a C_{1-20} hydrocarbyl group, X^- is anion, excluding halide), stated the chosen R^1, R^2, R^3, R^4, X^- to obtain low melting salts. They described (1): the total number of carbons usually 7-30, preferably 22-26; (2) one of R^1, R^2, R^3, and R^4 is a C_{8-20} alky group; (3) at least one of the R^1 to R^4 is a long straight alkyl chain at least containing 14 carbon atoms; (4) when anion is tosylate, at least one of the R^1, R^2, R^3, and R^4 is a branched alkyl group, and two, three or four can be branches. Suitable anions were mentioned were phosphate, nitrate, hexafluorophosphate (PF_6^-), tetrafluoroborate (BF_4^-), chloroaluminate ($AlCl_4^-$, $Al_2Cl_7^-$), carboxylates and sulfonates. A method to synthesise phosphonium sulfonates used reaction of a tertiary phosphine ($R^1R^2R^3P$) with a sulfonate ester (R^4X) (where R is same above, X = sulfonate). Anion exchange from a halide salt such as the chloride or bromide salt was used to prepare phosphonium hexafluorophosphates and tetrafluoroborates. The tetrachloroaluminate salt, formed by a phosphine mixed with trichloroaluminium was mentioned, but no examples of syntheses were given. Table 1.10 shows how the melting point is influenced by cations containing different alkyl group for alkylphosphonium tosylates, alkylphosphonium hexafluorophosphates, and alkylphosphonium tetrafluoroborates. It shows that a higher number of carbon atoms and branching will tend to result in a lower melting product. It was stated the trace levels of halide ion usually remained in the phosphonium salt when it was prepared from a phosphonium halide, and it was harmful for some reactions that are catalysed by a palladium or platinum catalyst [73].

Table 1.10: Influence of melting point of alkyl phosphonium tosylates/tetrafluoroborate/ hexafluorophosphates, through using different alkyl group [73]

	R^1	R^2	R^3	R^4	M.P. (°C)
Tosylates:	Et	Et	Et	Et	68-69
	n-Pr	*n*-Pr	*n*-Pr	Me	50-52
	n-Bu	*n*-Bu	*n*-Bu	Me	72-73
	i-Bu	*i*-Bu	*i*-Bu	Me	liquid
	i-Bu	*i*-Bu	*i*-Bu	Et	28-29
$[PF_6]^-$:	Pr	Pr	Pr	tetradecyl	44.5-45.5
	Bu	Bu	Bu	tetradecyl	38.0-39.0
	hexyl	hexyl	hexyl	tetradecyl	29-33
	Bu	Bu	Bu	Bu	161-163
	dodecyl	dodecyl	dodecyl	dodecyl	72-78
$[BF_4]^-$:	Bu	Bu	Bu	tetradecyl	32-35
	hexyl	hexyl	hexyl	tetradecyl	liquid

1.4.2 Phosphinate-based ionic liquids

To the best of this author's knowledge, there is not a lot of systematic synthesis, and discussion involving phosphinate-based ionic liquids in the literature. Only one Cytec patent (Novel phosphonium phosphinate compounds and their methods of preparation) [74] has been found. The patent gave phosphonium phosphinate compounds of general formula: $[R_1R_2R_3R_4P]^+[R_5R_6Y_1Y_2P]^-$, where R_1, R_2, R_3, R_4, R_5 and R_6 is independently a hydrogen or hydrocarbyl, Y_1 is O or S; and Y_2 is O or S. The patent described methods for preparing the phosphonium phosphinate compounds: (a) a phosphonium salt ($[R_1R_2R_3R_4P]^+X^-$) (wherein R_1 to R_4 is independently a hydrogen atom or a hydrocarbyl group, X^- is a leaving group, such as hydroxide, acetate, sulfate, or a halide preferably chloride, bromide or iodide) reacts with a phosphinic acid ($H^+[R_5R_6Y_1Y_2P]$) (R_5, R_6 is same as R_1 to R_4, Y_1, Y_2 is O or S) and a base, or, (b) a phosphonium salt reacts with a phosphinate salt

($M^{k+}[R_5R_6Y_1Y_2P]^-_k$) ($R_5$, R_6, Y_1, Y_2 in the same way as above, M^{k+} is H^+ or a metal cation with valency 'k'). It mentioned phosphonium phosphinates can be prepared by reaction a phosphonium hydroxide with a phosphinic acid, and recommended the reaction temperature was 45-70 °C to facilitate phase separation for preparing phosphonium phosphinates that have a small total number of carbons, of the order of 7-10 carbons. The examples do not discuss the hydroxide method and they used $(hexyl)_3P^+$tetradecyl chloride as starting material and then exchanged the anion to get the desired phosphonium phosphinate.

1.5 Aim of this research

The aim of this project was to investigate novel types of phosphorus-containing ionic liquids, specifically phosphinate-based and phosphonium-based ionic liquids. Synthesis, characterisation and applications of these types of ionic liquids comprise the major part of this project. Very little work has been done so far in the published literature on ionic liquids of these types. The lack of phosphonium/phosphinate-based ionic liquid publications, especially phosphinate-based ionic liquids provides a good reason for doing this current research. Additionally, the starting materials are commercially available or easily synthesised. Phosphonium salts are also much more thermally stable than the corresponding ammonium salts [39].

1.5.1 Methodology of syntheses

As discussed in Section 1.4.1.1, when ionic liquids are synthesised by quaternization of nitrogen or phosphorus centres to form chlorides, and then to exchange the chloride anion for the desired anion, the products would inevitably contain residual chloride ions, which is harmful for catalysts [73]. Additionally, anion exchange processes are wasteful and expensive [39]. These factors will increase the final cost of ionic liquids produced industrially, and limit the application range.

Halogen-free routes were used to synthesise phosphinate-based and phosphonium-based ionic liquids: (a) organophosphorus acids (R'R''PO_2H, R' = alkyl; R'' = R' or H) neutralised with quaternary ammonium hydroxides (R_4NOH, R = alkyl) or quaternary phosphonium hydroxides (R_4POH) to give [R_4N][R'R''PO_2]/[R_4P][R'R''PO_2] (Equation 1.4 (a)); (b) An excess of amine or pyridine was combined with the phosphinic acid to get [R_3NH][R'R''PO_2] or [pyH][R'R''PO_2] (Equation 1.4 (b) and (c)).

$$R'R''PO_2H + R_4EOH \rightarrow [R_4E][R'R''PO_2] + H_2O \quad (a)$$

$$R_3N + R'R''PO_2H \rightarrow [R_3NH][R'R''PO_2] \quad (b)$$

$$py + R'R''PO_2H \rightarrow [pyH][R'R''PO_2] \quad (c)$$

E = N, P;
R, R' = alkyl, R'' = R' or H

Equation 1.4: Methods of synthesis of phosphinate-based ionic liquids

These methods used to synthesise ionic liquids are particularly simple. For reaction (a) the only byproduct is water which could be removed by vacuum. So, if the starting material is very pure, the prepared ionic liquids should also be very pure. For reaction (b) and (c) the excess amine or pyridine can be easily removed under vacuum. The following organic acids: bis(2,4,4-trimethylpentyl)phosphinic acid ($(TMP)_2PO_2H$), mono-*n*-octylphosphinic acid ($octylPO_2H_2$), mono-*n*-hexylphosphinic acid ($hexylPO_2H_2$), di-*n*-octylphosphinic acid ($(octyl)_2PO_2H$), di-*n*-hexylphosphinic acid ($(hexyl)_2PO_2H$) and D-camphor-10-sulfonic acid ($camSO_3H$) were used to react with a base, such as, tetrabutylammonium hydroxide (Bu_4NOH), or tetraethylammonium hydroxide (Et_4NOH), or tetrabutylphosphonium hydroxide (Bu_4POH), or triethylamine (Et_3N) or pyridine to obtain phosphinate-based salts or phosphonium-based salts. The phosphinate-based salts, which are liquids at room temperature, were characterized by different techniques, such as NMR, UV-Visible, thermal gravimetric analysis (TGA) etc. More specific details are presented in Chapter 2. Some of these ionic liquids used as a media for preparing the transition metal nanoparticles, it will be presented in Chapter 3, and a literature review of application of ionic liquids is also presented in Chapter 3.

1.6 References

[1] Welton, T. *Chem. Rev*. **1999**, *99*, 2071-2083.

[2] (a) Welton, T. *Coord. Chem. Rev*. **2004**, *248*, 2459-2477.
(b) Dupont, J.; De Souza, R. F.; Suarez, P. A. Z. *Chem. Rev*. **2002**, *102*, 3667-3692.
(c) Sheldon, R. *Chem. Commun*. **2001**, 2399-2407.

[3] (a) AlNashef, I. M.; Mattews, M. A.; Weidner, J. W. In *Ionic Liquids as Green Solvents Progress and Prospects* Rogers, R. D., Seddon, K. R., Ed., American Chemical Society, Washington, DC 2003, pp 509-525.
(b) Ito, Y.; Nohira, T. *Electrochim. Acta* **2000**, *45*, 2611-2622.

[4] Rogers, R. D., Seddon, K. R. *Ionic Liquids: Industrial Applications for Green Chemistry*; ACS symposium series 818; American Chemical Society; Washington, DC, 2002.

[5] Wolfson, A.; Vankelecom, I. F. J.; Jacobs, P. A. *J. Organomet. Chem*. **2005**, *690*, 3558-3566.

[6] Sugden, S.; Wilkins, H. *J. Chem. Soc*. **1929**. 1291-1298 and references therein.

[7] (a) Hurley, F. H. U.S. Patent 2446331, August 3nd 1948 [Chem. Abstr. 1949, 43, P7645b].
(b) Hurley, F. H.; Wier, Jr, T. P. *J . Electrochem. Soc*. **1951,** *98*, 207-212.

[8] (a) Chum, H. L.; Koch, V. R.; Miller, L. L.; Osteryoung, R. A. *J. Am. Chem. Soc*. **1975**, *97*, 3264-3265.
(b) Robinson, J.; Osteryoung, R. A. *J. Am. Chem. Soc*. **1979**, *101*, 323-327.
(c) Wilkes, J. S.; Levisky, J. A.; Wilson, R. A.; Hussey, C. L. *Inorg. Chem*. **1982**, *21*, 1263-1264.

[9] Swain, C. G.; Ohno, A.; Roe, D. K.; Brown, R.; Maugh II, T. *J. Am. Chem. Soc*. **1967**, *89*, 2648-2649.

[10] (a) Scheffler, T. B.; Hussey, C. L.; Seddon, K. R; Kear, C. M.; Armitage; P. D. *Inorg. Chem*. **1983**, *22*, 2099-2100.
(b) Laher, T. M.; Hussey, C. L. *Inorg. Chem*. **1983**, *22*, 3247-3251.
(c) Scheffler, T. B.; Hussey, C. L. *Inorg. Chem*. **1984**, *23*, 1926-1932.

(d) Hitchcock, P. B.; Mohammed, T. J.; Seddon, K. R.; Zora, J. A.; Hussey, C. L.; Ward, E. H. *Inorg. Chim. Acta* **1986,** *113,* L25-L26.

[11] Dent, A. J.; Seddon, K. R.; Welton, T. *J. Chem. Soc., Chem. Commun.* **1990**, 315-316.

[12] Boon, J. A.; Levisky, J. A.; Pflug, J. L.; Wilkes; J. S. *J. Org. Chem*. **1986**, *51*, 480-483.

[13] Fry, S. E.; Pienta, N. J. *J. Am. Chem. Soc*. **1985**, *107*, 6399-6400.

[14] Chauvin, Y.; Gilbert, B.; Guibard, I. *J. Chem. Soc. Chem. Commun*. **1990**, 1715-1716.

[15] Carlin, R. T.; Wilkes, J. S. *J. Mol. Catal.* **1990**, *63*, 125-129.

[16] Wilkes, J. S.; Zaworotko, M. J. *J. Chem. Soc. Chem. Commun*. **1992**, 965-967.

[17] Chauvin, Y.; Mussmann, L.; Oliver, H. *Angew. Chem. Int. Ed. Engl.* **1995**, *34*, 2698-2700.

[18] Wasserscheid, P.; Keim, W. *Angew. Chem. Int. Ed.* **2000**, *39*, 3772-3789.

[19] (a) Bonhôte, P.; Dias, A. P.; Papageorgiou, N.; Kalyanasundaram, K.; Grätzel, M. *Inorg. Chem*. **1996**, *35*, 1168-1178.

(b) Davis Jr., J. H.; Forrester, K. J. *Tetrahedron Lett*. **1999**, *40*, 1621-1622.

(c) Davis Jr., J. H.; Forrester, K. J.; Merrigan, T. *Tetrahedron Lett*. **1999**, *39*, 8955-8958.

(d) Hagiwara, R.; Hirashige, T.; Tsuda, T. Ito, Y. *J. Fluorine Chem*. **1999**, *99*, 1-3.

(e) Hasan, M.; Kozhevnikov, I. V.; Siddiqui, M. R. H.; Steiner, A.; Winterton, N. *Inorg. Chem*. **1999**, *38*, 5637-5641.

[20] (a) Gordon, C. M.; Holbrey, J. D; Kennedy, A. R.; Seddon, K. R. *J. Mater. Chem*. **1998**, *8*, 2627-2636.

(b) Carmichael, A. J.; Hardacre, C.; Holbrey, J. D.; Nieuwenhuyzen, M.; Seddon, K. R. *Anal. Chem*. **1999**, *71*, 4572-4574.

(c) Holbrey, J. D.; Seddon, K. R. *J. Chem. Soc. Dalton Trans*. **1999**, *13*, 2133-2139.

[21] (a) Zim, D.; de Souza, R. F.; Dupont, J.; Monteiro, A. L. *Tetrahedron Lett*. **1998**, *39*, 7071-7074.

(b) Silva, S. M.; Suarez, P. A. Z.; de Souza, R. F.; Dupont, J. *Polymer Bull*. **1998**, *40*, 401-405.

(c) Dyson, P. J.; Ellis, D. J.; Parker, D. G.; Welton, T. *Chem. Commun.* **1999**, 25-26.

(d) Geldbach, T. J.; Dyson, P. J. *J. Organomet. Chem.* **2005**, *690*, 3552-3557.

(e) Gordon, C. M.; McCluskey, A. *Chem. Commun*. **1999**, 1431-1432.

(f) Earle, M. J.; McCormac, P. B.; Seddon, K. R. *Green Chem*. **1999**, *1*, 23-25.

(g) Adams, C. J.; Earle, M. J.; Seddon, K. R. *Green Chem.* **2000**, *2*, 21-23.

[22] Sheldon, R. *Chem. Commun.* **2001**, 2399-2407.

[23] Evans, D. F.; Yamauchi, A.; Wei, G. J.; Bloomfield, V. A. *J. Phys. Chem.* **1983**, *87*, 3537-3541.

[24] Lee, C. K.; Huang, H. W.; Lin, I. J. B. *Chem. Commun*. **2000**, 1911-1912.

[25] Davis, Jr., J. H.; Gordon, C. M.; Hilgers, C. Wasserscheid, P. In *Ionic Liquids in Synthesis*; Wasserscheid, P.; Welton, T., Ed.; GmbH & Co. KGaA, Weinheim, 2003; pp 7-21.

[26] Huddleston, J. G.; Willauer, H. D.; Swatloski, R. P.; Visser, A. E.; Rogers, R. D. *Chem. Commun*. **1998***,* 1765-1766.

[27] Lucas, P.; El Mehdi, N.; Ho, H. A.; Bélanger, D.; Breau, L. *Synthesis* **2000**, *9*, 1253-1258.

[28] Karodia, N.; Guise, S.; Newlands, C, Andersen, J.-A. *Chem. Commun*. **1998**, 2341-2342.

[29] Oye, H. A.; Jagtoyen, M.; Oksefjell, T.; Wilkes, J. S. *Mater. Sci. Forum* **1991**, *73-75*, 183-190.

[30] Williams, S. D.; Schoebrechts, J. P.; Selkirk, J. C.; Mamantov, G. *J. Am. Chem. Soc*. **1987**, *109*, 2218-2219.

[31] Chauvin, Y.; Olivier-Bourbigou, H. *CHEMTECH* **1995**, *25*, 26-30.

[32] Parshall, G. W. *J. Am. Chem. Soc*. **1972**, *94*, 8716-8719.

[33] Chauvin, Y.; Einloft, S.; Olivier; H. *Ind. Eng. Chem. Res*. **1995**, *34*, 1149-1155.

[34] Lecocq, V.; Graille, A.; Santini, C. C; Baudouin, A.; Chauvin, Y.; Basset, J. M.; Arzel, L.; Bouchu, D.; Fenet, B. *New J. Chem.* **2005**, *29*, 700-706.

[35] Abbott, A. P.; Capper, G.; Davies, D. L.; Rasheed, R. *Inorg. Chem*. **2004**, *43*, 3447-3452.

[36] Sitze, M. S.; Schreiter, E. R.; Patterson, E. V.; Freeman, R. G. *Inorg. Chem*. **2001**, *40*, 2298-2304.

[37] Swain, C. G.; Ohno, A.; Roe, D. K.; Brown, R.; Maugh, II, T. *J. Am. Chem. Soc*. **1967**, *89*, 2648-2649.

[38] Suarez, P. A. Z.; Dullius, J. E. L.; Einloft, S.; de Souza R. F.; Dupont, J. *Polyhedron* **1996**, *15*, 1217-1219.

[39] Bradaric, C. J.; Downard, A.; Kennedy, C.; Robertson, A. J.; Zhou, Y. *Green Chem*. **2003**, *5*, 143-152.

[40] Robertson, A. J. US01/12780, Date April 19, 2001.

[41] Seddon, R. K. *J. Chem. Tech. Biotechnnol*. **1997**, *68*, 351-356.

[42] Anthony, J. L.; Brennecke, J. F.; Holbrey, J. D.; Maginn, E. J.; Mantz, R. A.; Rogers, R. D.; Trulove, P. C.; Visser, A. E.; Welton, T. in *Ionic Liquids in Synthesis*; Wasserscheid, P.; Welton, T., Ed.; Wiley-WCH, Weinheim 2003; pp 41-55.

[43] Elaiwi, A.; Hitchcock, P. B.; Seddon, K. R.; Srinivasan, N.; Tan, Y. M.; Welton, T.; Zora, J. A. *J. Chem. Soc., Dalton Trans*. **1995**, *21*, 3467-3472.

[44] Fannin, Jr., A. A.; Floreani, D. A.; King, L. A.; Landers, J. S.; Piersma, B. J. Stech, D. J.; Vaughn, R. L.; Wilkes, J. S.; Williams, J. L. *J. Phys. Chem*. **1984**, *88*, 2614-2621.

[45] Gordon, J. E.; SubbaRao, G. N. *J. Am. Chem. Soc*. **1978**, *100*, 7445-7454.

[46] Carmichael, A. J.; Hardacre, C.; Holbrey, J. D.; Seddon, K. R.; Nieuwenhuyzen, M. In *Eleventh International Symposium on Molten Salts*, Vol. 99-41, Truelove, P. C.; De Long, H. C.; Stafford, G. R.; Deki, S. Eds.; The Electrochemical Society, Pennington, NJ, 1999.

[47] Ngo, H. L.; LeCompte, K.; Hargens, L.; McEwen A. B. *Thermochim. Acta* **2000**, *357-358*, 97-102.

[48] Robertson, A. J.; Seddon, K. CA Patent 2,343,456, March 30, 2001.

[49] http://pb.merck.de/servlet/PB/menu/1303700/index.html (18/02/2006).

[50] Baker, S. N.; Baker, G. A.; Kane, M. A.; Bright, F. V. *J. Phys. Chem. B*. **2001**, *105*, 9663-9668.

[51] Seddon, K R.; Stark, A.; Torres, M. J. *Pure Appl. Chem*. **2000**, *72*, 2275-2287.

[52] Sun, J.; Forsyth, M.; MacFarlane, D. R. *J. Phys. Chem. B*. **1998**, *102*, 8858-8864.

[53] Johnson, M. Ma, K. E. in *Proceedings of the Ninth International Symposium on Molten Salts* Hussey, D. S.; Newman, G.; Mamantov, G.; Ito, Y., Ed.; The

Electrochemical Society; Penington NJ, 1994, 94-13, pp 179-186.

[54] Mantz, R. A.; Trulove, P. C. in *Ionic Liquids in Synthesis*; Wasserscheid, P.; Welton, T., Ed.; Wiley-WCH, Weinheim 2003; pp 56-68.

[55] Anthony, J. L.; Maginn, E. J.; Brennecke, J. F. *J. Phys. Chem. B*. **2001**, *105*, 10942-10949.

[56] McEwen, A. B; Ngo, H. L.; LeCompte, K; Goldman, J. L. *J. Electrochem. Soc*. **1999**, *146*, 1687-1695.

[57] Jureviciute, I.; Bruckenstein, S.; Hillman, A. R. *J. Electroanal. Chem.* **2000**, *488*, 73-81.

[58] Brennecke, J. F.; Anthony, J. L.; Maginn, E. J. In *Ionic Liquids in Synthesis*; Wasserscheid, P.; Welton, T., Ed.; Wiley-WCH, Weinheim 2003; pp 81-93.

[59] Anthony, J. L.; Maginn, E. J.; Brennecke, J. F. *J. Phys. Chem. B*. **2002**, *106*, 7315-7320.

[60] Welton, T. In *Ionic Liquids in Synthesis*; Wasserscheid, P.; Welton, T., Ed.; Wiley-WCH, Weinheim, 2003; pp 94-103.

[61] Armstrong, D. W.; He, L.; Liu, Y. S. *Anal. Chem*. **1999**, *71*, 3873-3876.

[62] Buncel, E.; Rajagopal, S. *Acc. Chem. Res.* **1990**, *23*, 226-231.

[63] Carmichael, A. J.; Seddon, K. R. *J. Phys. Org. Chem*. **2000**, *13*, 591-595.

[64] Fletcher, K. A.; Storey, I. A.; Hendricks, A. E.; Pandey, S.; Pandey, S. *Green Chem*. **2001**, *3*, 210-215.

[65] Fry, A. J.; Britton, W. E. In *Laboratory Techniques in Electroanalytical Chemistry*; Kissinger, P. T.; Heineman, W. R., Ed.; Marcel Dekker, New York, 1984; pp 367-382.

[66] Schröder, U.; Wadhawan, J. D.; Compton, R. G.; Marken, F.; Suarez, P. A. Z.; Consorti, C. S.; de Souza, R. F.; Dupont, J. *New J. Chem*. **2000**, *24*, 1009-1015.

[67] Trulove, P. C. Mantz, R. In *Ionic Liquids in Synthesis*; Wasserscheid, P.; Welton, T., Ed.; Wiley-WCH, Weinheim 2003; pp 103-126.

[68] Perry, R. L.; Jones, K. M.; Scott, W. D.; Liao, Q.; Hussey, C. L. *J. Chem. Eng. Data* **1995**, *40*, 615-619.

[69] Del Sesto, R. E.; Corley, C.; Robertson, A.; Wilkes, J. S. *J. Organomet. Chem.* **2005***, 690*, 2536-2542.

[70] Henderson, Jr., W. A.; Buckler, S. A. *J. Am. Chem. Soc*. **1960**, *82*, 5794-5800.

[71] Henderson, Jr., W. A.; Streuli, C. A. *J. Am. Chem. Soc*. **1960**, *82*, 5791-5794.

[72] Freemantle, M. *Chem. Eng. News* **1998**, *76*, 32-37.

[73] Robertson, A. J. US01/12780, Date April 19, 2001.

[74] Robertson, A. J.; Seddon, K. CA Patent 2,343,456, March 30, 2001.

Chapter Two

Synthesis and characterisation of phosphinate-based ionic liquids

2.1 Introduction

The first ever entire organophosphorus chemistry book written in English, *Organophosphorus Compounds* [1], was only published in 1950. Organophosphorus chemistry has rapidly developed since then. Organophosphorus compounds are usually stable and easy to synthesise, reaction mechanisms of organophosphorus compounds have been extensively investigated, and industrial and commercial applications have been exploited by chemists. Phosphorus chemistry has also profited from the development of physical techniques, such as ^{31}P nuclear magnetic resonance spectroscopy, which is a powerful tool to help the investigation of organophosphorus chemistry [2].

The following formulae (Scheme 2.1) generally represent organophosphorus compounds where R represents combinations of organic substituents, such as mercapto, amino, etc., and X is O, S, ═NR, ═CR_2 or an acid radical [1].

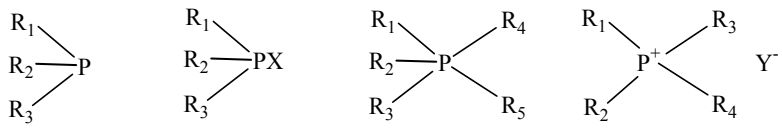

(a) (b) (c) (d)

When R_1, R_2, R_3 = alkyl groups or H as in (a) gives phosphines and in (b), if X = O in addition to the substituents present in (a), gives phosphine oxides; and when R_1 = alkyl, R_2 and R_3 = halides, R_4 and R_5 = an alkyl or a halide, then (c) = halogenophosphoranes; and finally when R_1, R_2, R_3, and R_4 are all = alkyl groups as in (d) gives phosphonium compounds.

Scheme 2.1: General formulae of organophosphorus compounds

2.1.1 Radical addition reaction for synthesis of P-C bonds

There are available multiple valencies for phosphorus, hence, the varied groups can be attached to phosphorus. Free-radical species, which have an odd electron centred primarily on phosphorus, are considered as very important. Some of them are shown in Scheme 2.2, where R represents alkyl, aryl, alkoxy, or aryloxy groups, halogen, hydrogen, and so on [3].

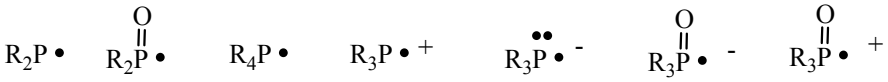

Scheme 2.2: Some of the odd electron centred free-radical species on phosphorus

Radical additions involving phosphorus-centered radicals in P-C bond forming reactions have been known for several decades [4]. It is a general reaction (see Scheme 2.3) for free radical addition of P-H bonds to olefins [5], and can involve phosphine (PH_3), substituted phosphine (RPH_2 or R_2PH) [6], phosphorous acid (H_3PO_3) [7] and esters [8], hypophosphorous acid (H_3PO_2) [9] and so on.

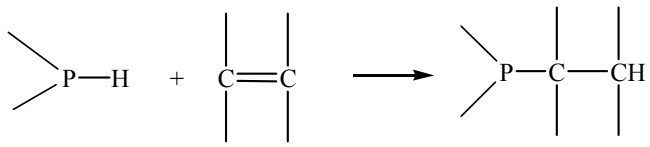

Scheme 2.3: Formation of a P-C bond through radical addition of a P-H bond to an olefin

Hypophosphorous acid is known to react with alkenes under the influence of radical initiators (Scheme 2.3). Williams and Hamilton studied the reaction of aqueous H_3PO_2 with *n*-1-olefins, as early as 1955 [9]. The suggested mechanism, shown in Scheme 2.4 for the addition of H_3PO_2 to alkenes, involves the generation of a H_3PO_2-derived radical, A, which attacks the double bond to produce a new radical B, which reacts with another H_3PO_2 molecule to generate another radical A.

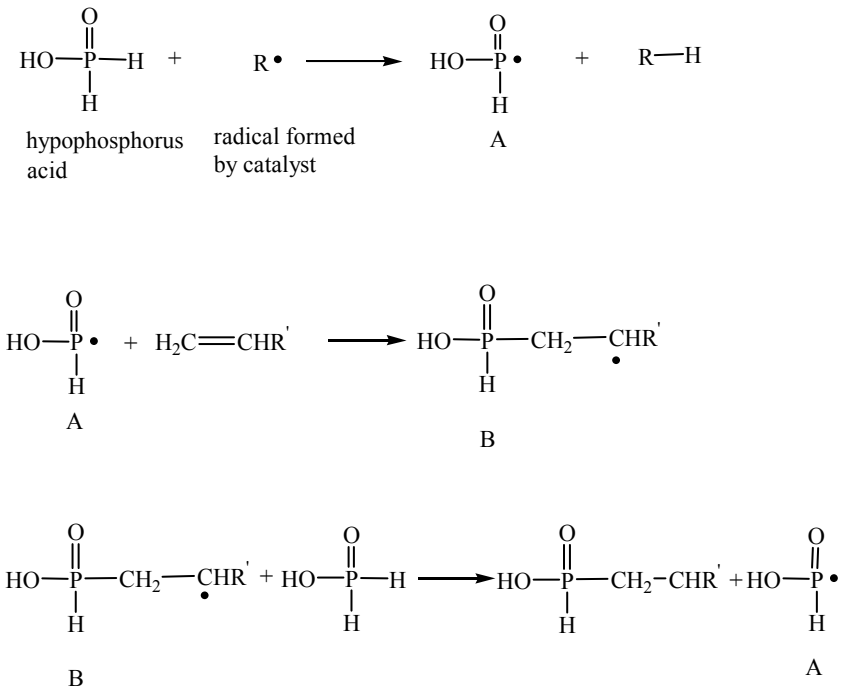

Scheme 2.4: The radical-catalysed addition of H_3PO_2 to alkene

Scheme 2.5 shows two possible modes of radical attack; radical intermediates B and C are generated by $H_2O_2P\cdot$ attack at position 1 and position 2 respectively. The protonation of B by a second hypophosphorous acid molecule produces the major addition product B'. Similarly, the protonation of C produces the minor addition product C'. The product C' is expected to exist only in trace amounts due to the radical attack on position 2 being more sterically hindered than at position 1 [10].

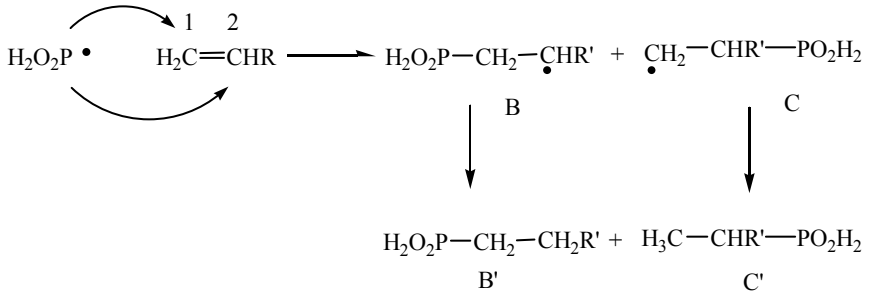

Scheme 2.5: The modes of radical addition to an unsaturated bond [10]

2.1.2 Phosphinate ionic liquids

The history and the methods of the synthesis of ionic liquids have been presented in Chapter 1. A Cytec patent [11] which covers the manufacture of phosphonium phosphinate ionic liquids has also been presented Section 1.4.2. The synthesised phosphonium phosphinates were not chloride free. Many ionic liquids synthesised by quaternization of nitrogen or phosphorus centres to form chlorides, and then anion exchange [12] [13]. Therefore, the products would inevitably contain residual chloride ions, which may be harmful for catalysts. Additionally, anion exchange processes are wasteful and expensive [14].

In this work, the intention was to prepare phosphinate-based ionic liquids, with triethylammonium, tetrabutylammonium, tetrabutylphosphonium and pyridinium counterions, ($[R_3R'E][R''_2PO_2]$), (R = alkyl group; R' = R, H; R'' = R, H, not more than one of R''are hydrogen; E = N, P) using halide-free routes. Simple reactions, involving neutralisation of organophosphorus acids with base in a suitable solvent were devised, followed by removal of all of volatiles under vacuum. The methodology is simple, convenient, and economic, and also is halide-free. When E = N, one of R'' is H, the $[R_3R'E][R''_2PO_2]$ is to be $[R_3R'N][R''PO_2H]$, this type of ionic liquid is new and it is also first time to be synthesised and reported.

One of the key points is choosing branched alkyl groups to prevent crystallisation [11] [15]. More details have presented in Chapter 1. Generally, as the degree of asymmetry and branching is increased, the melting point of salts will be decreased. As examples, OP(*n*-octyl)$_3$ is a solid, while OP(*iso*-octyl)$_3$ is a liquid, and also $Bu_2PO(OH)$ is solid, but *iso*-$Bu_2PO(OH)$ [1] is liquid. Conversely, increasing the total number of carbon atoms in the substituents R, R' and R'' will cause the melting point to increase, although this effect will be counteracted somewhat by asymmetry and branching [11].

2.2 Results and discussion

2.2.1 Synthesis of phosphinate-based ionic liquids and related compounds

2.2.1.1 Synthesis of di-*n*-alkylphosphinic acids

Two of the starting materials, di-*n*-octylphosphinic acid **1** and di-*n*-hexylphosphinic acid **2**, (dialkyl = di-*n*-alkyl, unless otherwise stated) were synthesised by a modification of the procedure described in the literature (Scheme 2.6), by the dibenzoyl peroxide-catalysed addition of 1-octene and 1-hexene respectively to hypophosphorous acid in *n*-butanol [9]. A large excess of alkene was used to ensure conversion to the dialkylphosphinic acid, giving the essentially pure product **1** [^{31}P-NMR ($CDCl_3$); δ 60.3] and product **2** [^{31}P-NMR ($CDCl_3$); δ 60.4] which were purified by removal of butanol, and recrystallisation from petroleum spirits, with yields around 40%. The yield was relatively low because the products are partly soluble in petroleum spirits at room temperature. The product di-*n*-alkylphosphinic acids are white crystalline compounds with high stability [9]. It might be expected that a 2-hexyldecylphosphinic acid, $C_{16}H_{33}PO_2H_2$ [16], and 2-butyloctylphosphinic acid, $C_{12}H_{25}PO_2H_2$, could be respectively found as impurities in the preparation of di-*n*-octylphosphinic acid **1** and di-*n*-hexylphosphinic acid **2** because telomerization [7a] could occur, and also expected accompanying 1-octylphosphinic acid, $C_8H_{17}PO_2H_2$ [16], and 1-hexylphosphinic acid, $C_6H_{13}PO_2H_2$. It was reported [7b] that there was an impurity, 2-hexyldecylphosphonic acid, in the synthesis of *n*-octylphosphonic acid from 1-octene and phosphorous acid, H_3PO_3. In the case of di-*n*-alkylphosphinic acids, these are solids and can be recrystallised to remove the 2-hexyldecylphosphinic acid, 2-butyloctylphosphinic acid 1-octylphosphinic acid and 1-hexylphophinic acid contaminants. The respective melting points of di-*n*-octylphosphinic acid and di-*n*-hexylphosphinic acid were 82 °C and 76 °C which are consistent with 85 °C [9] and 77-78.5 °C [17] in the literature. The same reactions in isopropanol were attempted, but **1** or **2** were not obtained.

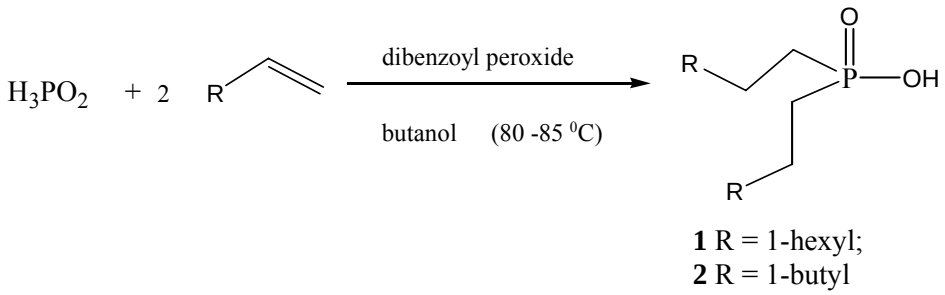

1 R = 1-hexyl;
2 R = 1-butyl

Scheme 2.6: Synthesis method for the preparation of **1** and **2**

2.2.1.2 Synthesis of mono-*n*-alkylphosphinic acids

Mono-*n*-alkylphosphinic acids (alkyl = mono-*n*-alkyl unless otherwise stated) are well known compounds. Accidentally, a method of making mono-*n*-alkylphosphinic acids was obtained from the failed synthesis of dialkylphosphinic acids in isopropanol. The present methodology was applied to the preparation of mono-*n*-alkylphosphinic acids by adjusting the ratio of reactants and the amount of catalyst in isopropanol (Scheme 2.7). An excess of hypophosphorous acid and less dibenzoyl peroxide was used to obtain around 50-60% yield of monoalkylphosphinic acid with about 92% purity, because of accompanying byproducts of dialkylphosphinic acids and isomeric alkylphosphinic acids, H_3C-CHR'-PO_2H_2 (R = butyl, and hexyl), (**C'** in Scheme 2.5) was observed in this reaction mixture. The byproducts cannot be successfully removed, as the monoalkylphosphinic acids are liquids. It has shown in the literature [16] that it is impossible to purify the product which is made by alkene addition to hypophosphorous acid. The mono-1-octylphosphinic acid **3** and mono-1-hexylphosphinic acid **4** give a peak in the ^{31}P - $\{^1H\}$ NMR spectrum at δ 37.

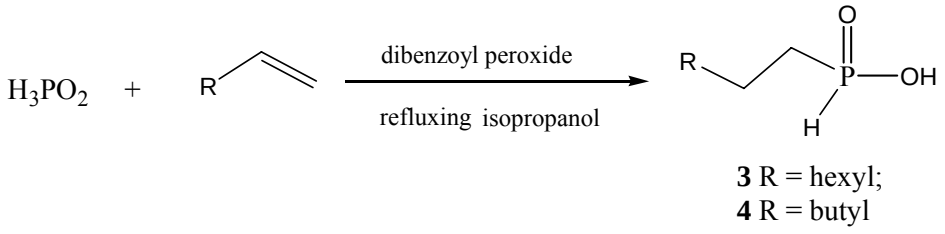

3 R = hexyl;
4 R = butyl

Scheme 2.7: Synthesis of **3** and **4**

2.2.1.3 Synthesis of ionic liquids

A chloride-free synthesis routine was selected for this research, because it is known that the presence of traces of chloride may adversely affect the rates of reactions which are catalysed by transition metals in ionic liquid media and/ or contaminate the reaction products [14] [18] [19] and can also affect the viscosity [19] [20]. The viscosity of ionic liquids depends on their tendency to form hydrogen bonding and the strength of their van der Waals interactions [21]. For example, for 1,3-dialkylimidazolium tetrachloroaluminate [22], there is an increase in viscosity of more than a factor of ten in ionic liquids because of the formation of hydrogen bonds between the hydrogen atoms of the imidazolium cation and the basic chloride ion, when the mole fraction of dialkylimidazolium tetrachloroaluminate melts/aluminium trichloride less than 0.5. However, in acidic mixtures, because of the presence of $AlCl_4^-$ and $Al_2Cl_7^-$, the negative charge is much better distributed, which results in the formation of weaker hydrogen bonds and a much lower viscosity [20].

Organophosphorus acids, such as di-*n*-alkylphosphinic acids (R_2PO_2H) and mono-*n*-alkylphosphinic acids (RPO_2H_2) were neutralised by quaternary ammonium hydroxides to give $[R_4N][R_2PO_2]$ and $[R_4N][RPO_2H]$. These syntheses involved reacting the acid and base in a suitable solvent and then removing volatiles under vacuum for 2-3 days with stirring until a constant weight was obtained. The titration method was necessary in some cases because the organophosphorus starting materials, such as RPO_2H_2 and bis(2,4,4-trimethylpentyl)phosphinic acid ($(TMP)_2PO_2H$) which is a commercial product, are not pure, so the amount of base to be used could not be calculated straightforwardly. Although the Cytec patent [11] covered ionic liquids with $R_2PO_2^-$ and RPO_2H^-, no examples such as RPO_2H^-, di-*n*-octylphosphinic acid and di-*n*-hexylphosphinic acid have been used. ($(TMP)_2PO_2H$), mono-*n*-octylphosphinic acid **3** ($octylPO_2H_2$) and hexylphosphinic acid **4** ($hexylPO_2H_2$) respectively, were titrated in methanol by an aqueous solution of tetra-*n*-butylammonium hydroxide (Bu_4NOH) with phenolphthalein indicator, until the endpoint (pale pink) (Equation 2.1). The ionic liquid products tetra-*n*-

butylammonium bis(2,4,4-trimetylpentyl)phosphinate ($[Bu_4N][(TMP)_2PO_2]$) **5,** tetra-*n*-butylammonium octylphosphinate ($[Bu_4N][octylPO_2H]$) **6**, and tetra-*n*-butylammonium hexylphosphinate ($[Bu_4N][hexylPO_2H]$) **7** were obtained as brown coloured, viscous liquids. Tetraethylammonium hydroxide (Et_4NOH) also was used in the synthesis of tetraethylammonium bis(2,4,4-trimethylpentyl)phosphinate ($[Et_4N][(TMP)_2PO_2]$), to give a waxy solid (M.P.>100 °C).

$$[Bu_4N]OH + RR'PO_2H \rightarrow [Bu_4N][RR'PO_2] + H_2O$$

5 R = R'=2,4,4- trimethylpentyl
6 R = *n*-hexyl, R'= H
7 R = *n*-octyl, R'=H

Equation 2.1: Synthesis of **5, 6** and **7**

Additionally, phosphonium phosphinate ionic liquids also were synthesised by neutralising tetrabutylphosphonium hydroxide with the organophosphorus acid. Similarly, $(TMP)_2PO_2H$, $otcylPO_2H_2$ **3** and $hexylPO_2H_2$ **4** were titrated in methanol by $[Bu_4P]OH$ with phenolphthalein indicator, until the endpoint (pale pink). After removing all volatiles, the ionic liquids tetrabutylphosphonium bis(2,4,4-trimethylpentyl)phosphinate ($[Bu_4P][(TMP)_2PO_2]$) **8**, tetrabutylphosphonium octylphosphinate ($[Bu_4P][octylPO_2H]$) **9**, and tetrabutylphosphonium hexylphosphinate ($[Bu_4P][hexylPO_2H]$) **10** were obtained (Equation 2.2). It would be expected that these ionic liquids should be colourless. However, the ionic liquids had a purple colour, caused by the phenolphthalein indicator, dependent on the pH. After several days, all of them became colourless, presumably because they gradually absorb traces of CO_2 and moisture from the atmosphere; most ammonium salts are hygroscopic [23]. One of the phosphonium ionic liquids, compound **8,** is hygroscopic too, as discussed later in this Chapter.

$$[Bu_4P]OH + RR'PO_2H \rightarrow [Bu_4P][RR'PO_2] + H_2O$$

8 R = R'= 2,4,4-trimethylpentyl
9 R = *n*-hexyl, R'= H
10 R = *n*-octyl, R'= H

Equation 2.2: Synthesis of **8, 9** and **10**

To see whether a chiral ionic liquid could be synthesised by this route a chiral organic acid, D-camphor-10-sulfonic acid (Figure 2.1), was reacted in methanol with solutions of $[Et_4N]OH$, $[Bu_4N]OH$ and $[Bu_4P]OH$. However, the resulting compounds were solids with relatively high melting points of 139-144 ºC, 139 ºC and 278-286 °C respectively. No further work was carried out with these systems.

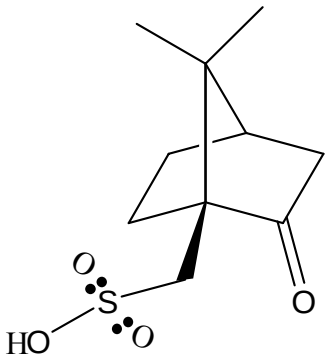

Figure 2.1: Molecular structure of D-camphor-10-sulfonic acid

A similar synthetic route was applied for the preparation of tetrabutylphosphonium/tetrabutylammonium dialkylphosphinate ionic liquids. Pure compound **1** or compound **2** was added to an equal number of moles of tetrabutylphosphonium hydroxide or tetrabutylammonium hydroxide, which was previously standardised by titration with hydrochloric acid (Equation 2.3). Water, which is the only byproduct, was removed under vacuum for 2-3 days with stirring until constant weight. The yields of colourless tetrabutylphosphonium di-*n*-octylphosphinate ($[Bu_4P][(octyl)_2PO_2]$) **11**, tetrabutylammonium di-*n*-octylphosphinate ($[Bu_4N][(octyl)_2PO_2]$) **12**, tetrabutylammonium di-*n*-hexylphosphinate ($[Bu_4N][(hexyl)_2PO_2]$) **13** were more than 99%, and were

higher than their monosubstituted phosphinic acid counterparts. $[Bu_4P][(hexyl)_2PO_2]$) was synthesised as a waxy solid, M.P. < 50 °C.

$$[Bu_4E]OH + R_2PO_2H \rightarrow [Bu_4E][R_2PO_2] + H_2O$$

11 R = octyl, E = P
12 R = octyl, E = N
13 R = hexyl, E = N

Equation 2.3: Synthesis of **11, 12** and **13**

Elemental analyses of **11** and **13** gave reproducible C, H, and N percentages that did not match with the theoretical values, although the products appeared pure by NMR. For example, for compound **11**, $([(C_4H_9)_4P][(C_8H_{17})_2PO_2])$, the respective percentage contents of C, and H were found to be 66.75 (70.03) and 13.03 (12.86) with theoretical values in parentheses. If it is assumed that the discrepancy is solely due to (0.9449 mole) H_2O, the respective percentage contents of C and H would be 66.75 and 12.81 which is very close to the experimental results. Similarly, for compound **13**, $([(C_4H_9)_4N][(C_6H_{13})_2PO_2])$, the respective percentage contents of C, H, and N are 65.20 (70.68), 13.15 (13.14) and 2.80 (2.94) from experiment (theoretical values in parentheses). On the assumption that **13** contained 2.221 mole H_2O, the responding percentage contents of C, H and N would be 65.20, 12.98, and 2.72 respectively, which are approximately the same as the observed values. It was also presumed that the starting materials di-*n*-octylphosphinic acid and di-*n*-hexylphosphinic acid might contain a trace of mono-*n*-octylphosphinic acid and mono-*n*-hexylphosphinic acid respectively as well (This point has been elaborated in dialkylphosphinic acids discussion part, Section 2.2.1.1), but not taken into account in calculation.

It is also possible to synthesise ionic liquids containing trialkylammonium and pyridinium cations, by a simple method. An excess of triethylamine was added to the different phosphinic acids, such as, $(TMP)_2PO_2H$, or acids **3** and **4**, stirred for several minutes and the excess unreacted base easily removed under

vacuum, producing colourless ionic liquids of triethylammonium bis(2,4,4-trimethylpentyl)phosphinate ($[Et_3NH][(TMP)_2PO_2]$) **14**, triethylammonium octylphosphinate ($[Et_3NH][octylPO_2H]$) **15** and triethylammonium hexylphosphinate ($[Et_3NH][hexylPO_2H]$) **16** in about 70% yield each (Equation 2.4). The yields of the triethylammonium ionic liquids are much lower than the tetrabutylammium analogues, because the substances with trialkylammonium ions easily decompose below 80 °C under vacuum [20]. Reactions of triethylamine with products **1** and **2** were also attempted, giving white solid products $[Et_3NH][(octyl)_2PO_2]$ and $[Et_3NH][(hexyl)_2PO_2]$ with M.P. 54-58 °C and 68-74 °C respectively.

$$Et_3N + RR'PO_2H \rightarrow [Et_3NH][RR'PO_2]$$

14 R = R' = 2,4,4-trimethylpentyl
15 R = *n*-octyl, R' = H
16 R = *n*-hexyl, R' = H

Equation 2.4: Synthesis of **14, 15** and **16**

The same method was used to synthesise the colourless ionic liquids pyridinium bis(2,4,4-trimethylpentyl)phosphinate ($[pyH][(TMP)_2PO_2]$) **17**, pyridinium octylphosphinate ($[pyH][octylPO_2H]$) **18** and pyridinium hexylphosphinate ($[pyH][hexylPO_2H]$) **19,** with yields around 70% (Equation 2.5).

$$py + RR'PO_2H \rightarrow [pyH][RR'PO_2]$$

17 R = R' = 2,4,4-trimethylpentyl
18 R = *n*-octyl, R' = H
19 R = *n*-hexyl, R' =H

Equation 2.5: Synthesis of **17, 18** and **19**

Pyridinium di-*n*-octylphosphinate ($[pyH][(octyl)_2PO_2]$) and pyridinium di-*n*-hexylphosphinate ($[pyH][(hexyl)_2PO_2]$) formed white solids with melting points of 81-82 °C and 75-77 °C respectively. Pyridine (py) is weaker base than

triethylamine and the R_2PO_2H is a weaker acid than RPO_2H_2. The pKa of $(TMP)_2PO_2H$ (5.42) < $(octyl)_2PO_2H$ (5.03) < $octylPO_2H_2$ (3.62) < $hexylPO_2H_2$, as this is because the pKa values of $RR'PO_2H$ increases with increasing steric of R and R'. Consequently, the acid strength of organophosphinic acids decreases through linear monoalkylphosphinic > branched monoalkylphosphinic > linear dialkylphosphinic > branched dialkylphosphinic [24]. So, bis(2,4,4-trimethylpentyl)phosphinic acid ($(TMP)_2PO_2H$) is the weakest acid among the $hexylPO_2H_2$, $octylPO_2H_2$, $(hexyl)_2PO_2H$, and $(octyl)_2PO_2H$. Thus the compound $[pyH][(TMP)_2PO_2]$ is the most unstable with respect to dissociation within the class of pyridinium ionic liquids.

In this research, generally, if pure starting materials are used, the product ionic liquids are colourless. However, the use of impure staring materials can result in impure or coloured ionic liquids. For example, a solution of Bu_4POH/Bu_4NOH develops a flocculent precipitate with time, and from this, ionic liquids with a yellow colour are formed. Hence, to obtain high purity ionic liquids it is necessary to use as high purity starting materials as possible, because purification of the product ionic liquid may be difficult.

2.2.2 NMR Spectroscopic characterisation

Di-*n*-octylphosphinic acid **1** and di-*n*-hexylphosphinic acid **2** were found to be very pure by NMR. Single peaks were observed in the ^{31}P NMR spectra for both compounds. Figure 2.2 shows the NMR spectra of mono-*n*-hexylphosphinic acid **4,** (CH_3-$(CH_2)_5$-P(O)(OH)(H)), where a small peak (δ 58) could be dihexylphosphinic acid, and another small peak (δ 42) which could be isomeric hexylphosphinic acid (Figure 2.2 (a)), that separated into two peaks in the proton-coupled spectrum, Figure 2.2 (b). In Figure 2.2 (c) a proton resonances at δ 11 was assigned to the acidic hydroxyl group, as integration of the OH to hexyl proton, 1:13.08, which was approximately 1:13 by calculation, and two signals (δ 7.7; δ 6.0) which from 'P-H', the ^1J coupling constant (538.7 Hz) was the same as that observed in the ^{31}P NMR spectrum.

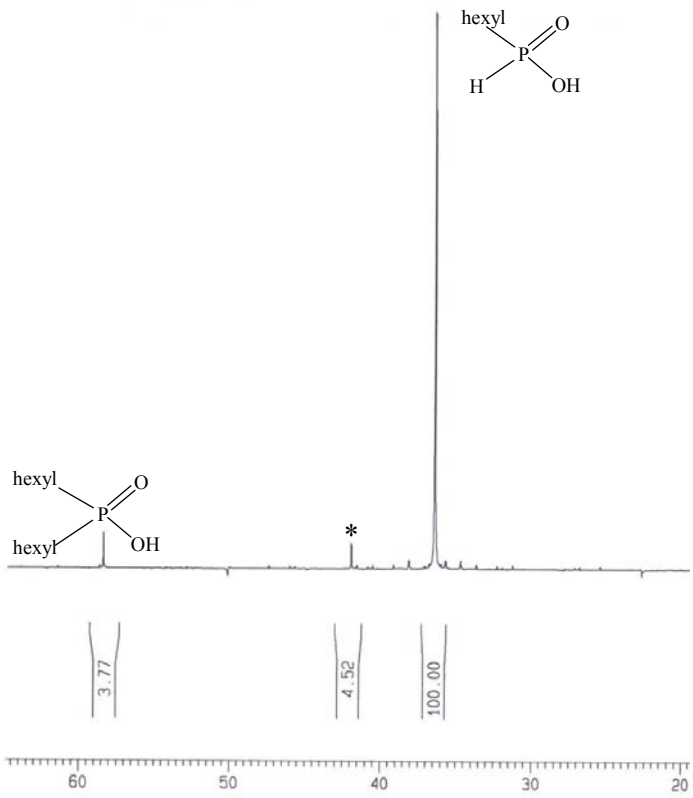
hexyl
O
P
H
OH
hexyl
O
P
hexyl
OH
*
3.77
4.52
100.00
60
50
40
30
20

(a)

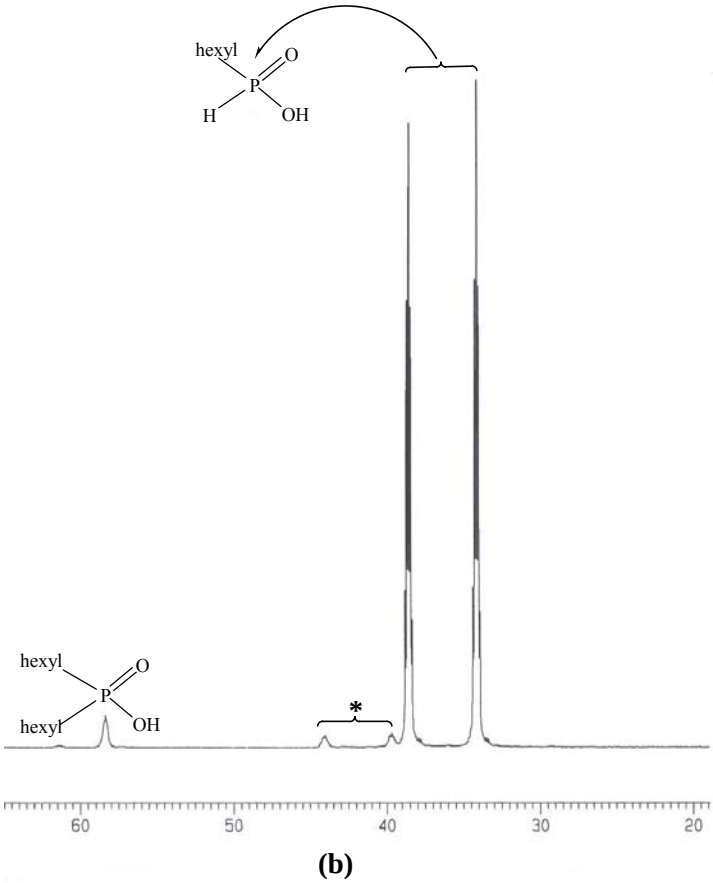
hexyl
O
P
H
OH
hexyl
O
P
hexyl
OH
*
60
50
40
30
20

(b)

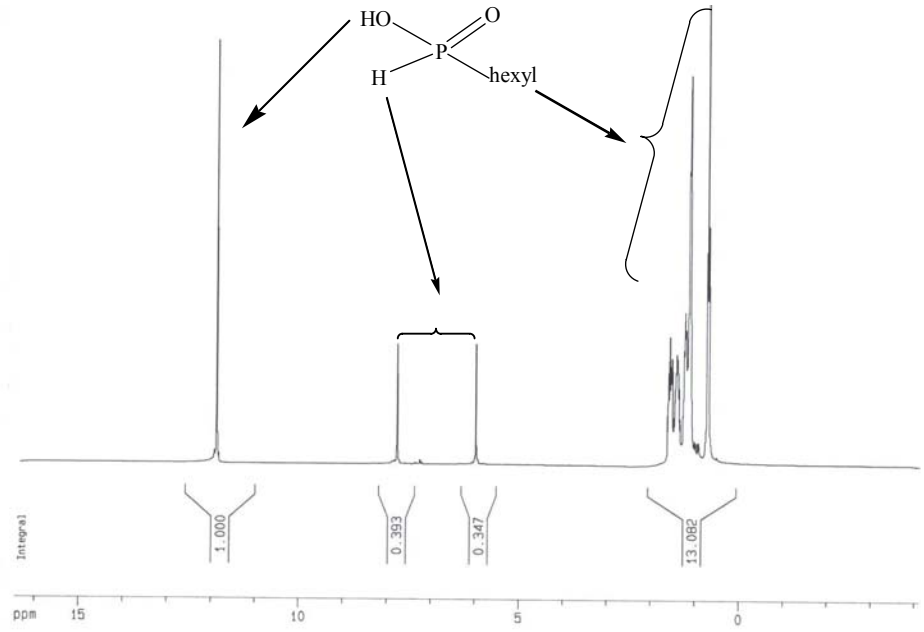

(c)

Figure 2.2: ^{31}P NMR (a) ^{31}P-{^{1}H}, (b) ^{31}P, and (c) ^{1}H NMR spectra of hexylphosphinic acid (**4)** in $CDCl_3$. The peak identified as "*" is possibly due to isomeric hexylphosphinic acid

A summary of the ^{31}P NMR data of the starting alkylphosphinic acids is presented in Table 2.1. *n*-OctylPO_2H_2 **3** and *n*-hexylPO_2H_2 **4** gave ^{1}J(PH) coupling constants of 539.6 Hz and 539.5 Hz respectively. The ^{31}P NMR shifts of (*n*-octyl)$_2PO_2H$ **1** and (*n*-hexyl)$_2PO_2H$ **2** [δ 60.3] are similar to that of di(*n*-octyl)phosphinic acid [δ 60.2] [25] from literature.

Table 2.1: ^{31}P NMR ($CDCl_3$) chemical shift data for compounds **1, 2, 3**, and **4**

Compound	Literature ^{31}P-{^{1}H}NMR	^{31}P-{^{1}H} NMR ($CDCl_3$)	^{1}J(PH, Hz)
n-octylPO_2H_2 **3**	37.8 ref. [26]	37.1	539.6
n-hexylPO_2H_2 **4**	37.8 ref. [26]	36.4	539.5
(*n*-octyl)$_2PO_2H$ **1**	60.2 ref. [25]	60.3	
(*n*-hexyl)$_2PO_2H$ **2**		60.3	

There is a change in ^{31}P NMR chemical shifts when the acid is converted to the anion, as shown by a comparison of Table 2.1 and Table 2.2. For example *n*-hexylPO_2H_2 **4** formed $[Et_3NH][hexylPO_2H]$ **16,** and the corresponding ^{31}P NMR chemical shift moves from 36.4 to 28.7 ppm.

Table 2.2: Chemical shift (δ) of ^{31}P NMR ($CDCl_3$) for some ionic liquids

Compound	^{31}P - $\{^1H\}$ NMR ($CDCl_3$)	
$[Bu_4P][(octyl)_2PO_2]$ **11**	34.5 (anion);	33.2 (cation)
$[Bu_4P][hexylPO_2H]$ **10**	24.1(anion);	33.5 (cation)
$[Et_3NH][hexylPO_2H]$ **16**	28.7	
$[Bu_4N][(hexyl)_2PO_2]$**13**	35.5	

2.2.3 ES-MS characterisation

Electrospray mass spectrometry (ES-MS) has been widely used to analyse the structure of a wide variety of substances involving inorganic [27] and organometallic compounds [28], such as positively charged phosphonium ions [29], ionic inorganic and organometallic compounds [30] [19], hydroxymethylphosphonium salts [31], phosphonic acids [32] and other organophosphorus acids [10]. However, very little information using ES-MS to study specific ionic liquids [19] [33] is available. An example of an ionic liquid, $[BMIM][PF_6]$ (BMIM = 1-butyl-3-methylimidazolium), was analysed by ES-MS by Dyson *et al*. to give a series of aggregate ions, $[BMIM]^+$, $[(BMIM)_2(PF_6)]^+$, $[(BMIM)_3(PF_6)_2]^+$, and $[(BMIM)_4(PF_6)_3]^+$ [33]. For salts of singly-charged ions (M^+X^-), the observed series of positive ions in the ES-MS not only depends on the cone voltage, but are also the solvating power of the different solvents. For many metal salts, aggregate ions are observed [19]. For salts of multiply-charged ions ($M^{2+}(X^-)_2$, $M^{3+}(X^-)_3$, etc.) and with higher charges, more complex patterns of ions are observed [34] [35] [19].

Compounds **1, 2, 3,** and **4** containing the –POOH group can lose a proton to generate the corresponding negative ion which was detected by ES-MS with higher aggregates also common [28]. For example, for $(hexyl)_2PO_2H$, higher aggregate ions such as $[2M-H]^-$ (*m/z* 468.2), $[3M-H]^-$ (*m/z* 702.9) and $[4M-H]^-$ (*m/z* 937.4) (where M is the neutral molecule) were observed in an ES-MS spectrum at cone voltage 50 V in methanol (Figure 2.3).

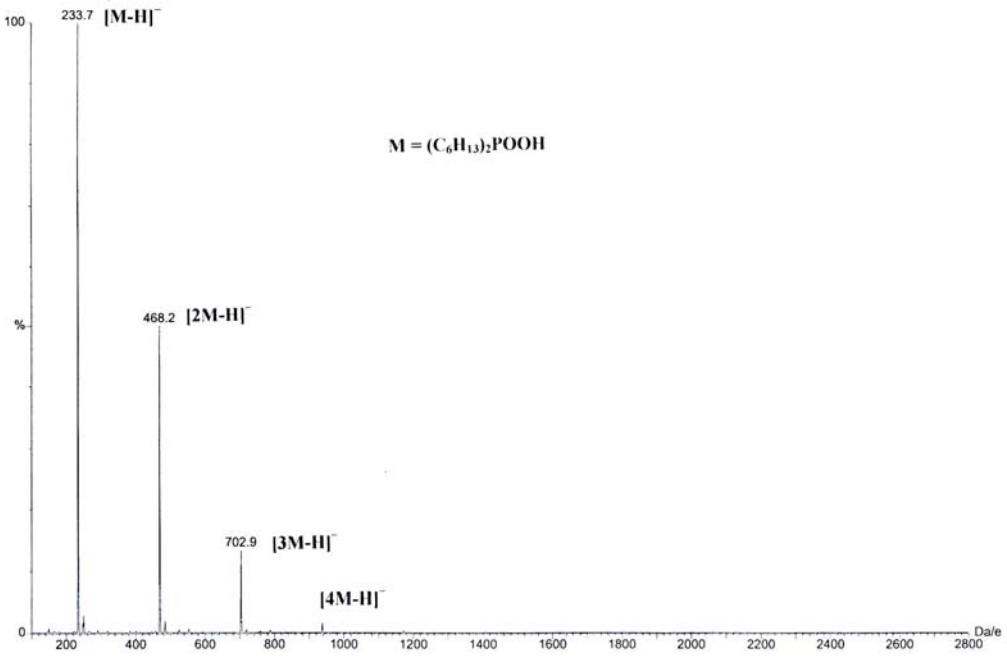

Figure 2.3: Negative-ion ES-MS spectrum of $(hexyl)_2PO_2H$ (M) (cone voltage: 50 V; solvent: methanol)

Compounds **5-19** gave easily detectable $[M]^+$ and $[X]^-$ ions using ES-MS. The general feature of all these ionic liquids is that their spectra gave the appearance of the intact positive and negative ions respectively, except $[M]^+$ of compound **17,** pyridinium bis(2,4,4-trimethylpentyl)phosphinate ($[pyH][(TMP)_2PO_2]$), which was synthesized by evaporating the excess pyridine under vacuum, as the pyridinium ions were easily decomposed, especially under vacuum. For the series of ionic liquids, $[Bu_4N][RR'PO_2]$, in the positive ion mode there is a base peak which is the principal ion $[Bu_4N]^+$ at *m/z* 242 with much weaker peaks being observed at *m/z* 186, 184, and 142 from Figure 2.4 (the cone voltage was 50 V), due to metastable decomposition of the parent ions producing

these fragment ions [30]. Higher aggregates, both in negative and positive ion, were detected, but the formed aggregates were different. For $[R_4N][RR'PO_2]$/ $[R_4P][RR'PO_2]$ ionic liquids, even $[M_6X_5]^-$ (M-cation; X-anion) aggregate ions, such as $[Bu_4N]_6^+[(hexyl)_2PO_2]_5^-$ can be detected (Figure 2.4). Surprisingly, for the series of $[R_3NH][RR'PO_2]$ ionic liquids such as $[Et_3NH][hexylPO_2H]$, no aggregation of ions were observed; but only $[M]^+$ and $[X]^-$. For $[Et_3NH][octylPO_2H]$, there are two peaks for $[HX_2]^-$ and $[X]^-$, and $[Et_3NH][(TMP)_2PO_2]$, gave a prominent peak corresponding to $[HX_2]^-$. This phenomenon probably indicates the proton from the cation is labile i.e. easy to deprotonate.

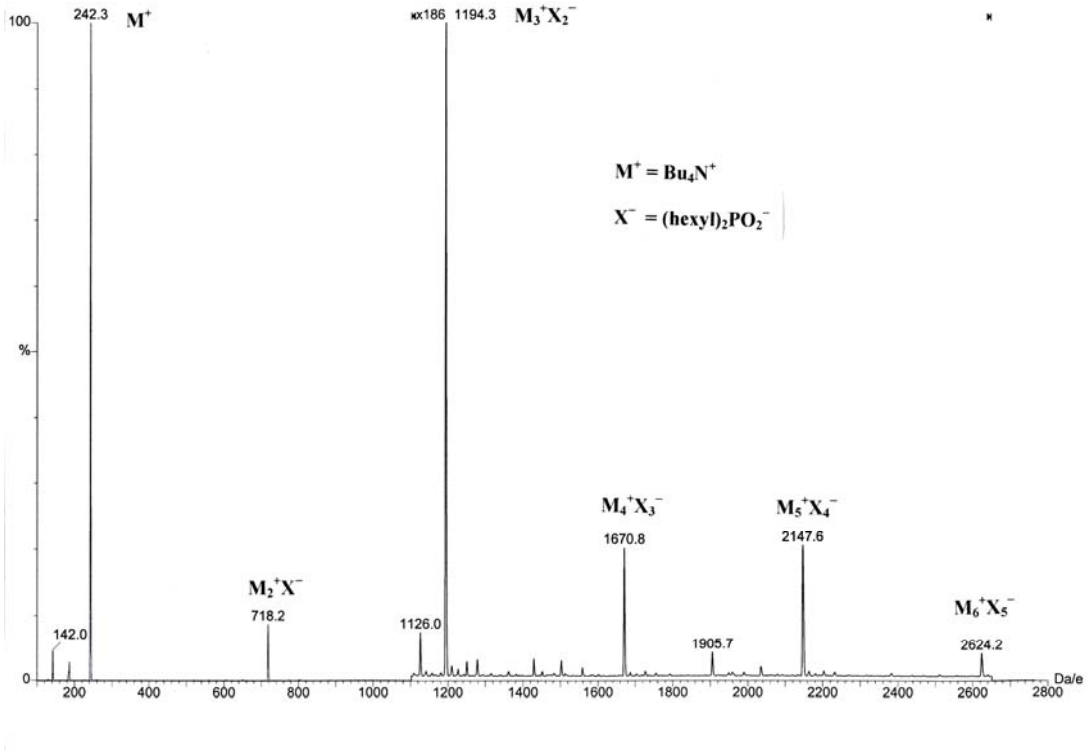

Figure 2.4: ES-MS spectrum of $[Bu_4N][(hexyl)_2PO_2]$ in positive ion mode. The region *m/z* 1100-2650 has been magnified 186 times to show weaker aggregate ions (cone voltage: 50 V; solvent: methanol)

In conclusion, the ions formed from the above ionic liquids can be assigned by their *m/z* values using ES-MS in negative ion and positive ion mode, except compound **17,** when *m/z* = 80, in which there is no peak in positive ion mode.

2.2.4 Physical properties of phosphinate ionic liquids

2.2.4.1 Melting point and glass transition temperature

Melting point is a key criterion when evaluating an ionic liquid. There are factors that provide a low melting point which is desired in an ionic liquid. In the published literature some structural aspects of low-melting salts such as low symmetry [36], weak intermolecular interactions (avoiding hydrogen bonding) [21] and good distribution of charge in the cation [37] were discussed. From Table 2.3 there is a decrease of melting point from cation Et_4N^+ to Bu_4N^+ to $BMIM^+$ for anion $camSO_3^-$ (see Figure 2.1), on the other hand, the anion influences the melting point too. For the well-known 1-ethyl-3-methylimidazolium (EMIM) ionic liquids, in most circumstances, an increasing anion size (with the same charge) causes a decrease in the melting point [20]. Table 2.3 shows for the cation Et_3NH^+ with anions $(octyl)_2PO_2^-$ and $(hexyl)_2PO_2^-$, the trend of melting point is similar to that of imidazolium salts.

Table 2.3: Influence of different cations and anions on the melting point of salts

Cation	Anion	Melting point (°C)	Reference
Et_4N^+	$camSO_3^-$	278-286	this work
Bu_4N^+	$camSO_3^-$	139	this work
Bu_4P^+	$camSO_3^-$	139-144	this work
$BMIM^+$	$camSO_3^-$	liquid	[38]
Et_3NH^+	$(octyl)_2PO_2^-$	54-58	this work
Et_3NH^+	$(hexyl)_2PO_2^-$	68-74	this work
Bu_4P^+	$(hexyl)_2PO_2^-$	15<M.P.<50	this work
$MMIM^+$	Cl^-	125	[20]
$EMIM^+$	Cl^-	87	[20]
$BMIM^+$	Cl^-	65	[20]
$EMIM^+$	NO_2^-	55	[39]
$EMIM^+$	NO_3^-	38	[39]
$EMIM^+$	BF_4^-	6[a]	[40]

a: Glass transition; $camSO_3$: D-camphor-10-sulfonate; MMIM: 1,3-dimethylimidazolium

Many ionic liquids are prone to supercooling [41], which makes it difficult to measure melting points. A lot of ionic liquids could form glasses, so the glass transition temperatures are usually reported instead of melting points [42]. Figure 2.5 shows the relationship of melting point and freezing point for ionic liquids reported in the literature. Three of the 1-methyl-3-ethylimidazolium ionic liquids showed substantial supercooling effects; the freezing points of **b** and **c** at around -40 °C were much lower than their melting point, however, phase transition of **a** was not observed in the studied temperature range [43].

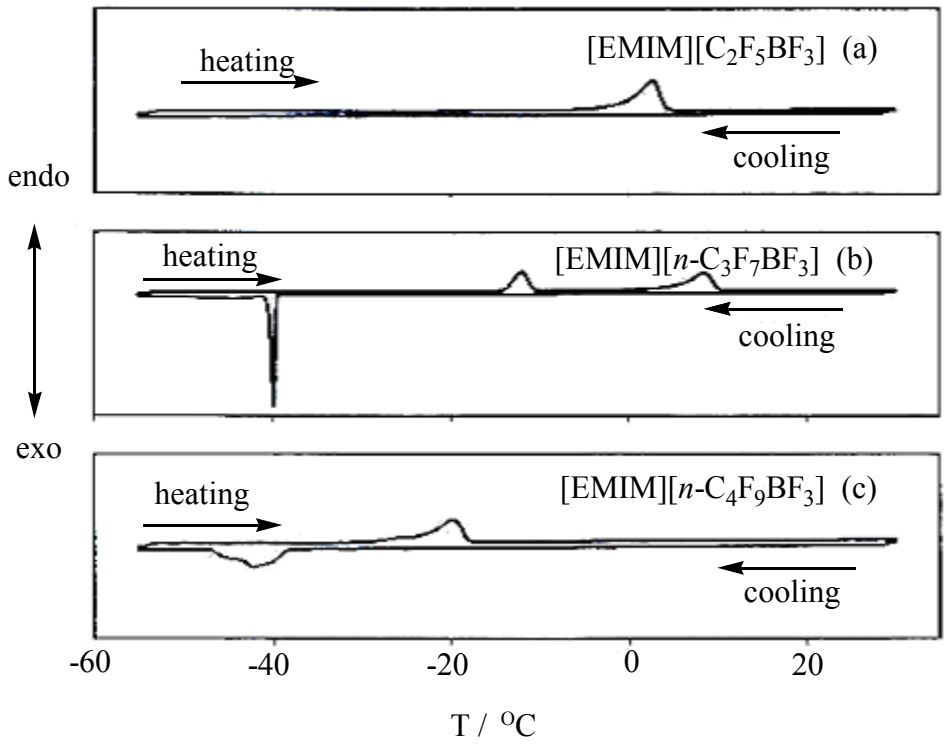

Figure 2.5: DSC curves of ionic liquids, [EMIM][$C_2F_5BF_3$], [EMIM][*n*-$C_3F_7BF_3$], [EMIM][*n*-$C_4F_9BF_3$] [43]

Compounds **5** to **19** remained in a liquid state at room temperature, except compound **13** which has a melting point around 15 °C. Compounds **8, 9, 10** and **11** containing [Bu_4P^+] have melting points lower than -10 °C; even after storing overnight at -10 °C in a freezer they are still fluid. Compounds containing [$Bu_4N]^+$, i.e. **5, 6, 12, 13,** formed a gel. Compounds **9**, **10** and **12** were tested by DSC to confirm the melting point or freezing point. Before starting the test,

samples were left for 30 minutes at -60 °C, and then heated to 30 °C and cooled down to -60 °C. On cooling, exothermic peaks were not observed. Compound **12** did not show a peak even down to -110 °C. On heating, compounds **9, 10,** and **12** also showed no endothermic peaks in the studied range.

2.2.4.2 Vapour pressure and thermal stability

There is a strong Coulombic force between cations and anions in ionic liquids. The force can be 100 kJ/mol (10 times that of water) between univalent opposite charges, and therefore, ionic liquids have an exceedingly low vapour pressure, even under high temperature or vacuum [44]. For example, in the synthesis of tetrabutylammonium/tetrabutylphosphonium ionic liquids under vacuum for several days at 75 °C, the yield was still over 99%.

Thermal stability is often reported as the thermal gravimetric analysis (TGA) onset temperature [42]. The thermal stability of ionic liquids depends on the strength of their heteroatom-carbon and their heteroatom-hydrogen bonds [20]. It is also dependent on the sample pan composition with certain ions [41]. Ionic liquids obtained by direct protonation of amines have restricted thermal stability, because the trialkylammonium ions are relatively easily decomposed at a temperature below 80 °C in vacuum [20]. Similarly, for the pyridinium ionic liquids, the pyridine can be lost under vacuum due to the pyridinium ionic liquid dissociating as follows: $pyH^+ \rightleftharpoons py + H^+$. Pyridine is weak base and $(TMP)_2PO_2H$ a weak acid, so the resulting salt is unstable towards dissociation.

Table 2.4 displays the onset temperature of decomposition (T_{onset}) for all the ionic liquids investigated as well as some literature data. The thermal stability of the tetrabutylammonium, triethylammonium and pyridinium ionic liquids is generally lower than those tetrabutylphosphonium ionic liquids. At high temperatures, both phosphonium and ammonium salts can decompose by internal displacement (Equation 2.6). Ammonium salts start to decompose at 100 °C and phosphonium salts start decomposing at 150 °C [45]. Generally phosphonium salts are more thermally stable than ammonium salts [18] [14].

$$[R_4E]^+X^- \quad \rightarrow \quad R_3E + R\text{-}X \ (E = N, P)$$

Equation 2.6: Decomposition of phosphonium/ammonium salts at high temperatures [45]

The tetrabutylphosphonium ionic liquids appear to be more thermally stable than their analogous tetrabutylammonium ionic liquids by at least 50 °C in this work. For the hexylphosphinate/octylphosphinate ionic liquids, the thermal stability decreases through the cation series of $[Bu_4P]^+$, $[pyH]^+$, and $[Bu_4N]^+$. Generally, it could be said that the P-C bond of these compounds is more stable than the analogue of N-C bond compounds, and the imidazolium cations tend to be thermally more stable than the tetraalkylammonium cations from Table 2.4 entry 17 and 18.

The thermal stability of ionic liquids is also strongly related to the nature of the anion. For example, $[EMIM][BF_4]$ and $[EMIM][(CF_3SO_2)_2N]$ decomposition temperatures are 300 °C [46] and 455 °C [21] respectively.

For ionic liquids containing $[Et_3NH]^+$ and $[pyH]^+$ ions, the thermal stability decreases through $[(TMP)_2PO_2]^-$, $[octylPO_2H]^-$, and $[hexylPO_2]^-$, and for $[Bu_4P]^+$ ionic liquids, the trend of thermal stability decreases through $[(octyl)_2PO_2]^-$, $[(TMP)_2PO_2]^-$, $[hexylPO_2H]^-$ and $[octylPO_2H]^-$. For $[Bu_4N]^+$ ionic liquids (see Table 2.4), the trend of thermal stability decreases in the order by $[(CF_3SO_2)_2N]^-$, $[(hexyl)_2PO_2]^-$, $[octylPO_2H]^-$, $[hexylPO_2H]^-$ and $[(octyl)_2PO_2]^-$.

Table 2.4: Decomposition temperature of ionic liquids

Entry	Product	T_{onset} (°C)	Reference
1	$[Bu_4N][(octyl)_2PO_2]$ **12**	178	this work
2	$[Et_3NH][hexylPO_2H]$ **16**	183	this work
3	$[Bu_4N][hexylPO_2H]$ **7**	185	this work
4	$[Bu_4N][octylPO_2H]$ **6**	187	this work
5	$[pyH][hexylPO_2H]$ **19**	214	this work
6	$[Et_3NH][octylPO_2H]$ **15**	219	this work
7	$[Bu_4N][(TMP)_2PO_2]$ **5**	230	this work
8	$[pyH][octylPO_2H]$ **18**	232	this work
9	$[Bu_4N][(hexyl)_2PO_2]$ **13**	243	this work
10	$[Bu_4P][octylPO_2H]$ **9**	249	this work
11	$[Et_3NH][(TMP)_2PO_2]$ **14**	253	this work
12	$[pyH][(TMP)_2PO_2]$ **17**	258*	this work
13	$[Bu_4P][hexylPO_2H]$ **10**	275	this work
14	$[Bu_4P][(TMP)_2PO_2]$ **8**	280	this work
15	$[Bu_4P][(octyl)_2PO_2]$ **11**	358	this work
16	$[Bu_4N][(CF_3SO_2)_2N]$	403	[41]
17	$[Et_4N][(CF_3SO_2)_2N]$	439	[41]
18	$[EMIM][(CF_3SO_2)_2N]$	455	[41]
19	$[EMIM][BF_4]$	300	[46]

*No pyridine H resonances were observed in the ^1H NMR spectrum; presumably due to loss of the pyridine under vacuum
$[EMIM][(CF_3SO_2)_2N]$:1-ethyl-3-methylimidazolium bis(trifluoromethylsulfonyl)imide

Clearly, the $[Bu_4P][(octyl)_2PO_2]$ is the most stable ionic liquid in this work and Figure 2.6 shows its thermogravimetric analysis (TGA) profile. The TGA curve demonstrates that when $[Bu_4P][(octyl)_2PO_2]$ is dried, the weight loss is approximately zero at around 100 °C. It is also very stable as decomposition does not occur until over 300 °C.

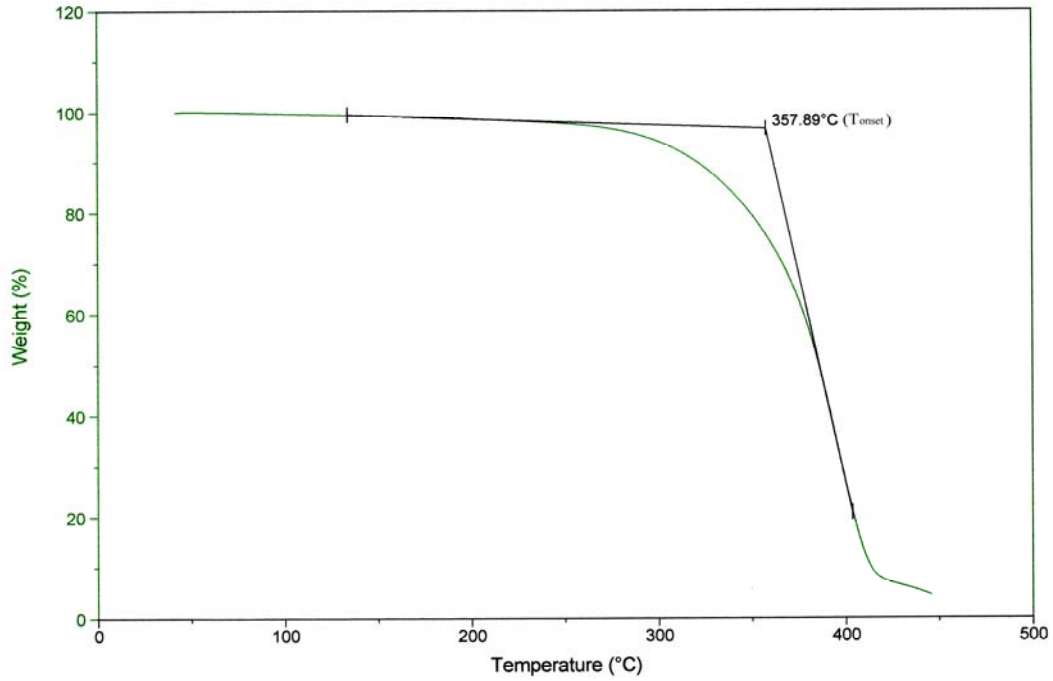

Figure 2.6: Themogravimetric analysis (TGA) of $[Bu_4P][(octyl)_2PO_2]$ ionic liquid

2.2.4.3 Viscosity

It has been shown that the viscosity of imidazolium ionic liquids is influenced by their ability to hydrogen bond and by the strength of their van der Waals interactions, which is strongly dependent on the type of anion present [21].

For ionic liquids of 1-alkyl-3-methylimidazolium bis(trifluoromethylsulfonyl)imide ([Cn-MIM][$(CF_3SO_2)_2N$]) and [Cn-MIM][PF_6], there is a increase in viscosity when n, the number of carbon atoms in the alkyl group, is increased, and there is a marked decrease in viscosity as the temperature is increased. This is shown in Figure 2.7 and 2.8 [47].

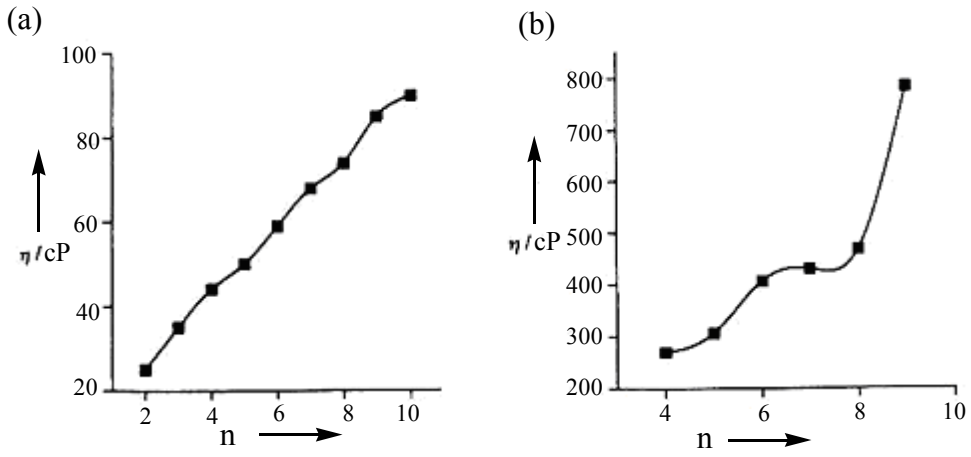

Figure 2.7: Influence of the 1-alkyl group on the viscosity of the $[C_n\text{-MIM}][(CF_3SO_2)_2N]$ and $[C_n\text{-MIM}][PF_6]$ [47]

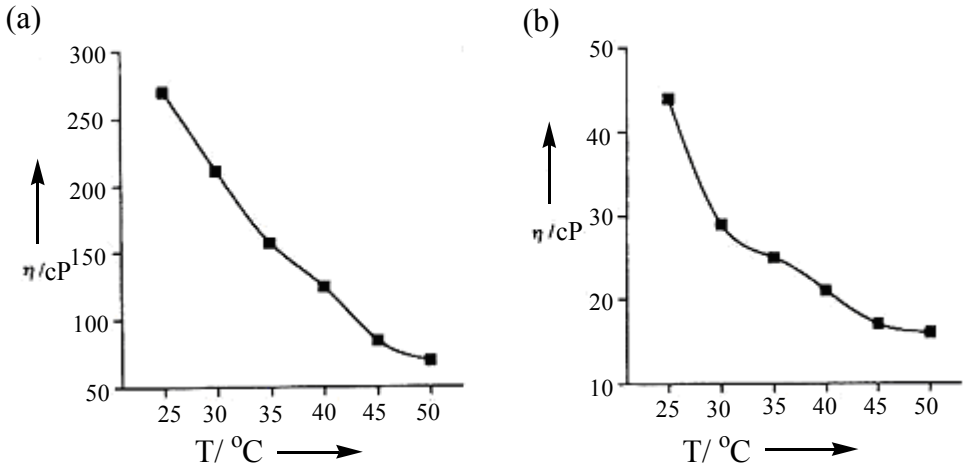

Figure 2.8: Influence of temperature on the viscosity of the $[C_n\text{-MIM}][(CF_3SO_2)_2N]$ and $[C_n\text{-MIM}][PF_6]$ [47]

The viscosity of the ionic liquids varies considerably, and while it is not easy to say any strict conclusions, it would appear the compounds from Table 2.5, except compounds **5** and **6,** that there is a steady increase in viscosity with the lengthening of the alkyl chain connecting the phosphorus, presumably as a result of the increased van der Waals interactions. Table 2.5 also shows the viscosities of ionic liquids containing the cations $[Et_3NH]^+$ and $[pyH]^+$ which have similar viscosities to dialkylimidazolium ionic liquids but have lower viscosities than ionic liquids containing cations $[Bu_4P]^+$ and $[Bu_4N]^+$.

Table 2.5: Viscosity comparison of some ionic liquids and common solvents

solvent	viscosity (Pa s, 25 °C)	viscosity (Pa s, 60 °C)	reference
water	0.001		[48]
benzene	0.000604		[48]
glycerol	0.934		[48]
[BMIM][BF_4]	0.219		[49]
[Bupy][$(CF_3SO_2)_2N$]	0.057		[49]
[pyH][hexylPO_2H] **19**	0.058	0.0188	this work
[Et_3NH][hexylPO_2H] **16**	0.0781	0.0231	this work
[Et_3NH][octylPO_2H] **15**	0.104	0.0276	this work
[pyH][octylPO_2H] **18**	0.113	0.0284	this work
[pyH][$(TMP)_2PO_2$] **17**	0.144	0.0244	this work
[Et_3NH][$(TMP)_2PO_2$] **14**	0.298	0.0418	this work
[Bu_4P][hexylPO_2H] **10**	0.694	0.0926	this work
[Bu_4N][$(TMP)_2PO_2$] **5**	1.52	0.225	this work
[Bu_4N][octylPO_2H] **6**	1.68	0.139	this work
[Bu_4N][hexylPO_2H] **7**	2.42	0.179	this work
[Bu_4N][$(hexyl)_2PO_2$] **13**	4.23	0.227	this work
[Bu_4P][$(TMP)_2PO_2$] **8**	6.1	0.225	this work

BMIM---1-*n*-butyl-3-methylimidazolium
EMIM---1-*n*-ethyl-3-methyllimidazolium
Bupy--- N-butylpyridinium
[$(CF_3SO_2)_2N$]---bis((trifluoromethyl)sulfonyl)imide

On increasing the temperature, the ionic liquids are more mobile, as expected. The viscosity of the ionic liquids is also very sensitive to dissolved solutes. It can be reduced by adding reactants or catalysts [14]. For example, addition of traces of water to [Bu_4P][$(octyl)_2PO_2$] decreases the viscosity as shown in Table 2.6.

Table 2.6: Viscosity comparison of $[Bu_4P][(octyl)_2PO_2]$ containing added water, at 25 °C and 60 °C

% of water added to IL	viscosity (Pa s, 25 °C)	viscosity (Pa s, 60 °C)
0	0.582	0.0756
1	0.559	0.0712
3	0.464	0.0576
5	0.397	0.0512

2.2.4.4 Solvent polarities

Solvent polarity has a great influence on the results of chemical reactions and on the characteristics observed with spectroscopic techniques. However, solvent polarity cannot simply be defined using properties such as, dielectric constant, refractive index and dipole moment, because particular solvent-solute interactions are not taken into account. A wide variety of solvent polarity scales based on empirical parameters have been developed, such as Z-Values [50] and solvatochromic dyes [51] [52] [53]. Solvatochromic dyes change colour according to the polarity of the liquid in which they are dissolved. A bathochromic red shift with increasing solvent polarity is called positive solvatochromism and oppositely a hypsochromic blue shift with increasing solvent polarity is called negative solvatochromism [52] (for more details see Chapter 1).

In order to understand more about the nature of the ionic liquids reported in this thesis, and how they compare with conventional solvents, a Nile Red dye (Figure 2.9) was used to study their polarity. When Nile Red is dissolved in an increasingly polar solvent, the wavelength of its visible absorption maximum (λ_{max}) moves to longer wavelengths (lower energies). Nile Red is positively solvatochromic and displays one of the largest bathochromic shifts known. For example, there is a change in λ_{max} of 110 nm from water to pentane [53].

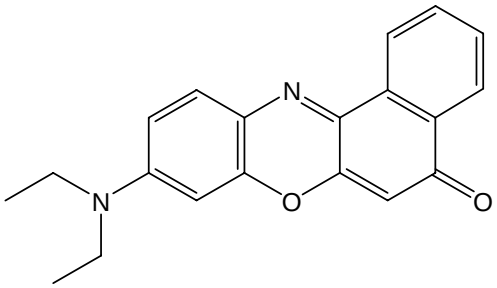

Figure 2.9: Molecular structure of the Nile Red dye

The wavelengths of maximum absorption (λ_{max}) and the molar transition energies (E_{NR}) for Nile Red dissolved in the ionic liquids and some common solvents are summarized in Table 2.7. Absorption spectra of Nile Red in several conventional solvents were obtained and most found a good agreement with published data [53]. All absorption spectra were recorded from 200 nm to 800 nm, and gave a single maximum in the visible region.

For $[Bu_4N]^+$ and $[Bu_4P]^+$-containing ionic liquids, the polarity decreases through the anion series of $[hexylPO_2H]^-$, $[octylPO_2H]^-$, $[(octyl)_2PO_2]^-$ and $[(TMP)_2PO_2]^-$. Similarly, the same trend was observed for $[pyH]^+$ and $[Et_3NH]^+$ salts of the anion series $[hexylPO_2H]^-$, $[octylPO_2H]^-$, and $[(TMP)_2PO_2]^-$. This decrease in polarity correlates with lengthening and branching the alkyl chain.

A decrease in the polarity of $[RR'PO_2]^-$-containing ionic liquids was observed from $[Bu_4N]^+$, $[Bu_4P]^+$, $[pyH]^+$ and $[Et_3NH]^+$. This decrease due to increasing cation size from $[Bu_4N]^+$ to $[Bu_4P]^+$. $[Et_3NH]^+$ should be more polar than $[Bu_4N]^+$, but the opposite result was observed, probably due to formation of the H-bonding between $[Et_3NH]^+$ and $[RR'PO_2]^-$, which reduces the polarity.

Table 2.7: Wavelengths of maximum absorption (λ_{max}) and transition energies (E_{NR}) for Nile Red dissolved in ionic liquids and some common organic solvents

Ionic liquid	λ_{max} (nm)	E_{NR} (kcal/mol)
acetic acid (glacial, 99.8%)	561.0	50.96
$[Bu_4N][hexylPO_2H]$ **7**	553.0	51.70
methanol	552.6	51.83
$[Bu_4N][octylPO_2H]$ **6**	551.0	51.89
$[Bu_4P][hexylPO_2H]$ **10**	550.3	51.96
$[Bu_4P][octylPO_2H]$ **9**	549.5	52.03
1-butanol (95 %)*	548.0	52.17
$[Bu_4N][(octyl)_2PO_2]$ **12**	546.0	52.37
pyridine (distilled)	545.0	52.46
$[Bu_4P][(octyl)_2PO_2]$ **11**	544.5	52.51
$[Bu_4N][(TMP)_2PO_2]$ **5**	543.0	52.65
$[pyH][hexylPO_2H]$ **19**	542.5	52.70
$[Et_3NH][hexylPO_2H]$ **16**	541.5	52.80
$[pyH][octylPO_2H]$ **18**	540.5	52.90
$[Bu_4P][(TMP)_2PO_2]$ **8**	539.8	52.97
$[Et_3NH][octylPO_2H]$ **15**	538.5	53.09
acetone	533.0	53.64
$[pyH][(TMP)_2PO_2]$ **17**	532.0	53.74
$[Et_3NH][(TMP)_2PO_2]$ **14**	530.0	53.95
benzene (multisolvent 99.8%)*	524.3	54.53

Transition energy, E, of the solvatochromic band calculated by $E = 28591.44/\lambda_{max}$ (nm) in kcal/mol [53]; * The data agree with [53].

2.2.4.5 Hygroscopicity

Most ammonium and imidazolium ionic liquids are hygroscopic; hydration will often occur if used in open vessels [23]. From Figure 2.10 it was confirmed that phosphonium phosphinate ionic liquids are also hygroscopic. An experiment to investigate the hygroscopicity of an ionic liquid was carried out by exposing a weighed sample of the ionic liquid to the atmosphere, and monitoring the weight increase. Figure 2.10 shows that the weight of ionic liquid increased dramatically by 10.7% in the first 139 minutes, and then stabilised. The total increase of weight by water was 13.3%.

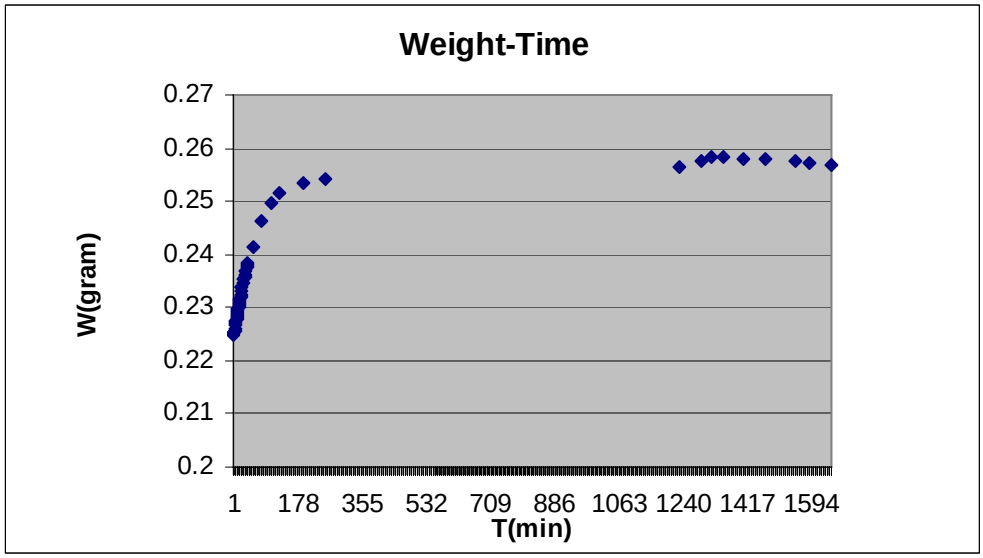

Figure 2.10: Weight change in an open vessel of compound **8**

2.2.4.6 Refractive index and miscibility with water

Table 2.8 shows the values of refractive index of ionic liquids, and it shows that: for anions $[(TMP)_2PO_2]^-$, $[octylPO_2]^-$, $[hexylPO_2]^-$ and $[(octyl)_2PO_2]^-$, the refractive indices of the salts formed, from the largest to the smallest is as

follows: tetrabutylphosphonium salts, ($[Bu_4P]^+$) > tetrabutylammonium salts ($[Bu_4N]^+$) > pyridinium salts ($[pyH]^+$), triethylammonium salts ($[Et_3NH]^+$).

Similarly, for the cation $[Bu_4P]^+$or $[Bu_4N]^+$ the corresponding salts formed with the anions (shown below), have refractive indices which can be arranged in the following order:

$[octylPO_2]^-$ or $[hexylPO_2]^-$ > $[(TMP)_2PO_2]^-$ > $[(octyl)_2PO_2]^-$.

A white cloudy emulsion was formed when an ionic liquid, when mixed with water, was immiscible. The exception was compound **17,** which formed two phases. For compound **17**, as mentioned before, the formed $[pyH]^+$ easily dissociates. The equilibrium moves in the dissociation direction when under vacuum, so compound **17** could be just $(TMP)_2PO_2H$, as no pyridine H resonances were observed in the ^1H NMR spectrum.

Table 2.8: Refractive index and miscibility with water of ionic liquids

Ionic liquid	Refractive index (27 °C)	Miscibility with water
$[Bu_4P][hexylPO_2H]$ **10**	1.4758	immiscible
$[Bu_4P][octylPO_2H]$ **9**	1.4747	immiscible
$[Bu_4P][(TMP)_2PO_2]$ **8**	1.4710	miscible
$[Bu_4P](octyl)_2PO_2]$ **11**	1.4701	miscible
$[Bu_4N][octylPO_2H]$ **6**	1.4696	immiscible
$[Bu_4N][hexylPO_2H]$ **7**	1.4695	immiscible
$[Bu_4N][(TMP)_2PO_2]$ **5**	1.4658	immiscible
$[Bu_4N][(octyl)_2PO_2]$ **12**	1.4657	immiscible
$[pyH][octylPO_2H]$ **18**	1.4586	immiscible
$[pyH][(TMP)_2PO_2]$ **17**	1.4557	immiscible
$[Et_3NH][(TMP)_2PO_2]$ **14**	1.4554	immiscible
$[Et_3NH][octylPO_2H]$ **15**	1.4535	immiscible
$[pyH][hexylPO_2H]$ **19**	1.4528	immiscible
$[Et_3NH][hexylPO_2H]$ **16**	1.4524	miscible

2.2.5 Conclusions

The prepared starting materials di-*n*-octylphosphinic acid and di-*n*-hexylphosphinic acid are very pure as seen by ^{31}P NMR spectra, and mono-*n*-octylphosphinic acid and mono-*n*-hexylphosphinic acid contain impurities which could be di-*n*-alkylphosphinic acid and *iso*-alkylphosphinic acid.

A number of phosphinate-based ionic liquids have been synthesized by directly neutralizing organophosphorus acids with bases, and some of their properties were studied in this work. Generally, the ionic liquids synthesised are colourless, but impure starting materials form ionic liquids with a yellow colour. The formed tetraalkylphosphonium/tetraalkylammonium phosphinate ionic liquids were viscous, hygroscopic liquids, but were more thermally stable than trialkylammonium and pyridinium analogues. The trialkylammonium/pyridinium ionic liquids have lower viscosity and are easier to synthesise than tetraalkylphosphonium/tetraalkylammonium ionic liquids. The refractive index decreases in this order: tetraalkylphosphonium, tetraalkylammonium, trialkylammonium and pyridinium. Solvatochromic dyes measured the solvent polarity of these phosphinate ionic liquid. A decrease in the polarity of $[RR'PO_2]^-$-containing ionic liquids was observed from $[Bu_4N]^+$, $[Bu_4P]^+$, $[pyH]^+$ to $[Et_3NH]$. For $[Bu_4N]^+$, $[Bu_4P]^+$, $[pyH]^+$ and $[Et_3NH]^+$ ionic liquids, the polarity decreases through the anion series of $[hexylPO_2H]^-$, $[octylPO_2H]^-$, $[(octyl)_2PO_2]^-$ and $[(TMP)_2PO_2]^-$.

2.3 Experimental

2.3.1 Materials

Tetra-*n*-butylammonium hydroxide solution (40.30% in water), and tetra-*n*-butylphosphonium hydroxide solution (40.42% in water) were purchased from Fluka and Aldrich respectively, and were standardised by titration with 0.0975 mol/L hydrochloric acid using phenolphthalein as an indicator. They were used without further purification. Bis(2,4,4-trimethylpentyl)phosphinic acid (about 85%) (CYANEX 272) was generously donated by CYTEC Industries and used without further purification. Dibenzoyl peroxide (70%) and 1-hexene (97%) were purchased from Aldrich. 1-Octene (98%) and aqueous hypophosphorous acid (50% w/w) were obtained by Riedel-de Haen and Rhodia Consumer Specialties Limited respectively. Triethylamine (99.5%) from Ajax Chemicals and pyridine was a laboratory grade reagent, were distilled before use. Nile Red was purchased from Sigma-Aldrich Inc, and used without purification.

2.3.2 Instrumentation

^{31}P and ^{1}H NMR spectra were recorded on a Bruker Avance 300 MHz spectrometer. Solvents were assigned the following chemical shift values with respect to $SiMe_4$: $CDCl_3$, 7.26 (^{1}H), 77.06 (^{13}C); d^6-DMSO, 2.6 (^{1}H), 39.5 (^{13}C); D_2O, 3.5 (MeOH, ^{1}H), 49.3 (MeOH, ^{13}H). ^{31}P chemical shift assignment was with respect to a simple external reference of 85% phosphoric acid. The spectrometer was operated at 75.47 MHz for ^{13}C, 300.13 MHz for ^{1}H and 121.51 MHz for ^{31}P.

Positive- and negative-ion electrospray mass spectra were recorded with a VG Platform II electrospray mass spectrometer on samples dissolved in methanol. The cone voltage was 50 V.

Thermogravimetric analysis (TGA) was performed on a SDT 2960 Simultaneous DTA-TGA thermal analysis system. An average sample weight of 4 mg was placed in an aluminium pan and heated at 10 °C min^{-1} from 25 °C to 450 ºC under an argon atmosphere. The onset of decomposition was defined as the decomposition temperature (T_{onset}).

Melting points for liquids at ambient temperature and freezing point were measured by a DSC 2920 Differential Scanning Calorimeter. An average sample weight of 5 mg was sealed in an aluminium pan and quenched, initially to -60 °C (-110 °C in one case) for 30 minutes and then heated and cooled at 10 °C min^{-1}, between -60 °C (-110 °C in one case) and 30 °C under a flow of argon. Melting points for compounds which are solids at room temperature were measured by a Reichert melting-point microscope.

The C, H, and N analyses were performed by the Microanalytical Laboratory of the University of Otago. Viscosity measurements were carried out on a Paar Physica UDS 200 rheometer at the Chemistry Department of the University of Auckland, New Zealand.

The UV-Visible absorption spectra of the solvatochromic Nile Red dye were recorded on a Cary 100 Scan UV Visible spectrophotometer. Solutions were measured using quartz cuvettes of 0.5 cm path length and the absorption spectra were determined over the spectral range from 200 to 800 nm. Solutions of the dye, dissolved in the ionic liquids, were examined at different concentrations in order to find the optimum concentration range for absorption measurements. A Nile Red concentration was chosen such that absorbances would fall in the range 0.4-1.5. This was achieved by preparing a concentrated solution of Nile Red in ionic liquid by stirring for several hours, of which 2-10 drops were transferred to a vial with about 2 g of ionic liquid.

2.3.3 Syntheses

2.3.3.1 Synthesis of di-*n*-octylphosphinic acid 1

To a solution of 1-octene (20.4 g, 98%, 0.179 mol) and hypophosphorous acid (10 mL, 50.4%, 92.1 mmol) in butan-1-ol (45 mL) was added dibenzoyl peroxide (4.95 g, 70%, 14.3 mmol). The reaction mixture was stirred at 80-85 ºC for 48 hours. Water (100 mL) was added, and the butan-1-ol was removed by rotary evaporation. After cooling, the reaction mixture was filtered using a Buchner funnel. The crude product was obtained as a slightly yellow oily semisolid and was recrystallised from hexane to give white crystals (12.1 g, 41.7 mmol 47%), M.P. 82 ºC. ^{31}P - {^{1}H} NMR ($CDCl_3$): δ 60.3; ^{31}P- NMR ($CDCl_3$) (proton coupled): δ 60.3. ES-MS: negative ion *m/z*, 288.9 $[M]^-$.

2.3.3.2 Synthesis of di-*n*-hexylphosphinic acid 2

A similar procedure for **1** was used, using 1-hexene (50.1 g, 97%, 0.578 mol) instead of octene, hypophosphorous acid (32 mL, 50.4%, 0.295 mol) and dibenzoyl peroxide (15.0 g, 70%, 43.3 mmol) in butan-1-ol (100 mL). After removing butan-1-ol, the mixture was extracted with diethyl ether (150 mL) and the solvent was removed by rotary evaporation. After cooling, the reaction mixture was filtered using a Buchner funnel. The crude product was obtained as a slightly yellow oily semisolid and was recrystallised from hexane to give white crystals (29.1 g, 0.124 mol, 43%), M.P. 76 ºC. ^{31}P - {^{1}H} NMR ($CDCl_3$): δ 60.4; ^{31}P- NMR ($CDCl_3$) (proton coupled): δ 60.4. ES-MS: negative ion *m/z*, 233.7 $[M]^-$.

2.3.3.3 Synthesis of *n*-octylphosphinic acid 3

To a stirred, refluxing solution of 1-octene (37.7 g, 0.329 mol) and hypophosphorous acid (106 mL, 50.4%, 0.987 mol) in isopropanol (100 mL) was added, in six portions over 27 hours, benzoyl peroxide (0.47 g, 1.35 mmol). After

cooling, water (150 mL) was added, and the isopropanol was removed by rotary evaporation. The mixture was transferred to a separating funnel, extracted with dichloromethane (100 mL followed by 2 × 30 mL) and the dichloromethane extracts combined. The dichloromethane solution was washed with water (3 × 100 mL). The solvent was removed from the solution, firstly by rotary evaporation, and then on the vacuum line. This gave the product as a colourless oily liquid (28.8 g, 0.162 mol, 51% yield), ^{31}P- {^{1}H} NMR ($CDCl_3$): δ 37.1; ^{1}J(PH): 539.6 Hz; ES-MS: negative ion *m/z*, 177.3 $[M]^-$.

2.3.3.4 Synthesis of *n*-hexylphosphinic acid 4

The same procedure for **3** was followed, using 1-hexene (44.3 g, 97%, 0.512 mol) instead of octene, with hypophosphorous acid (165 mL, 50.4%, 1.54 mol). The product was obtained as a colourless oily liquid (46.6 g, 0.311 mol, 61% yield). ^{31}P - {^{1}H} NMR ($CDCl_3$): δ 36.4; ^{1}J(PH): 539.5 Hz; ES-MS: negative ion *m/z*, 149.2 $[M]^-$.

2.3.3.5 Synthesis of $[Bu_4N][(TMP)_2PO_2]$ 5

Bis(2,4,4-trimethylpentyl)phosphinic acid (0.39 g, 1.33 mmol) in methanol (1 mL) was titrated with an aqueous solution of tetrabutylammonium hydroxide, using phenolphthalein as indicator, until the endpoint (a pale pink colour), and the volatiles were then evaporated under vacuum. Compound **5** was obtained as a brown, viscous liquid (0.65 g). ES-MS: positive ion *m/z*, 242.0 $[M]^+$; negative ion *m/z*, 288.8 $[M]^-$.

2.3.3.6 Synthesis of $[Bu_4N][octyl\,PO_2H]$ 6

The same procedure for **5** was followed, using compound **3** (0.40 g, 2.25 mmol) instead of bis(2,4,4-trimethylpentyl)phosphinic acid. The product was obtained as a brown liquid (0.89 g). ES-MS: positive ion *m/z*, 242.2 $[M]^+$; negative ion *m/z*, 176.8 $[M]^-$.

2.3.3.7 Synthesis of [Bu_4N][hexyl PO_2H] 7

The same procedure for **5** was followed, using compound **4** (0.40 g, 2.68 mmol) instead of bis(2,4,4-trimethylpentyl)phosphinic acid. The product was obtained as a brown liquid (0.99 g). ES-MS: positive ion *m/z*, 241.6 $[M]^+$; negative ion *m/z*, 148.1 $[M]^-$.

2.3.3.8 Synthesis of [Bu_4P][$(TMP)_2PO_2$] 8

The same procedure for **5** was followed, using tetrabutylphosphonium hydroxide instead of tetrabutylammonium hydroxide and bis(2,4,4-trimethylpentyl)phosphinic acid (0.34 g, 1.17 mmol) was used. The product was obtained as a purple liquid (0.61 g). ES-MS: positive ion *m/z*, 259.3 $[M]^+$; negative ion *m/z*, 289.1 $[M]^-$.

2.3.3.9 Synthesis of [Bu_4P][octylPO_2H] 9

The same procedure for **8** was followed, using compound **3** (0.31 g, 1.72 mmol) instead of $(TMP)_2PO_2H$. **9** was obtained as a purple liquid (0.73 g). ES-MS: positive ion *m/z*, 259.8 $[M]^+$; negative ion *m/z*, 177.5 $[M]^-$.

2.3.3.10 Synthesis of [Bu_4P][hexylPO_2H] 10

The same procedure for **8** was followed, using compound **4** (0.44 g, 2.94 mmol) instead of $(TMP)_2PO_2H$. **10** was obtained as a purple liquid (1.15 g). ES-MS: positive ion *m/z*, 259.3 $[M]^+$; negative ion *m/z*, 148.7 $[M]^-$.

2.3.3.11 Synthesis of [Bu_4P][$(octyl)_2PO_2$] 11

A mixture of compound **1** (2.64 g, 9.12 mmol) and tetrabutylphosphonium hydroxide (6.24 g, 40.42% 9.12 mmol) was stirred at room temperature for 30 minutes. Water was removed by rotary evaporation, and then on the vacuum line.

The product was obtained as a colourless liquid (4.70 g, 8.57 mmol, 98%). ES-MS: positive ion *m/z*, 259.8 $[M]^+$; negative ion *m/z*, 289.9 $[M]^-$. The respective percentage contents of C, and H presented as found, followed by theoretical values in parentheses, are 66.75 (70.03) and 13.03 (12.86).

2.3.3.12 Synthesis of $[Bu_4N][(octyl)_2PO_2]$ 12

The same procedure for **11** was followed, using tetrabutylammonium hydroxide (2.31 g, 40.30%, 3.60 mmol) instead of tetrabutylphosphonium hydroxide and compound **3** (1.04 g, 3.60 mmol) was used. The product was obtained as a colourless viscous liquid (1.78 g, 3.34 mmol, 93%). ES-MS: positive ion *m/z*, 242.3 $[M]^+$; negative ion *m/z*, 289.1 $[M]^-$.

2.3.3.13 Synthesis of $[Bu_4N][(hexyl)_2PO_2]$ 13

The same procedure for **12** was followed, using compound **2** (2.49 g, 10.6 mmol) instead of compound **1** and tetrabutylammonium hydroxide (6.86 g, 40.30%, 10.6 mmol) was used. The product was obtained as a colourless, viscous liquid (4.91 g, 10.3 mmol, 97%). On storing, the colour became yellow. ES-MS: positive ion *m/z*, 242.3 $[M]^+$; negative ion *m/z*, 233.1 $[M]^-$. The respective percentage contents of C, H, and N presented as found, followed by theoretical values in parentheses, are 65.20 (70.68), 13.15 (13.14) and 2.89 (2.94).

2.3.3.14 Synthesis of $[Et_3NH][(TMP)_2PO_2]$ 14

An excess amount of triethylamine (5 mL, 68.0 mmol) was added to liquid bis(2,4,4-trimethylpentyl)phosphinic acid (4.01 g, 13.8 mmol) and stirred. The excess triethylamine was removed by rotary evaporation, and then under vacuum. The product was obtained as a colourless liquid (4.09 g, 10.4 mmol, 76%). ES-MS: positive ion *m/z*, 102.1 $[M]^+$; negative ion *m/z*, 289.3 $[M]^-$.

2.3.3.15 Synthesis of $[Et_3NH][octylPO_2H]$ 15

The same procedure for **14** was followed, using octylphosphinic acid (3.42 g, 19.2 mmol) instead of bis(2,4,4-trimethylpentyl)phosphinic acid. The product was obtained as a colourless liquid (3.80 g, 13.6 mmol, 71%). ES-MS: positive ion *m/z*, 102.1 $[M]^+$; negative ion *m/z*, 177.2 $[M]^-$.

2.3.3.16 Synthesis of $[Et_3NH][hexylPO_2H]$ 16

The same procedure for **14** was followed, using hexylphosphinic acid (4.07 g, 27.2 mmol) instead of bis(2,4,4-trimethylpentyl)phosphinic acid. The product was obtained as a colourless liquid (4.74 g, 18.9 mmol, 69%). ES-MS: positive ion *m/z*, 102.1 $[M]^+$; negative ion *m/z*, 149.1 $[M]^-$.

2.3.3.17 Synthesis of $[pyH][(TMP)_2PO_2]$ 17

To a solution of bis(2,4,4-trimethylpentyl)phosphinic acid (4.28 g, 14.8 mmol) in methanol (5 mL), an excess of pyridine (6 mL, 72.2 mmol) was added and stirred. The volatiles were removed by rotary evaporation, and then under vacuum (54 hr, 1 mmHg). The product was obtained as a colourless liquid (4.24 g, 11.5 mmol, 78%). ES-MS: positive ion *m/z*, pyH^+ not observed (expected *m/z* 80.1); negative ion *m/z*, 289.5 $[M]^-$.

2.3.3.18 Synthesis of $[pyH][octylPO_2H]$ 18

The same procedure for **17** was followed, using compound **3** (3.54 g, 12.2 mmol) instead of bis(2,4,4-trimethylpentyl)phosphinic acid. The product was obtained as a slightly yellow liquid (3.53 g, 13.7 mmol, 69%). ES-MS: positive ion *m/z*, 80.0 $[M]^+$; negative ion *m/z*, 177.3 $[M]^-$.

2.3.3.19 Synthesis of [pyH][hexylPO$_2$H] 19

The same procedure for **17** was followed, using compound **4** (3.46 g, 23.0 mmol) instead of bis(2,4,4-trimethylpentyl)phosphinic acid. The product was obtained as a colourless liquid (3.39 g, 14.8 mmol, 64%). ES-MS: positive ion *m/z*, 80.1 $[M]^+$; negative ion *m/z*, 149 $[M]^-$.

2.3.3.20 Investigation of hygroscopicity of compound 8

The ionic liquid, $[Bu_4P][(TMP)_2PO_2]$ (0.22468 g), was exposed to the atmosphere on a dried (constant weight) watch-glass. Weight gain was monitored using a 5 digit balance.

2.4 References

[1] Kosolapoff, G. M. *Organophosphorus Compounds*, John Wiley & Sons: New York, 1950.

[2] Moedritzer, K.; Maier, L.; Groenweghe, L. C. D. *J. Chem. Eng. Data* **1962**, *7*, 307-310.

[3] Bentrude, W. G. Phosphorus Radicals. In *Free radicals*; J. K. Kochi, Ed.; Wiley: New York, 1973; pp 595-663.

[4] (a) Walling, C.; Pearson, M. S. *Top. Phosphorus Chem.* **1996**, *3*, 1-56.
(b) Halmann, M. *Top. Phosphorus Chem*. **1967**, *4*, 49-84.
(c) Bentrude, W. G. In *The Chemistry of Organophosphorus Compounds: Primary, Secondary and Tertiary Phosphines, Polyphosphines and Heterocyclic Organophosphorus(III) Compounds*; F. R. Hartley, Ed., John Wiley & Sons, 1990; pp 531-566.

[5] Stacey, F. W.; Harris Jr, J. F. In *Organic Reactions*; R. Adams, Ed.; Krieger R.E., Huntington, N.Y., 1963; pp 150-268.

[6] (a) Stiles, A. R.; Rust, F. F.; Vaughan, W. E. *J. Am. Chem. Soc.* **1952**, *74*, 3282-3284.
(b) Rauhut, M. M.; Currier, H. A.; Semsel, A. M.; Wystrach, V. P. *J. Org. Chem*. **1961**, *26*, 5138-5145.

[7] (a) Griffin, C. E. *J. Org. Chem*. **1960,** *25*, 665-666.
(b) Griffin, C. E.; Wells, H. J. *J. Org. Chem*. **1959**, *24*, 2049-2051.

[8] (a) Barnes, Jr., G. H.; David, M. P. *J. Org. Chem.* **1960**, *25*, 1191-1194.
(b) Kharasch, M. S.; Mosher R. A.; Bengelsdorf, I. S. *J. Org. Chem*. **1960**, *25*, 1000-1006.
(c) Stiles, A. R.; Vaughan, W. E.; Rust, F. F. *J. Am. Chem. Soc*. **1958**, *80*, 714-716.

[9] Williams, R. H.; Hamilton, L. A. *J. Am. Chem. Soc.* **1955**, *77*, 3411-3412.

[10] Leach, M. Ph. D. Thesis, University of Waikato, Hamilton, NZ, 1999.

[11] Robertson, A. J.; Seddon, K. CA Patent 2,343,456, March 30, 2001.

[12] Huddleston, J. G.; Visser, A. E.; Reichert, W. M.; Willauer, H. D.; Broker, G. A; Rogers, R. D. *Green Chem*. **2001**, *3*, 156-164.

[13] Sheldon, R. *Chem. Commun*. **2001**, 2399-2407.

[14] Bradaric, C. J.; Downard, A.; Kennedy, C.; Robertson, A. J.; Zhou, Y. *Green Chem*. **2003**, *5*, 143-152.

[15] Robertson, A. J. US01/12780, April 19, 2001.

[16] Peppard, D. F; Mason, G. W; Lewey, S. *J. Inorg. Nucl. Chem.* **1965**, *27*, 2065-2073.

[17] Williams, R. H; Hamilton, L. A. *J. Am. Chem. Soc.* **1952,** *74*, 5418-5420.

[18] Bradaric, C. J.; Downard, A.; Kennedy, C.; Robertson, A. J.; Zhou, Y. *The Strem Chemiker* **2003**, *XX 1*.

[19] Henderson, W.; McIndoe, J. S. *Mass Spectrometry of Inorganic and Organometallic Compounds*; John Wiley & Sons: England, 2005.

[20] Wasserscheid, P; Keim, W. *Angew. Chem. Int. Ed.* **2000**, *39*, 3772-3789.

[21] Bonhôte, P.; Dias, A. P.; Papageorgiou, N.; Kalyanasundaram, K.; Grätzel, M. *Inorg. Chem.* **1996**, *35*, 1168-1178.

[22] Fannin, Jr., A. A.; Floreani, D. A.; King, L. A.; Landers, J. S.; Piersma, B. J. Stech, D. J.; Vaughn, R. L.; Wilkes, J. S.; Williams, J. L. *J. Phys. Chem*. **1984**, *88*, 2614-2621.

[23] Welton, T. *Chem. Rev*. **1999**, *99*, 2071-2083.

[24] Martinez, M; Miralles, N.; Sastre, A. Bosch, E. *Talanta* **1993**, *40*, 1339-1343.

[25] Martinez, M; Herranz, C; Miralles, N; Sastre, A. M. *AFINIDAD* **1996**, *53*, 404-406.

[26] Deprèle, S.; Montchamp, J. *J. Org. Chem.* **2001**, *66*, 6745-6755.

[27] Colton, R.; D' Agostino, A.; Traeger, J. C. *Mass Spectrom. Rev*. **1995**, *14*, 79-106.

[28] Henderson, W; Nicholson, B. K.; McCaffrey, L. J. *Polyhedron* **1998**, *17*, 4291-4313.

[29] Colton, R; Traeger, J. C.; Harvey, J. *Org. Mass Spectrom.* **1992**, *27*, 1030-1033.

[30] Colton, R.; Traeger, J. C. *Inorg. Chim. Acta* **1992**, *201*, 153-155.

[31] Henderson, W.; Olsen, G. M. *Polyhedron* **1996**, *15*, 2105-2115.

[32] Borrett, V. T.; Colton, R.; Traeger, J. C. *Eur. Mass Spectrom*. **1995**, *1*, 131-140.

[33] Dyson, P. J.; McIndoe, J. S.; Zhao, D. *Chem. Commun.* **2003**, 508-509.

[34] Blades, A. T.; Jayaweera, P.; Ikonomou, M. G.; Kebarle, P. *Int. J. Mass*

Spectrom. Ion Proc. **1990**, *101*, 325-336.

[35] Blades, A. T.; Jayaweera, P.; Ikonomou, M. G.; Kebarle, P. *Int. J. Mass Spectrom. Ion Proc*. **1990**, *102*, 251-267.

[36] Seddon, R. K. *J. Chem. Tech. Biotechnnol.* **1997**, *68*, 351-356.

[37] Stegemann, H.; Rohde, A.; Reiche, A.; Schnittke, A.; Füllbier, H. *Electrochim. Acta* **1992**, *37*, 379-383.

[38] Nobuoka, K.; Kitaoka, S.; Kunimitsu, K.; Iio, M.; Harran, T.; Wakisaka, A.; Ishikawa, Y. *J. Org. Chem*. **2005**, *70*, 10106-10108.

[39] Wilkes, J. S.; Zaworotko, M. J. *J. Chem. Soc. Chem. Commun*. **1992**, *13*, 965-967.

[40] Holbrey, J. D.; Seddon, K. R. *J. Chem. Soc. Dalton Trans*. **1999**, *13*, 2133-2139.

[41] Ngo, H. L.; LeCompte, K.; Hargens, L.; McEwen A. B. *Thermochim. Acta,* **2000**, *357-358*, 97-102.

[42] Wilkes, J. S. *J. Mol. Catal. A: Chem.* **2004**, *214*, 11-17.

[43] Zhou, Z. B.; Takeda, M.; Ue, M. *J. Fluorine Chem.* **2004**, *125*, 471-476.

[44] Gu, Y. L.; Peng, J. J.; Qiao, K.; Yang, H. Z.; Shi, F.; Deng, Y. Q. *Prog. Chem.* **2003**, *15*, 222-242.

[45] Wolff, M. O.; Alexander, K. M.; Belder, G. *Chim. Oggi* **2000,** 29-32.

[46] Mutch, M. L.; Wilkes, J. S. *Proc. Electrochem. Soc*. **1998**, *98*, 254-260.

[47] Dzyuba, S. V.; Bartsch, R. A. *Chemphyschem* **2002**, *3,*161-166.

[48] http://pb.merck.de/servlet/PB/menu/1303700/index.html (18/02/2006).

[49] Dyson, P. J.; Laurenczy, G.; André Ohlin, C.; Vallance, J.; Welton, T. *Chem. Commun.* **2003**, *19*, 2418-2419.

[50] Kosower, E. M. *J. Am. Chem. Soc*. **1958**, *80*, 3253-3260.

[51] Herfort, I. M.; Schneider, H. *Liebigs Ann. Chem*. **1991**, 27-31.

[52] Buncel, E.; Rajagopal, S. *Acc. Chem. Res.* **1990**, *23*, 226-231.

[53] Deye, J. F.; Berger, T. A.; Anderson, A. G. *Anal. Chem*. **1990**, *62*, 615-622.

Chapter Three

Application of ionic liquids: Synthesis of transition metal nanoparticles in phosphinate-based ionic liquids

3.1 Introduction

A good review of ionic liquids in catalysis has been presented by Welton [1a] and a very recent review of imidazolium ionic liquids for catalysis, organic synthesis, extraction, and construction of nanostructure materials has also been discussed by Lee [1b]. During the last decade, room temperature ionic liquids have been employed in catalytic chemistry especially in organic synthesis. Whenever the solvent (ionic liquid) leads to a faster reaction, the new solvent could be viewed as being a catalyst. If one of the ions of the ionic liquid acts as a catalyst activator, for example, a chloroaluminate(III) derived ionic liquid, it could be considered as a co-catalyst. Ionic liquids also could act as a ligand source [1a]. In recent years, increasing uses for ionic liquids in areas such as biotechnology, photochemistry etc. have been reported. Novel applications have also been gradually discovered in electrochemistry [2] and sonochemistry [3]. Therefore, with continuous development of applications, ionic liquids have significant future.

In this work, a series of phosphinate-based ionic liquids were synthesised (Chapter 2), such as $[Bu_4P][RR'PO_2]$ (R = alkyl; R'= R or H) and $[Et_3NH][RR'PO_2]$, and in this Chapter were employed to prepare transition metal (Au, Rh, and Ir) nanoparticles as protecting agents and/or reducing agents. The nanoparticles were characterized by different techniques, such as SEM, TEM, UV-Visible, Zetasizer and IR-spectroscopy.

3.1.1 Ionic liquids as solvents for transition metal catalyzed reactions

3.1.1.1 Hydrogenation reactions

Hydrogenation of olefins using transition metal catalysts is one of the first and most important catalytic reactions. Successful recycling of these metals and ligands, which are usually very expensive, is a prerequisite and makes possible large-scale and industrial applications.

Ionic liquids have been used in organic synthesis as either a catalyst and/ or solvent. In 1995, de Souza [4] and Chauvin [5] reported the first successful hydrogenation reactions in ionic liquids. The Rh catalysts, $RhCl(PPh_3)_3$ and $[Rh(COD)_2][BF_4]$ (COD = cycloocta-1,5-diene) were used in the hydrogenation of cyclohexene in 1-*n*-butyl-3-methylimidazolium tetrafluoroborate ([BMIM][BF_4]) and 1-*n*-butyl-3-methylimidazolium hexafluorophosphate ([BMIM][PF_6]) were investigated by de Souza. This catalytic hydrogenation reaction was a two-phase system, and at the end of the reaction, the product was easily removed by decantation and the Rh catalyst remained in the ionic liquid phase [4]. Chauvin *et al*. investigated the biphasic hydrogenation of 1-pentene in [BMIM][SbF_6] using $[Rh(NBD)(PPh_3)_2][PF_6]$ (NBD = norbornadiene) as a catalyst. The rate of this reaction was five times faster than the homogeneous reaction in acetone [5]. The ionic liquid, [BMIM][SbF_6] was employed for hydrogenation of cyclohexadiene to cyclohexene in biphasic reaction system with 98% selectivity at 96% conversion. The catalyst, which was dissolved in the ionic liquid, could be reused [5].

Pt-catalysed hydrogenation of alkenes and arenes, such as 1-hexene, cyclohexene, benzene, and 2,3-dimethyl-1-butene [6] and Ir-catalysed [7], Pd-catalysed [8], and Co-catalyzed [9] hydrogenation of olefins have also been reported to be successful in ionic liquids.

A stereoselective hydrogenation in ionic liquids [10] was studied by Steines, *et al*. (Scheme 3.1). A more than threefold increase of the hydrogenation of cis-3-hexanoic acid was obtained in ionic liquid than in glycol.

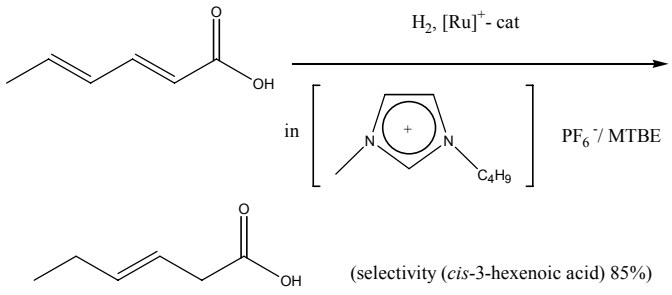

Scheme 3.1: A stereoselective hydrogenation of sorbic acid [10]

Enantioselective hydrogenation [5] [11] in ionic liquids has also been described; α-acetamidocinnamic acid was hydrogenated to (S)-phenylalanine in 64% ee (ee = enantiomeric excess) in the presence of a $[Rh(COD)\{(-)diop\}]PF_6$ catalyst (diop = 4,5-bis[p[(diphenylphosphanyl)-methyl]-2,2-dimethyl-1,3-dioxolan-4,5-diol) in $[BMIM][SbF_6]$ [5].

Reactions of $Ru(COD)Cl_2$/BINAP/NEt_3 catalysed (BINAP = 2,2'-bis(diphenylphosphanyl)-1,1'-binaphthyl) hydrogenation of 2-phenylacrylic acid to 2-phenylpropionic acid (Scheme 3.2) in $[BMIM][BF_4]$, were obtained with ee around 80% [11]. The obtained enantioselectivities of these reactions were similar or higher than those in homogeneous organic media.

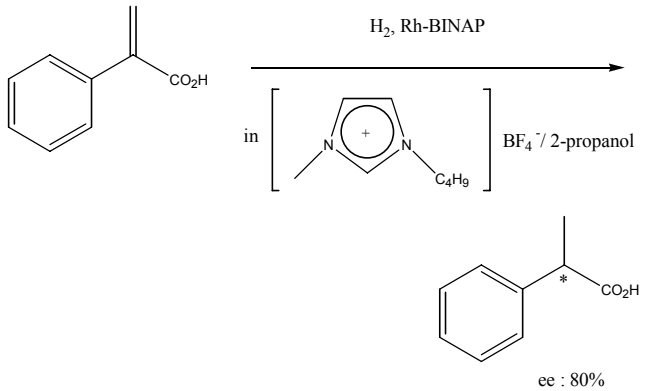

Scheme 3.2: Enantioselective hydrogenation of 2-phenylacrylic acid [11]

Recently, Dupont *et al*. studied an asymmetric hydrogenation of α-acetamidocinnamic acid in 1-*n*-butyl-3-methylimidazolium tetrafluoroborate ([BMIM][BF_4]) and its hexafluorophosphate analogue ([BMIM][PF_6]) by a Rh(I)-catalyst [12]. The remarkable effects in the conversion and enantioselectivity of these reactions were described as the molecular hydrogen concentration in the ionic catalyst layer, rather than the hydrogen pressure in the gas phase. As shown in Table 3.1, with increasing the solubility of molecular hydrogen in the liquid phase, the enantioselectivity and conversion increase. The enantioselectivity and conversion in [BMIM][BF_4] is much higher than in [BMIM][PF_6], because of the higher solubility of hydrogen in [BMIM][PF_6]. The solubility of hydrogen in [BMIM][BF_4] was nearly four times higher than in [BMIM][PF_6].

Table 3.1: The asymmetric hydrogenation of (Z)-α-acetamidocinnamic acid: the effect of hydrogen concentration in the liquid phase on the conversion and the enantioselectivity [12]

Entry	Cat. phase	P (atm)	Sol. H_2 (mol L^{-1})	Conversion (%)	ee (%)
1	[BMIM][PF_6]	5	4.4×10^{-3}	7	66
2	[BMIM][PF_6]	50	4.4×10^{-2}	26	81
3	[BMIM][PF_6]	100	8.9×10^{-1}	41	90
4	[BMIM][PF_6]	50	1.5×10^{-1}	73	93
5	^{i}PrOH	50	129.3	99	94

3.1.1.2 Oxidation reactions

Ionic liquids have also been employed as solvents in oxidation reactions [13] [14] [15]. Song and Roh [13] investigated the conversion of alkenes to epoxides, such as, 2,2-dimethylchromene with a chiral Mn(III) catalyst (salen) ([N,N'-bis(3,5-di-*tert*-butylsalicylidene)-1,2-cyclohexanediamine]manganese(III) chloride) and NaOCl in a mixture of [BMIM][PF_6]-CH_2Cl_2 (1:4, v/v) (Scheme 3.3). The catalyst activity was apparently enhanced through the addition of the ionic liquid to the organic solvent. Also Song and Roh studied Cr(salen)-catalysed asymmetric ring opening reactions of epoxides in ionic liquids [14]. Methyltrioxorhenium-catalyzed epoxidations in ionic liquids were reported by Owens and Abu-Omar [15].

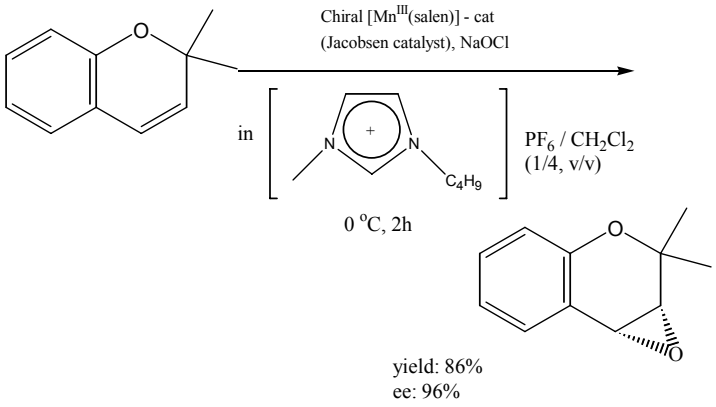

Scheme 3.3: Oxidation of 2, 2-dimethylchromene [14]

3.1.1.3 Hydroformylation reactions

Tetraethylammonium trichlorostannate melt ($[(C_2H_5)_4N][SnCl_3]$), (melting point 78 °C), was employed for the platinum-catalyzed hydroformylation of olefin by Parshall as early as 1972 [16]. Wasserscheid *et al*. have studied the platinum-catalyzed hydroformylation of 1-octene in an ionic liquid of BMIM trichlorostannate. High activity of the platinum catalyst was achieved with turnover frequency (TOF = mol of 1-octene converted per mol of Pt-catalyst per hour) 126 [17].

The rhodium-catalyzed hydroformylation of 1-hexene in phosphonium salts, (with melting points > 70 °C), was studied [18]. Also the rhodium-catalyzed hydroformylation of olefin in room temperature ionic liquids was investigated by Chauvin *et al*. in 1995 [5] [19]. For example, the hydroformylation of 1-pentene with $[Rh(CO)_2(ACAC)]/PPh_3$ (ACAC = acetylacetonate) in $[BMIM][PF_6]$ was achieved with TOF = 333 h^{-1}.

3.1.1.4 Alkoxycarbonylation reactions

Monteiro *et al*. investigated the palladium-catalyzed alkoxycarbonylation of styrene and styrene derivatives in a two-phase system [20] (Scheme 3.4). Using a catalytic system composed of $PdCl_2(PhCN)_2$, (+)-NMDPP

(neomenthyldiphenyldiphosphine) and TsOH (*p*-toluenesulfonic acid), the reaction of styrene with carbon monoxide and isopropanol in [MBIM][BF_4]/cyclohexane, gave the product (isopropyl 2-phenylpropionate) in high yield (89%) and very high regioselectivity (α:β = 99.5:0.5).

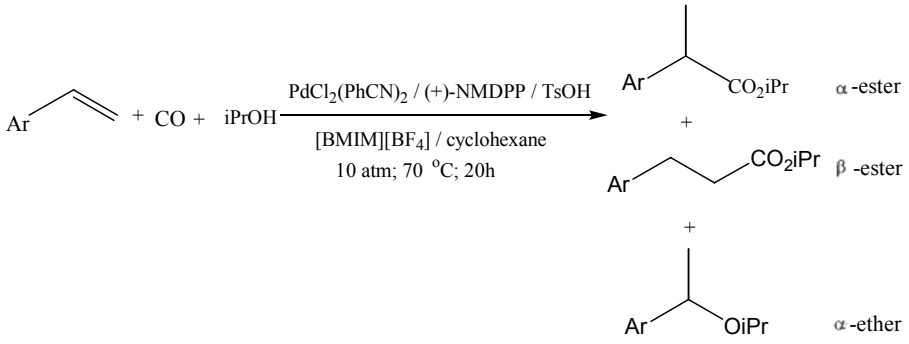

Scheme 3.4: Alkoxycarbonylations of styrene [20]

3.1.1.5 Heck reactions

It was first described by Kaufmann *et al*. in 1996 that ionic liquids can be employed as reaction media for the palladium-catalyzed Heck reaction [21]. Bromobenzene was successfully reacted with butyl acrylate to form butyl *trans*-cinnamate in high yield in molten tetraalkylammonium bromide ([R_4N][Br]) and tetraalkylphosphonium bromide ([R_4P][Br]) salts. Later, the Heck reaction in low melting salts was studied by Herrmann and Böhm [22]. These results showed that molten salts as reaction media have advantages over conventional, molecular solvents such as dimethylformamide (DMF), especially for the conversion of industrially important chloroarenes in the Heck reaction. The yield of stilbene increases from 20% (in DMF) to over 99% (in [Bu_4N][Br]) in the reaction of bromobenzene and styrene using diiodo-bis(1,3-dimethylimidazoliun-2-ylidene) palladium(Π) as catalyst, and the catalyst could be reused up to thirteen times.

Additionally, the Heck reaction in ionic liquids using a three-phase catalyst system was performed with excellent yield by Seddon's group [23]. After the reaction, the catalyst, ([$BMIM]_2[PdCl_4$]) remains in the ionic liquid phase, the products are in the organic phase, and by-products of the reaction, the salt

($[Hbase]^+X^-$) is in the aqueous layer. Allowing for ionic liquid and catalyst recycling, the product and by-products can easily separated.

Heterogeneous Heck reaction catalyzed by Pd/C in ionic liquid was studied by the Hagiwara group (Scheme 3.5) [24]; they found that the catalyst system was easily re-usable without losing catalytic activity.

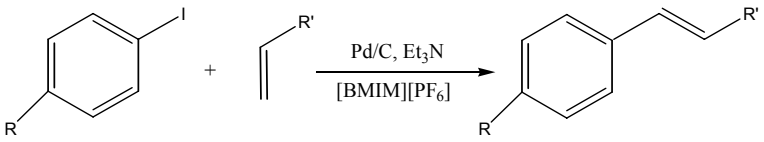

R = H; 4-OMe; 4-Me; 4-COMe
R'= CN; Ph; COMe; COEt

Scheme 3.5: Pd/C-catalyzed Heck reactions of with olefins in ionic liquids [24]

3.1.1.6 Hydrodimerizations or telomerizations

Hydrodimerization of 1,3-butadiene by palladium compounds in [BMIM][BF_4] was performed by Dupont *et al*. [25]. Two-phase dimerization of ethylene [26] and *n*-butene [27] using nickel complexes in 1-*n*-butyl-3-methyl-imidazolium chloroethylaluminate ionic liquid was reported by the Dupont and de Souza group. An example of telomerization of butadiene with methanol using ionic liquid as solvent in the palladium-catalyst (palladium(II) acetate with either triphenylphosphine or sodium diphenylphosphinobenzene-3-sulfonate) was studied by Niccolai and Basset *et al*. [28].

3.1.1.7 Trost-Tsuji couplings

The nucleophilic allylic substitution reaction using palladium(0)-catalysis to form C-C bonds can also be successfully performed in ionic liquids. Xiao *et al*. investigated monophasic reaction of 3-acetoxy-1,3-diphenylprop-1-ene and dimethyl malonate with $Pd(OAc)_2/PPh_3$ (1/4) catalyst and K_2CO_3 as base in [BMIM][BF_4] [29]. Biphasic Trost-Tsuji coupling reaction was studied by de

Bellefon *et al*. [30]. It was indicated that reaction in the ionic liquid had clear advantages over the reaction in the aqueous biphasic system. A tenfold increase was observed in the rate of reaction, because of the better solubility of the substrate (ethyl cinnamyl carbonate) in the ionic liquid. Furthermore, the selectivity of the [BMIM]Cl-/methylcyclohexane has significantly improved in the reaction, because the formation of cinnamylalcohol (by reaction of water) was stopped and the formation of phosphonium salts (by reaction of the Pd-allyl complex with TPPTS as ligand) (TPPTS = triphenylphosphine trisulfonate, sodium salt) was suppressed in the ionic liquid.

3.1.1.8 Oligomerizations

Though many cationic transition metal complexes are excellent oligomerization catalysts [31], these complexes usually are poorly soluble in non-polar solvents. An ionic liquid solvent of higher polarity was employed with the substrate for the coordination sites at the catalytic centre to improve solubility of the metal complex.

The oligomerization of short-chain alkenes in chloroaluminate melts using a nickel catalyst is one of the best studied applications of transition metal catalysts in ionic liquids. The oligomerization of *n*-butenes in ionic liquids of aluminium trichloride or ethylaluminium dichloride and 1-methyl-3-butylimidazolium chloride using Ni catalyst ($Ni(MeCN)_6[BF_4]$) was investigated by Chauvin *et al*. [32]. The Ni oligomerization catalyst in chloroaluminate melts has been given particular attention since it has been commercially and industrially used, under the named Difasol process [33].

3.1.1.9 Transition metal nanoparticles in ionic liquid for hydrogenation and Heck reactions

Nanoparticle catalysts have attracted increased attention in recent years because they have unique properties [34] [35]. Metallic nanoparticles are kinetically unstable towards agglomeration to the bulk metal; therefore, they must

be protected by stabilizing agents, such as, quaternary ammonium salts, soluble polymers, and polyoxoanions [34]. Recently, nanoparticles stabilized by an ionic liquid [BMIM][PF_6] have been reported [6] [7]. The Fonseca group reported [BMIM][PF_6] ionic liquid was a suitable medium for the synthesis and stabilization of Ir nanoparticles, and also was an ideal medium in recyclable biphasic catalytic systems for hydrogenation of alkenes [7]. A total turnover (TTO) of 3509 in 32 hours has been achieved for arene hydrogenation by the Ir(0) nanoparticles (2.0-2.5 nm) in solventless conditions [36]. Rhodium nanoparticles stabilized by ionic copolymers in [BMIM][BF_4] were investigated and had a TTO of 20000 and a TOF of 250 h^{-1} for benzene hydrogenation [37]. This showed that ionic liquids combined with ionic copolymer stabilizers provide a good pathway for formation of stable and active nanoparticle catalysts.

Transition metal Pd nanoparticles in [BMIM][PF_6] ionic liquid in Heck reaction was investigated by Dupont *et al*. [38]. They demonstrated the changes in shape and in size of colloidal Pd catalysts after the Heck reaction in [BMIM][PF_6] (Figure 3.1).

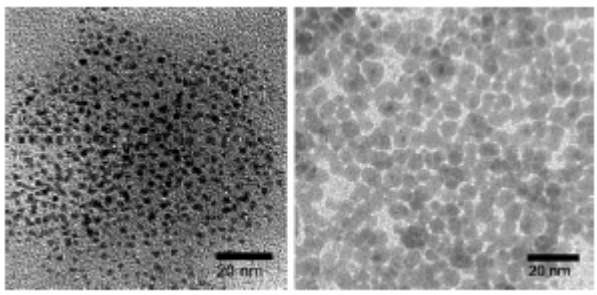

Figure 3.1: Part of the TEM micrographs showing the Pd nanoparticles dispersed in [BMIM][PF_6] ionic liquid before (left) and after (right) catalysis, observed at 200 kV [38]

They indicated that Pd nanoparticles dispersed in the ionic liquids performed as a reservoir of catalytically active Pd species (Figure 3.2).

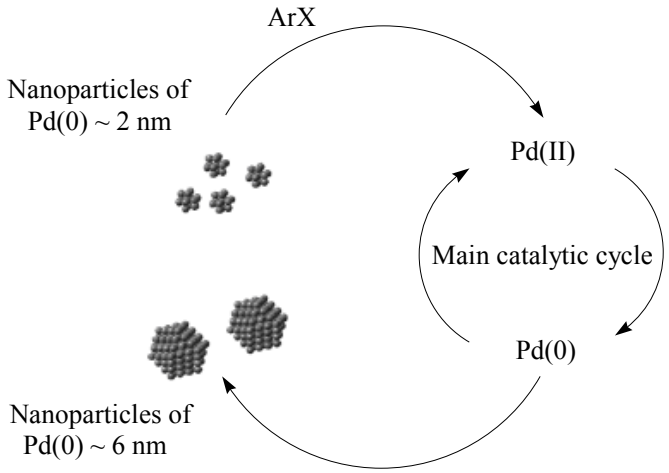

Figure 3.2: Possible pathways involved in the Heck reaction promoted by Pd nanoparticles dispersed in imidazolium ionic liquids [38]

For example, after reaction, iodobenzene had 92% conversion, the product was formed in 87% yield, and also metal leaching from the ionic phase to the organic phase had happened [38].

3.1.2 Transition metal nanoparticles in ionic liquids

3.1.2.1 Nanoparticles

Nanoparticles are nearly monodispersed particles that are generally defined as having 1-50 nm diameters, a size range where metals can demonstrate size-dependent properties. The smaller the cluster of atoms, the higher the percentage of atoms are on the surface [39], therefore, a nanoparticle of 10 nm diameter would have 10% of its atoms on the surface. If a nanoparticle diameter is 1 nm, it would have 100% of atoms on the surface [40].

Nanoparticles have been of interest over the past decade, because of their unique physical and chemical properties [41]. They also have many potential utilities, such as, quantum dots used as microelectronic quantum devices [42], application in microelectronics [43], chemical sensors [44], light-emitting diodes [45], application in biology and medicine, drug and gene delivery [46] cell-separation [47], industrial lithography [48], photochemistry [49] and in paint &

coatings industry giving improved resistance to chipping, scratching and water spotting [50]. Nanoparticles are also used as new types of catalysts with higher activity and selectivity for organo synthesis in common solvents [51] and ionic liquids [6] [7] [36] [37] [38] etc.

3.1.2.2 Synthesis of metal nanoparticles

Several synthetic methods have been used in the literature to synthesize metal nanoparticles, such as, chemical reduction of a metal salt; thermal, photochemical, or sonochemical decomposition of a metal(0) complex; hydrogenation of a coordinating olefinic moiety; metal vapour synthesis, and electrochemical reduction [52]. Metallic nanoparticles can be generally synthesised by two main ways: (Figure 3.3) (i) physical methods using mechanical subdividing of metallic aggregates or (ii) chemical methods using nucleating and growing metallic atoms [53].

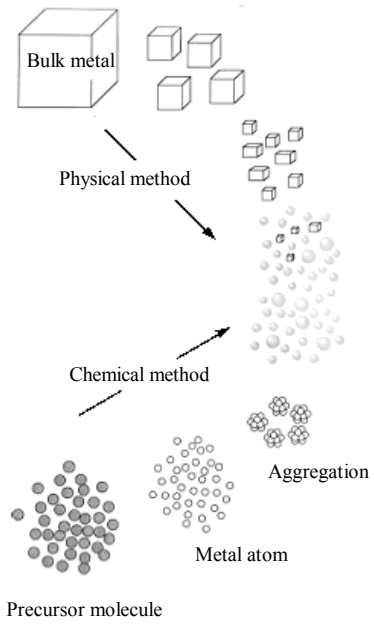

Figure 3.3: Schematic illustration of preparative methods of metal nanoparticles [53]

Five examples are presented below for synthesis of nanopartices in order to provide an overall perspective of nanocluster chemistry. These systems are those where nanoparticles were widely studied and very well characterized by different techniques.

One of the first examples of a ligand-stabilized nanocluster is $Au_{55}(PPh_3)_{12}Cl_6$ (Figure 3.4) which was synthesised by Günter Schmid *et al*. [54]. Diborane (B_2H_6) reduction of a benzene solution of PPh_3AuCl at 50-60 °C gave the nanocluster in 14 Å size [39a]. The diborane reduces Au(I) to Au(0) and complexes excess phosphine [55], a black solid was isolated.

$$Au_{55}[P(C_6H_5)_3]_{12}Cl_6$$

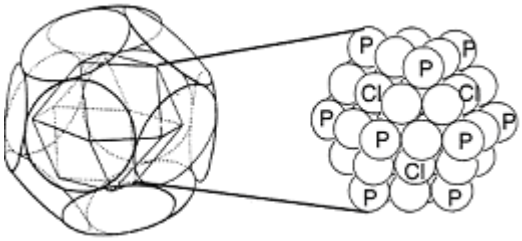

Figure 3.4: Schmid's proposed structural model for the $Au_{55}(PPh_3)_{12}Cl_6$ ligand-stabilized nanocluster. The image on the left [55] contains the metal core surrounded by the phosphine ligand shell radii while the inset on the right [56] shows the cubic close packed structure of the Au_{55} metal core alone with the proposed phosphine and chloride ligand binding sites at each metal (labelled P and Cl, respectively) [39a]

Moiseev *et al*.'s giant cationic palladium clusters (with approximate formulae $Pd_{\sim 561}L_{\sim 60}(OAc)_{\sim 180}$ [57] (Figure 3.5) [L=1,10-phenanthroline or 2,2′-bipyridine] and $Pd_{\sim 561}phen_{\sim 60}O_{\sim 60}(PF_6)_{\sim 60}$) is one of the most-studied catalytic nanocluster systems in the literature [39a]. A overall stoichiometry of synthesis reaction was given $[Pd_4phen(OCOCH_3)_2H_4]_n$ ($n \approx 100$) (Equation 3.1) [57] [58], which was followed by reacting with oxygen, then washing with benzene and vacuum drying to form $[Pd_9phen(OAc)_3]_{60}$ or $Pd_{\sim 561}phen_{\sim 60}(OAc)_{\sim 180}$ (Figure 3.5).

$$4Pd_3(OCOCH_3)_6 + 3phen + 15H_2 \rightarrow 3Pd_4phen(OCOCH_3)_2H_4 + 18CH_3COOH$$

Equation 3.1: Synthesis of $Pd_4phen(OCOCH_3)_2H_4$

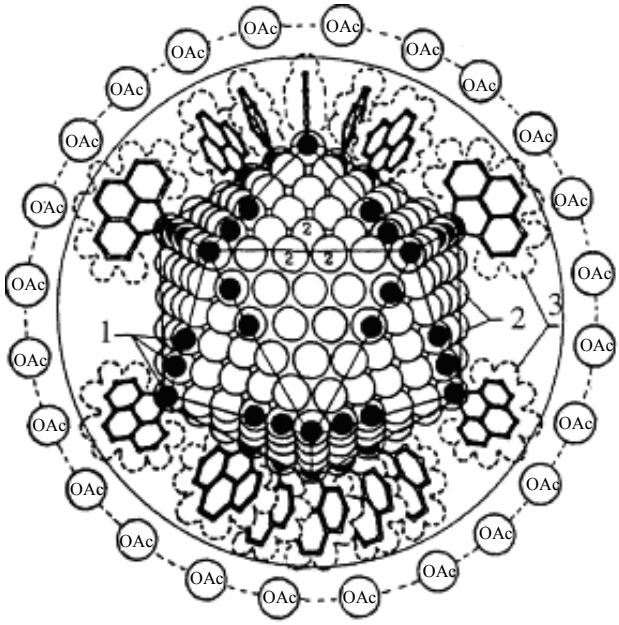

1—Pd atoms coordinated with phenanthroline ligands; 2—Pd atoms accessible for coordination with OAc^- anions or molecules of substrates or solvent; 3—van der Waals surface of coordinated phenanthroline ligands.

Figure 3.5: The idealized model of $Pd_{\sim 561}phen_{\sim 60}(OAc)_{\sim 180}$ [57]

A wide range of metals and extensive use of nanoclusters as heterogeneous catalysts is Bönnemann's nanocluster systems [59] [60] [61] [62] [63] [64] [65]. Transition metal nanoclusters were synthesised through reducing metal salts in tetrahydrofuran (THF) using tetraalkylammonium hydrotriorganoborates. Most metals in groups 6-11 were applied. Equation 3.2 is a typical preparative route [59], where M = metals of groups 6-11; X = Cl, Br; n = 1, 2, 3; and R = alkyl, C_6-C_{20}.

$$MX_n + nNR_4(BEt_3H) \rightarrow M_{colloid} + NR_4X + nBEt_3 + n/2H_2$$

Equation 3.2: Synthesis of transition metal nanoclusters [59]

An impressive, size-selective electrochemical-based synthetic procedure for the preparation of transition metal nanoclusters has been developed by Manfred Reetz *et al*. [66]. A sacrificial anode was used as a metal source and a

supporting electrolyte as a nanocluster stabilizing agent in the synthesis of $(C_8H_{17})_4NBr$-stabilized Pd nanoclusters in CH_3CN/THF. Reetz mentioned the precise mechanism of colloid formation was difficult to determine, but a rudimentary mechanism has been proposed (Figure 3.6). The bulk metal was oxidized at the anode, then the metal cations move to the cathode, and reduction took place with formation of metal(0). Agglomeration was prevented by the presence of the ammonium stabilizing agent.

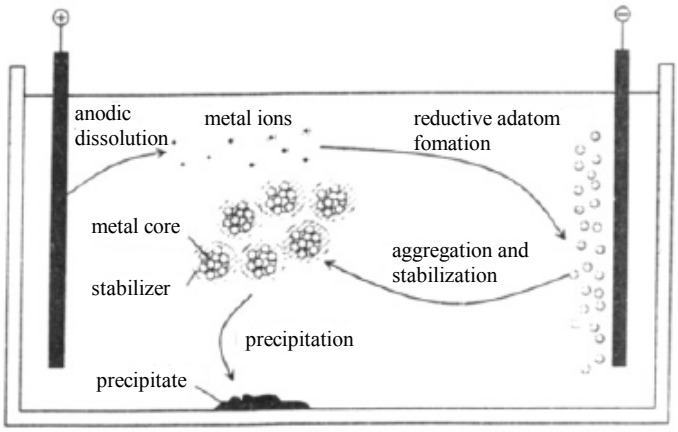

Figure 3.6: Formation of produced tetraalkylammonium stabilized metal clusters in electrochemistry [66]

Finke *et al*. have investigated in-depth kinetic and mechanistic studies [67] of the active catalyst of the nanocluster chemistry, when the polyoxoanion-supported Ir(I) organometallic complex ($[(n\text{-}C_4H_9)_4N]_5Na_3[(1,5\text{-}COD)Ir{\cdot}P_2W_{15}Nb_3O_{62}]$), was reacted with H_2, with or without cyclohexene as a substrate for hydrogenation catalysis. Scheme 3.6 shows the overall, average stoichiometry of the $Ir(0)_{\sim 300}$ nanoclusters [68].

$$300[(1,5\text{-COD})Ir{\cdot}P_2W_{15}Nb_3O_{62}]^{8-} + 750\ H_2 \longrightarrow$$

$$300\ \bigcirc + 1\ Ir(0)_{\sim 300} + 300\ P_2W_{15}Nb_3O_{62}^{9-} + 300\ H^+$$

Scheme 3.6: The formation of the resultant Ir(0) nanocusters [68]

A pictorial representation of the $Ir(0)_{\sim 300}$ nanoclusters in the 20 Å and 12 × 15 Å $P_2W_{15}Nb_3O_{62}^{9-}$ shown in Figure 3.7.

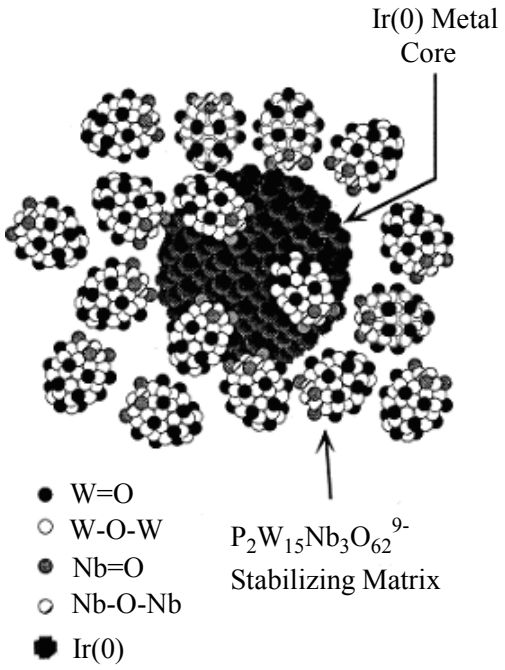

Figure 3.7: Idealized, roughly-to-scale representation of a $P_2W_{15}Nb_3O_{62}^{9-}$ polyoxoanion and Bu_4N^+ stabilized $Ir(0)_{\sim 300}$ nanocluster, $[Ir(0)_{\sim 300}(P_4W_{30}Nb_6O_{123}^{16-})_{\sim 33}](Bu_4N)_{\sim 300}Na_{\sim 228}$. For the sake of clarity, only 17 of the polyoxoanions are shown, and the polyoxoanion is shown in its monomeric, $P_2W_{15}Nb_3O_{62}^{9-}$ form (and not as its Nb-O-Nb bridged, anhydride, $P_4W_{30}Nb_6O_{123}^{16-}$ form). The ~330 Bu_4N^+ and ~228 Na^+ cations have been deliberately omitted [69]

3.1.2.3 Stabilization of metal nanoparticles

Whatever the method used, a stabilizing agent is always necessary to prevent aggregation into larger particles. Usually nanoparticle stabilization can be divided into two categories: (i) charge stabilization and (ii) steric stabilization [70]. In a recent review, four kinds of stabilization procedures were suggested by Roucoux *et al*. [34]. They are (i) the electrostatic stabilization through surface adsorbed anions, (ii) steric stabilization through the presence of bulky groups, (iii) the combination of these two kinds of stabilization with the electrosteric stabilization such as surfactants, and (iv) stabilization with a ligand.

Electrostatic stabilization is based upon generating a double electric layer on the metallic nanoparticle surface (Figure 3.8) [34] when ions of the counter

sign are adsorbed. The nanoparticle containing an electrical double-layer repels the neighbouring nanoparticle, because of Coulombic repulsion between the particles. The electrostatic repulsion could prevent particle aggregation if the electric potential of the double layer is high enough [39a] [71].

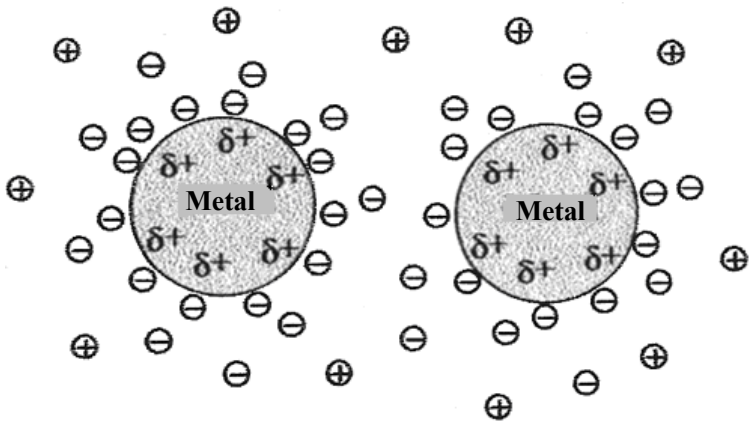

Figure 3.8: Schematic representation of electrostatic stabilization [34]

In the second case, protecting molecules which have a considerable length interact attractively with the surface of the nanoparticle. The molecules involved are usually macromolecules, such as polymers [72] or oligomers to prevent mutual approach of metal surfaces at bonding distance (Figure 3.9) [34].

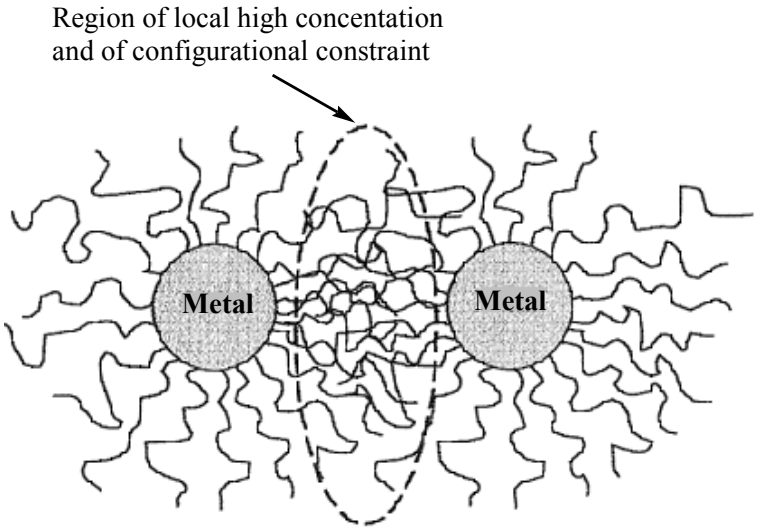

Figure 3.9: Schematic representation of steric stabilization [34]

Both electrostatic and steric stabilization can be combined together to maintain the stability of metallic nanoparticles [73] [74]. This kind of stabilization is dependant on ionic surfactants. These compounds with a polar head group are able to generate an electric double layer, and side chains provide steric repulsion. The electrostatic and steric stabilization can be obtained from polyoxoanions, such as the ammonium (Bu_4N^+)/polyoxoanion ($P_2W_{15}Nb_3O_{62}^{9-}$) as well [74].

Stabilization can occur by coordinating metallic nanoparticles with ligands, such as phosphines [75] [76] [77], thiols [78] [79], amine [80] [81], and carbon monoxide [82] and so on.

3.1.3 Infrared spectra of CO chemisorbed on transition metal catalysts

The infrared absorption bands of CO chemisorption on metal catalyst are very strong and easy to measure. The very high extinction coefficient for the $\upsilon(CO)_{ads}$ stretch makes easy the detection by infrared spectroscopy of monomolecular layer of CO adsorbed on metal catalyst. Usually two finely divided catalysts derived from the same metal will give different CO spectra; these can be attributed to different surface environments. A lot of data from the literature can be confusing and not consistent due to identical conditions not being followed, however the data are valuable when they are interpreted [83] and compared with the presently studied system. IR spectra of CO adsorbed to metal, the "linear" (terminal) CO bonding gives peaks at 2130 to 2000 cm^{-1} while two fold bridged bonded CO gives peaks from 1880 to 2000 cm^{-1} [83] [84]. CO stretching frequencies less than 1850 cm^{-1} due to 3-fold bridge-bonded CO species can also be observed [83].

3.1.3.1 IR spectra of CO adsorbed on rhodium

Introduction

The spectra of CO adsorbed on evaporated rhodium films [85] [86] [87] [88] [89] [90] are very variable. Normally linear-bonded CO bands are dominant, but sometimes bridge-bonded CO absorption peaks are also rather strong in the range of 1885 to 1820 cm^{-1} [89]. These lower wavenumber peaks suggest 3-fold or 4-fold bridged species.

The first reported IR spectrum from CO adsorbed on rhodium was by Yang *et al*. [91]. They reported on the basis of extensive infrared studies for CO chemisorbed on the surface of rhodium supported on a high surface area, non-porous alumina. Yang *et al*. investigated spectra as a function of CO coverage for adsorption and desorption on a series of rhodium surfaces, and the reaction of the chemisorbed CO with oxygen, hydrogen and water. Three types of surface species were proposed (Figure 3.10) and their corresponding infrared band assignments for low and high coverage on various rhodium surfaces are shown in Table 3.2; Spectra for CO adsorbed on rhodium reported by other workers are also shown in Table 3.2.

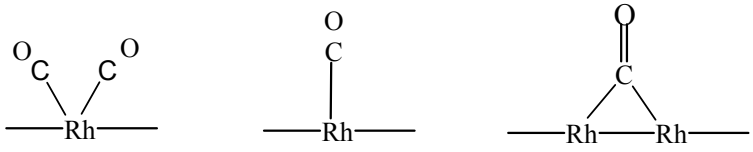

Gem-dicarbonyl Rh species (2 CO's per Rh atom)

Single linear CO

Two-fold bridged CO (1 CO per 2 neighbouring Rh atoms)

Figure 3.10: Three types of the species on rhodium for chemisorbed CO [91]

Table 3.2: Stretching frequencies (cm^{-1}) of CO chemisorbed on rhodium

Substrate (support)	ν CO					Comments	Ref. no.
Rhodium (a) Evaporated films*							
CaF_2 or CsI (2111)		2055a		1905	1852	evaporation film	[86]
NaCl			2000		1820		[89]
Metal	2078	2060				Rh(110) crystal	[87]
NaCl			2020		1885	evaporation film	[85]
NaCl			2015		1860	evaporation film	[90]
Ta		2060				low coverage	[92]
	2080					high coverage	[92]
Rhodium (b) supported metal particles							
SiO_2		2065	2005		1895		[93]
Al_2O_3	2095		2027			2% Rh unsintered	[91]
Al_2O_3	2095	2055	2027	1905		8-16% Rh, unsintered	[91]
Al_2O_3	2108	2062	2040	1925		8-16% Rh, sintered	[91]
Al_2O_3	2096		2025			0.2% Rh	[94]
Al_2O_3		2063	2030			2.2% Rh	[94]
Al_2O_3	2103	2055		1900		10% Rh	[94]

a: Underlining denotes relatively strong absorptions.
*: Metal films were prepared by evaporation under vacuum or in the presence of argon or CO.

Infrared spectra of CO adsorbed on poly(vinyl alcohol)-protected rhodium hydrosols was studied by Mucalo *et al*. [95]. It showed spectra of linear and two-fold-bridging CO on rhodium metal surfaces sites, assigned in the region 2030-2040 cm^{-1} and 1890-1900 cm^{-1} respectively.

3.1.3.2 IR spectra of CO adsorbed on iridium

Introduction

Infra-red absorption spectra of evaporated Ir metal films with adsorbed carbon monoxide have been investigated before by Baker *et al*. [96]. CO adsorbed on the bare Ir film at very low temperatures (< -100 °C) gave a weak band (Figure

3.11 **a**). With an increase of the temperature and time of treatment with CO, the stronger bands appeared at the same wavenumber (Figure 3.11 **b** and **c**).

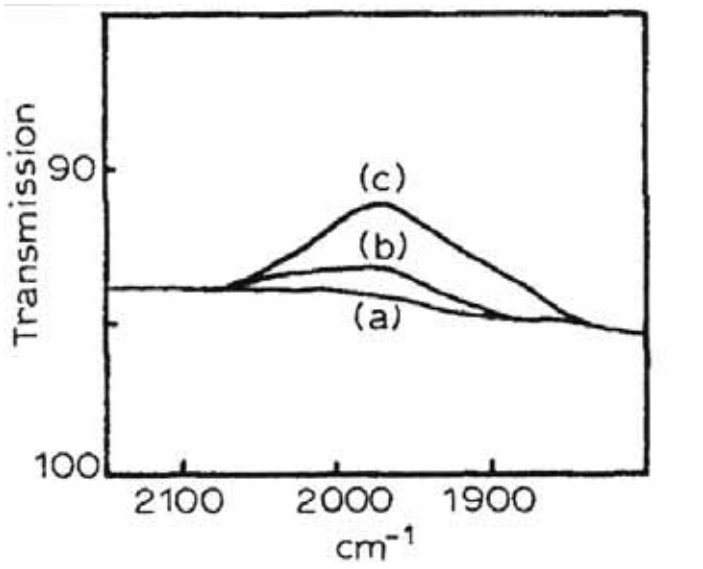

Figure 3.11: IR spectra of CO adsorbed on iridium at different temperatures and treatment times (a) at low temperature (b) at 170 °K, (c) after 4 hours at room temperature [96]

Infrared spectra of CO chemisorbed on Ir were also reported by Lynds [97]. This study found that changing the surface coverage of CO from high to low coverage caused a shift of the main absorption band from 2074 to 2044 cm^{-1}.

3.1.4 Aim of this chapter

In this chapter the application of these new phosphinate-based ionic liquids, as solvents/or reducing agents in preparation of metal nanoparticle systems are investigated. In recent years, metal nanoparticle particles have been of much interest. In order to stabilise metal nanoparticles, a stabilizing agent needs to be used. A variety of protecting agents have been used in the literature, for example phosphines [75] [76] [77], thiols [78] [79], amines [80] [81], and carbon monoxide [82] etc; however, using an ionic liquid as protecting agents are rare. So, the synthesis of Au, Rh and Ir nanoparticles in a series of phosphinate-based ionic liquids and their characterization was investigated.

3.2 Results and discussion

3.2.1 Synthesis of metal nanoparticles in phosphinate ionic liquids

Four kinds of transition metal compounds were individually employed to generate metal nanoparticles in different ionic liquids. These compounds are tetrahydrothiophene gold(I) chloride ($(CH_2)_4SAuCl$), tetramethylammonium tetrachloroaurate ($[Me_4N][AuCl_4]$), di-μ-chloro-bis-(1,5-cyclooctadiene)diiridium(I) ($[IrCl(COD)]_2$) and rhodium(Ⅲ) chloride hydrate ($RhCl_3 \cdot xH_2O$). Reactive ionic liquids ($[R_4E][RHPO_2]$, E = N, P) which contain a P-H bond will show reducing properties, and may be able to generate metal nanoparticles from metal salt precursors without external reducing agents, whereas unreactive ionic liquids ($[R_4E][R_2PO_2]$, E = N, P) presumably need to use added reducing agent in order to generate the nanoparticles.

3.2.1.1 Synthesis of Au(0) nanoparticles in "reactive" ionic liquids from $(CH_2)_4SAuCl$

When a grey-white powder of $(CH_2)_4SAuCl$ was dissolved in "reactive" ionic liquids (containing the RPO_2H^- anion, such as $[Et_3NH][hexylPO_2H]$ or $[Bu_4P][hexylPO_2H]$), the colour of mixture changed from pink, purple, to black in 5 minutes at room temperature. In this system, the ionic liquid is not only the solvent, but also the reductant to reduce Au(I) to Au(0) nanoparticles (**20a, 20b**), which were detected by Scanning Electron Microscopy (SEM), Zetasizer and UV-Visible spectroscopy. A possible equation for the conversion could be as shown in Equation 3.3:

$$2(CH_2)_4SAuCl + RHPO_2^- + H_2O \rightarrow 2Au^0 + RPO_3^{2-} + 3H^+ + 2Cl^- + 2(CH_2)_4S$$
$$\text{or } 2(CH_2)_4SAuCl + RHPO_2^- + 3OH^- \rightarrow 2Au^0 + RPO_3^{2-} + 2H_2O + 2Cl^- + 2(CH_2)_4S$$

Equation 3.3: A possible reaction equation between $(CH_2)_4SAuCl$ and reactive ionic liquid

If the phosphinic acid is oxidised, the phosphonic acid is most likely to be formed. To prove that phosphonic acid was formed, a standard RPO_3H_2 was compared. The synthesis of RPO_3H_2 (R = Bu) was attempted using alkene and H_3PO_3 (Equation 3.4) [98].

$$RCH = CH_2 + HP(O)(OH)_2 \rightarrow RCH_2CH_2P(O)(OH)_2$$

Equation 3.4: Synthesis of alkylphosphonic acid [98]

Unfortunately this synthesis method was not very successful because of telomerization (Scheme 3.7) [99] and purification of the product did not prove successful.

$$\underset{}{RCH = CH_2} + \underset{\text{II}}{\cdot P(O)(OH)_2} \rightarrow \underset{\text{III}}{R\dot{C}HCH_2P(O)(OH)_2}$$

$$R\dot{C}HCH_2P(O)(OH)_2 + HP(O)(OH)_2 \rightarrow \underset{\text{I}}{RCH_2CH_2P(O)(OH)_2} + \text{II}$$

$$\text{III} + RCH = CH_2 \rightarrow \underset{\text{IV}}{R\dot{C}HCH_2CHRCH_2P(O)(OH)_2}$$

$$\text{IV} + HP(O)(OH)_2 \rightarrow \underset{\text{V}}{RCH_2CH_2CHRCH_2P(O)(OH)_2} + \text{II}$$

Scheme 3.7: Telomerization in the synthesis of alkylphosphonic acid [99]

Using another route, RPO_2H_2 was directly oxidised using SO_2. After bubbling of SO_2 the yellow powder, sulfur (S_8), was precipitated from the reaction mixture (Equation 3.5) and the semicrystals were obtained after filtration and removal of volatiles. The $C_6H_{13}PO_3H_2$ reacted with Bu_4POH to give $[(Bu_4P)_2][C_6H_{13}PO_3]$.

$$2C_6H_{13}PO_2H_2 + SO_2 \rightarrow 2C_6H_{13}PO_3H_2 + 1/8S_8$$

Equation 3.5: Oxidation of *n*-hexylphosphinic acid to *n*-hexylphosphonic acid

NMR data for $[(Bu_4P)_2][C_6H_{13}PO_3]$ did not exactly match that of $[(Bu_4P)_2][C_6H_{13}PO_3]$ which was produced from the $(CH_2)_4SAuCl$-$[Bu_4P][hexylPO_2H]$ reaction mixture. It is possible the tetrahydrothiophene gold(I) complex interacted with the ionic liquid in some way. Consistent with this, the NMR shift of protons depends on the ratio of thiophene to ionic liquid [100].

A similar phenomenon was observed in the mixture of $(CH_2)_4SAuCl$ with $[Bu_4P][hexylPO_2H]$. ^{31}P NMR (proton coupled) chemical shifts varied with the molar ratio of the $(CH_2)_4SAuCl$ to the ionic liquid, as shown in Figure 3.12. With the increase of the molar ratio, the peaks 2 and 3 which were from "$[P(H)O_2]^-$" moved up to higher chemical shifts, and the marked "$*$" peak which was presumably "$[RPO_3]^{2-}$", also slightly moving up to same direction, while the peak 1 which were from "$[Bu_4P]^+$" kept the same position. It is therefore difficult to correlate the peak labelled "$*$" ($[RPO_3]^{2-}$), produced in the above reaction, with that obtained by SO_2 oxidation of $R(H)PO_2H$, by proton coupled ^{31}P NMR.

The reaction of a mixture of $(CH_2)_4SAuCl$ and $[Bu_4P][hexylPO_2H]$ was also tested by ES-MS. In the negative ion mode there was a peak which was from $[hexylPO_3]^{2-}$ at *m/z* 164. This confirms that the reaction of Au(I) with $[hexylPO_2H]^-$ had indeed formed Au(0) and $[hexylPO_3]^{2-}$.

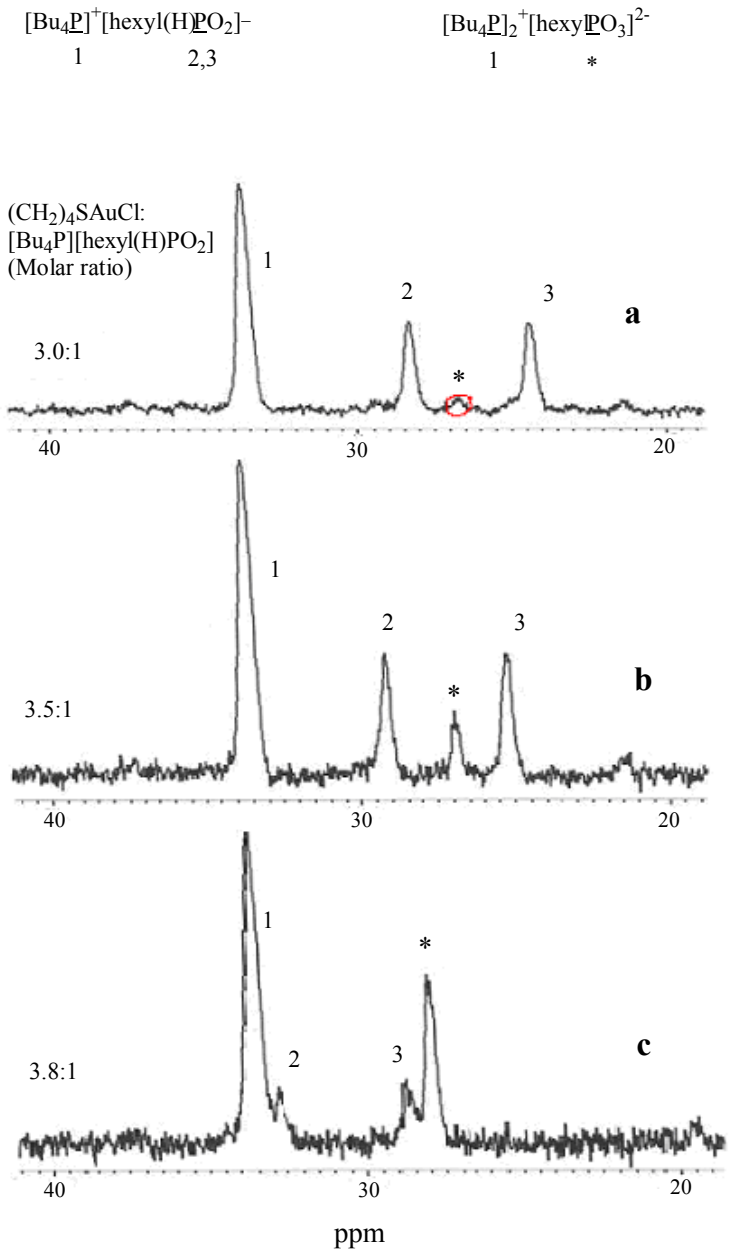

Figure 3.12: ^{31}P NMR (proton coupled) signals in solutions ($CDCl_3$) containing different molar ratios of $(CH_2)_4SAuCl$/$[Bu_4P][hexylPO_2H]$

3.2.1.2 Synthesis of Au(0) nanoparticles in "unreactive" ionic liquid from $(CH_2)_4SAuCl$

After preparation of Au(0) nanoparticles (**20a, 20b**) in reactive ionic liquid (Section 3.2.1.1), accordingly, synthesis of Au(0) nanoparticles (**20c**) was attempted in "unreactive" ionic liquids using $(CH_2)_4SAuCl$ at room temperature.

$(CH_2)_4SAuCl$ reacted in $[Bu_4P][(octyl)_2PO_2]$ at room temperature without any reducing agent, and Au(0) nanoclusters of about 2 nm size were shown to be present by UV-Visible spectroscopy, by comparing spectra of proven size of Au particles in published literature. The nanoparticles were more easily aggregated than **20b** when the $[Bu_4P][(octyl)_2PO_2]$ was removed. It was confirmed through comparing their UV-Visible spectra (see Section 3.2.2) and the SEM images (see Section 3.2.5).

The metal nanoclusters formed in ionic liquids were more stable than in common solvents. For example, compound **20b** in $[Bu_4P][hexylPO_2H]$, no precipitates were found in this pink colloidal ionic liquid solution, and they remained stable for several months, as illustrated by UV-Visible spectroscopy. On the other hand, after ionic liquid was removed, during acetone washing, the golden solid gradually appeared around the wall of the vessel from black solid (**20a, 20b,** and **20c)**; furthermore, after storing in the test tube with a lid for a couple of days, all particles became golden in colour. It demonstrated that these gold nanoparticles aggregate easily without ionic liquids.

3.2.1.3 Synthesis of Au(0) nanoparticles in "reactive" and "unreactive" ionic liquids from $[Me_4N][AuCl_4]$

In these cases, there is no apparent difference for reducing Au(0) **21** from $[Me_4N][AuCl_4]$ using hydrogen gas in "reactive" and "unreactive" ionic liquid. $[Me_4N][AuCl_4]$ easily dissolved in $[Bu_4P][hexylPO_2H]$, $[Bu_4P][(octyl)_2PO_2]$, and $[Bu_4P][(TMP)_2PO_2]$. Reduction, as shown by formation of a "black solution" only can be obtained with the help of reducing agents, such as H_2. The black particles **21** separated by centrifugation with acetone or ethanol are more stable than the compounds **20**, but aggregation producing golden yellow particles were formed around the wall of the sample container still was observed. Compound **21** was tested by TEM and SEM. After ethanol (13 × 10 mL) washing, the isolated nanoparticles, **21a,** were measured by elemental analysis (C: 0.38%; H: 0.12%; N = Nil). If the anion of phosphinate ionic liquid presumedly combine to the nanoparticles surface after removing extra ionic liquid, the molar ratio of H:C would be 2.21 from the formula calculation. The actual molar ratio of H:C is

3.76:1 (from test) which is higher than the theoretical formula calculation (2.2:1). It is possible that hygroscopic $[Bu_4P][(TMP)_2PO_2]$ absorbed water (see Figure 2.9), causing the molar ratio (H:C) to be higher.

3.2.1.4 Synthesis of Ir(0) nanoparticles in "unreactive" ionic liquid from $[Ir(COD)Cl]_2$

Ir(0) was generated by H_2 (1 atm) reducing $[Ir(COD)Cl]_2$ in $[Et_3NH][(TMP)_2PO_2]$, $[Bu_4P][(TMP)_2PO_2]$, and $[Bu_4P][(octyl)_2PO_2]$ to give black solutions **22a**, **b**, and **c** respectively. Compound **22a** produced black particles separating from $[Et_3NH][(TMP)_2PO_2]$ ionic liquid, and were tested by SEM.

Interestingly, compounds **22b** which generated in $[Bu_4P][(TMP)_2PO_2]$ and **22c** which generated in $[Bu_4P][(octyl)_2PO_2]$ were not successfully separated by centrifugation. It is postulated that the nanoparticles were too small to allow centrifugation. To determine whether the Ir nanoparticles existed in the "black solution", carbon monoxide was employed to confirm. The CO easily adsorbs to the Ir metal surface to form characteristic CO-absorption IR spectra between 2100 cm^{-1} and 1700 cm^{-1} [101], and can be detected (more detail see Section 3.2.4.2). Using H_2 (1 atm) to reduce $[Ir(COD)Cl]_2$ in the reactive ionic liquid, such as $[Et_3NH][hexylPO_2H]$ and $[Bu_4P][octylPO_2H]$ was also investigated. Surprisingly, formation of dark solutions did not occur, though the colour of solution darkened slightly from yellow to brown yellow.

3.2.1.5 Synthesis of Rh(0) nanoparticles in "unreactive" ionic liquid from $RhCl_3 \cdot xH_2O$

A black Rh(0) reaction mixture was obtained by reducing a solution of $RhCl_3 \cdot xH_2O$ in $[Bu_4P][(TMP)_2PO_2]$ or $[Bu_4P][(octyl)_2PO_2]$ using H_2 (1 atm). The size of these particles was extremely small, the sizes being less 2 nm. The sample also did not pass the size measurement test using Zetasizer, resulting in a particle size < 2 nm. Using centrifugation (3000 rpm, up to 30 min) it was not possible to obtain a solid precipitate from the reaction mixture. The characterization of

particles was carried out using CO adsorption as described in Section 3.2.4.1. Additionally, the sample before reaction, and after reacting with H_2, and with CO was tested by UV-Visible spectroscopy, as detailed in the next Section.

3.2.2 UV-Visible spectroscopic characterisation of metal nanoparticles

UV-Visible spectroscopy is particularly powerful in characterizing nanoparticles whose plasmon resonance lies in the visible range, such as, gold [39a]. A broad absorption at around 530 nm characteristic of a surface plasmon absorption band of gold particles indicates the formation of particles with a diameter of several nanometers [102] [103]. Furthermore, when the plasmon absorbance increased in the UV-Visible spectrum, indicated the core size of gold nanoparticles was larger [104] [105], and no significant plasmon resonance at 520 nm indicated the gold nanoparticles were around 2 nm in diameter [105] [106]. Extracts were prepared by Yao *et al.* [105]. They stated an aqueous solution containing a Au nanoparticles sample was mixed with toluene containing tetraoctylammonium bromide ($[(C_8H_{17})_4N][Br]$) and stirred vigorously, followed by the extraction of the toluene phase as extract 1; after the toluene phase was removed, a fresh $[(C_8H_{17})_4N][Br]$/toluene solution was used for the second extraction from the water phase, and this toluene phase was extract 2; the same procedure was used to give extract 3. Yao *et al*. also demonstrated the absorption spectra of gold nanoparticles for extracts 1, 2, and 3 with different size respectively (Figure 3.13). In the absorption spectrum, extract 1 showed no surface plasmon band, the average diameter of particles with a yellow colour for extract 1 was 2.61 ± 0.33 nm, illustrated by TEM. The extract 2 with a dark-brown colour and 3 with a light-blue colour showed a similar surface plasmon band (~ 530 nm) in the absorption spectra, the average diameter of particles were 3.01 ± 0.55 nm and 4.29 ± 0.96 nm respectively [105].

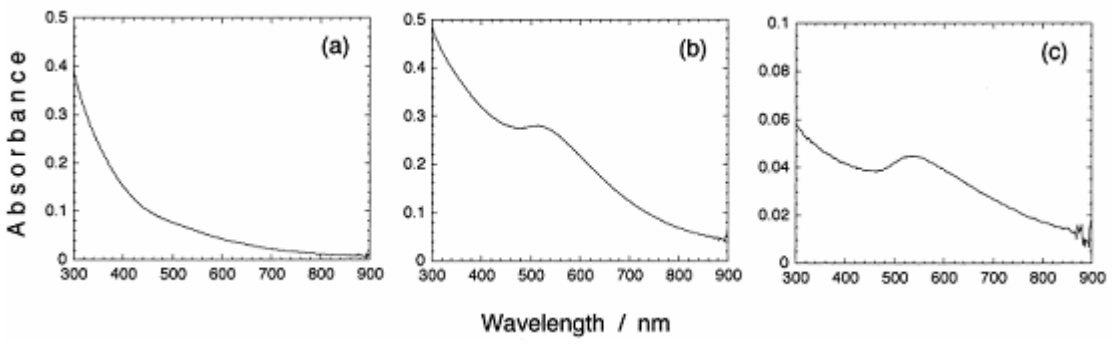

Figure 3.13: Absorption spectra of transferred gold nanoparticles in toluene obtained by stepwise extraction procedures. (a), (b), and (c) were extracts 1, 2 and 3 respectively [105]

Figure 3.14 (fresh sample (**b**), and after two months (**a**)) showed the UV-Visible spectra of Au(0) **20b** produced from $(CH_2)_4SAuCl$ in $[Bu_4P][hexylPO_2H]$. There was a surface plasmon band around (~ 520 nm) for both of them; plasmon absorbance of (**a**) has slightly increased compared to (**b**). These plasmon absorbances in the UV-Visible spectra are similar to those in Figure 3.13, so the estimated size of the Au(0) particles are 2-5 nm.

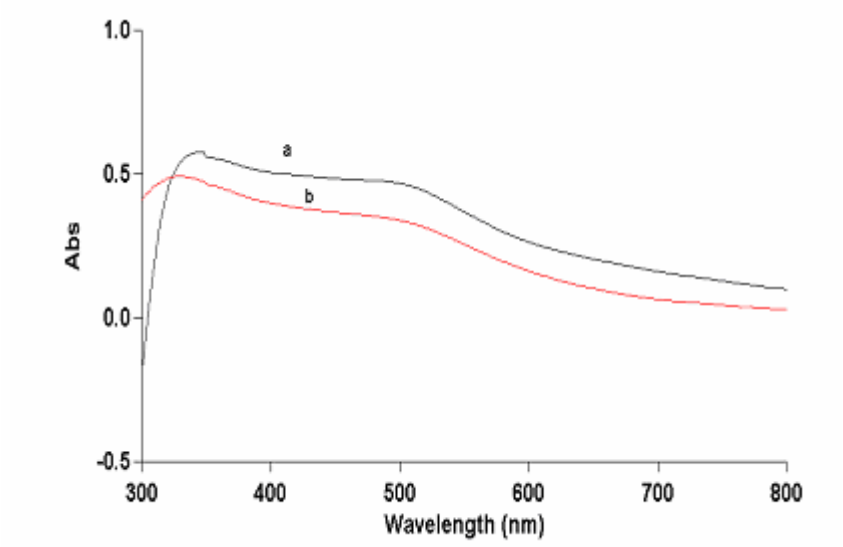

Figure 3.14: UV-Visible spectrum of Au(0) **20b** in $[Bu_4P][hexylPO_2H]$ (**b**: fresh sample; **a**: sample **b** stored in a sealed flask for two month)

The size of the Au(0) nanoparticles **20c** appear to be smaller than those formed in $[Bu_4P][hexylPO_2H]$ **20b**, because no surface plasmon band [105] [106] is observed in the absorption spectrum of **20c** (Figure 3.15).

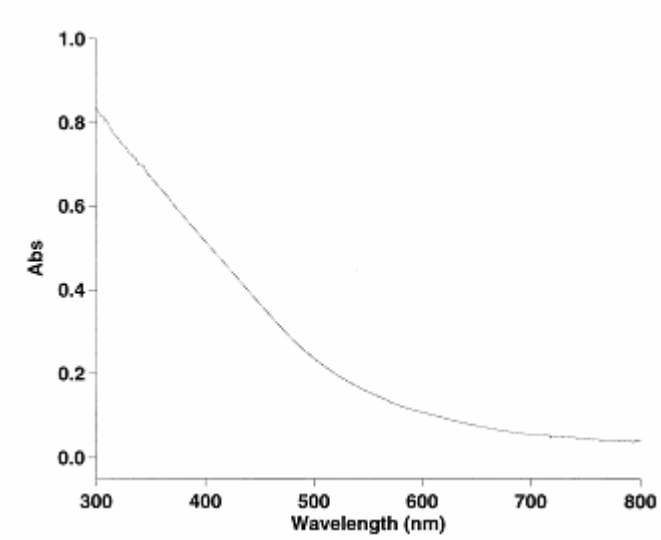

Figure 3.15: UV-Visible spectrum of Au(0) **20c** in $[Bu_4P][(octyl)_2PO_2]$

Figure 3.16 shows the UV-Visible spectra of Rh metal particles which are spherical particles with 10 nm diameter in size, in vacuo and water from the literature [107]. Figure 3.17 also shows the UV-Visible spectra of $RhCl_3$ in the water-in-CO_2 microemulsion and before and after H_2 treated and corresponded the size of particles were less 10 nm which illustrated by TEM [108].

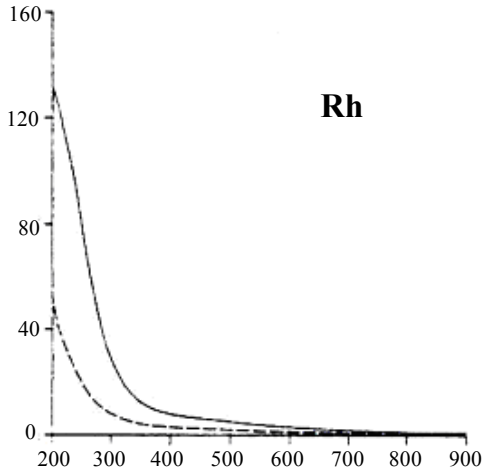

Figure 3.16: Calculated absorption spectra of 10 nm diameter spherical particles of the metallic elements: (----) in vacuo and (—) in water. (The spectra are presented as the absorption cross-section C plotted the wavelength, A = CNl/2.303 where l = pathlength; N = containing particles per unit volume)[107]

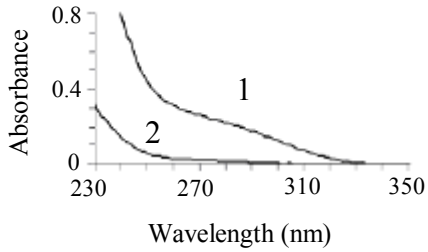

Figure 3.17: UV-Visible spectra of $RhCl_3$ in the water-in-CO_2 microemulsion before (1) and after (2) injection of H_2 gas [108]

Absorption spectra of $RhCl_3 \cdot xH_2O$ in $[Bu_4P][(TMP)_2PO_2]$ (**a**), treated with H_2 (**b**) and treated with H_2 and CO (**c**) are shown in Figure 3.18. The solution (**a**) is dark red and solutions (**b**) and (**c**) are the same colour, brown black. Spectrum (**b**) and (**c**) are the same, and in (**a**) there is small band around at 550 nm. The spectra of (**b**) and (**c**) are similar, suggesting Rh(0) particle sizes of 10 nm particles (Figure 3.16) [107]. Figure 3.18 (a) and (c), looks similar as the spectra in Figure 3.16 and 3.17, but move to the high wavelength. Probably, the media in which particles are dispersed could affect the absorbance spectrum.

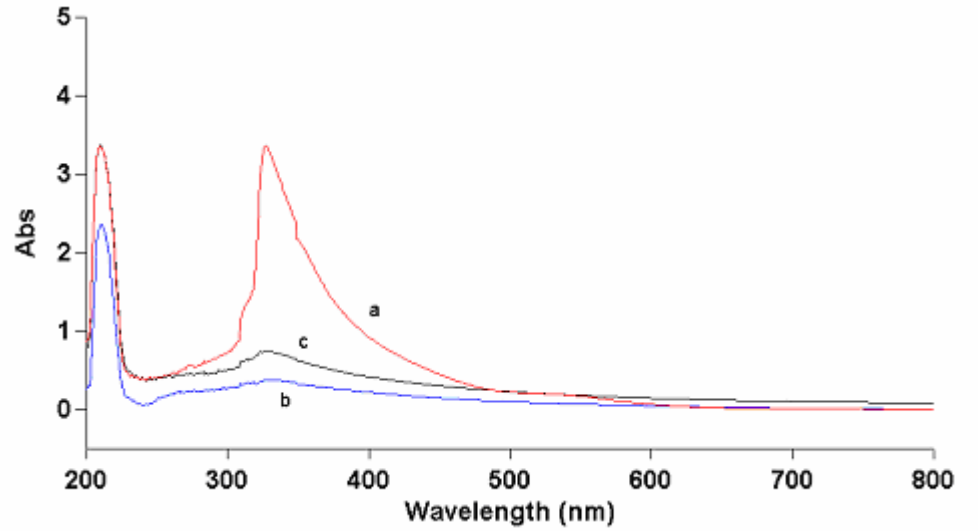

Figure 3.18: UV-Visible spectrum of $RhCl_3 \cdot xH_2O$ in $[Bu_4P][(TMP)_2PO_2]$ a: before H_2 treatment; b: after H_2 treatment; c: after H_2 treatment and CO treatment.(dispersed in acetone solution for measurement)

3.2.3 Determination of the particle size distributions of the Au(0) nanoparticle preparation in $[Bu_4P][hexylPO_2H]$, using the Malvern 3000 HS Zetasizer

The Malvern Zetasizer 3000 HS is an instrument dedicated to the study of colloidal particles. It can measure particle size distributions on stable colloids and zeta potential on stable colloids or unstable, colloidally sized suspended matter. It covers the particle size range 2 to 3000 nm. Particle sizes are determined by the technique of photon correlation spectroscopy (PCS) which involves determining the velocity distribution of colloidal particle movement based on light scattering measurements. The scattering efficiency depends on the size of particles and exhibits a d^6 (d = diameter) dependence which means that the larger the particles are, the more efficiently they scatter the laser light [109]. So the consequence of this is that if there are a few large particles in a colloid that mainly consists of a lot of very small particles, the large particle will scatter light much more efficiently than a small particle to an extent depending on its diameter raised to the sixth power. Even though a peak may appear at large particle sizes, this may only represent a small percentage of the total particle population, i.e. the smaller particles may be in the majority, but would scatter less light. As a result, when the sample particles are polydisperse, photon correlation data analysis becomes more complex [109]. Scheme 3.8 is shown the effective factor of the scattering intensity (I) to the polarizability (α), the particles' size frequency distribution (N(d)) and the Mie factors (p(q,d)), which is the deviation of the particles from Rayleigh scattering (suitable small particles). When the Mie factors are ignored, the distribution of particle sizes, which is weighted (volumed) according to the scattering powers of the various particles and a correspondingly weighted (volumed) average diameter, will be obtained [109].

$$I(q,d) = N(d)\,\alpha^2\,p(q,d)$$

Scheme 3.8: The relationship of Intensity of scattering and particles of diameter (d) at scattering vector (q) [109]

Figure 3.19 shows the size distributions (**i:** intensity-based, **ii:** volume-based) of colloidal particles of Au(0) produced from $(CH_2)_4SAuCl$ in $[Bu_4P][hexylPO_2H]$. Figure 3.19 (i) illustrates the above discussed d^6 scattering dependence. Even though Figure 3.19 (i) shows that the intensity due to particles less than 5 nm in size (peak **a**) is very low, Figure 3.19 (ii) which is volume based shows that the smaller particles (peak **a**) are more dominant in the colloid compared to the larger particles (peak **b**). 40% of the particles detected exist in the particle size range less than 5 nm compare to less than 15% for the large particles. So most particles in the colloid are small nano-sized particles (< 5 nm), and less than 15% are larger particles (50 nm).

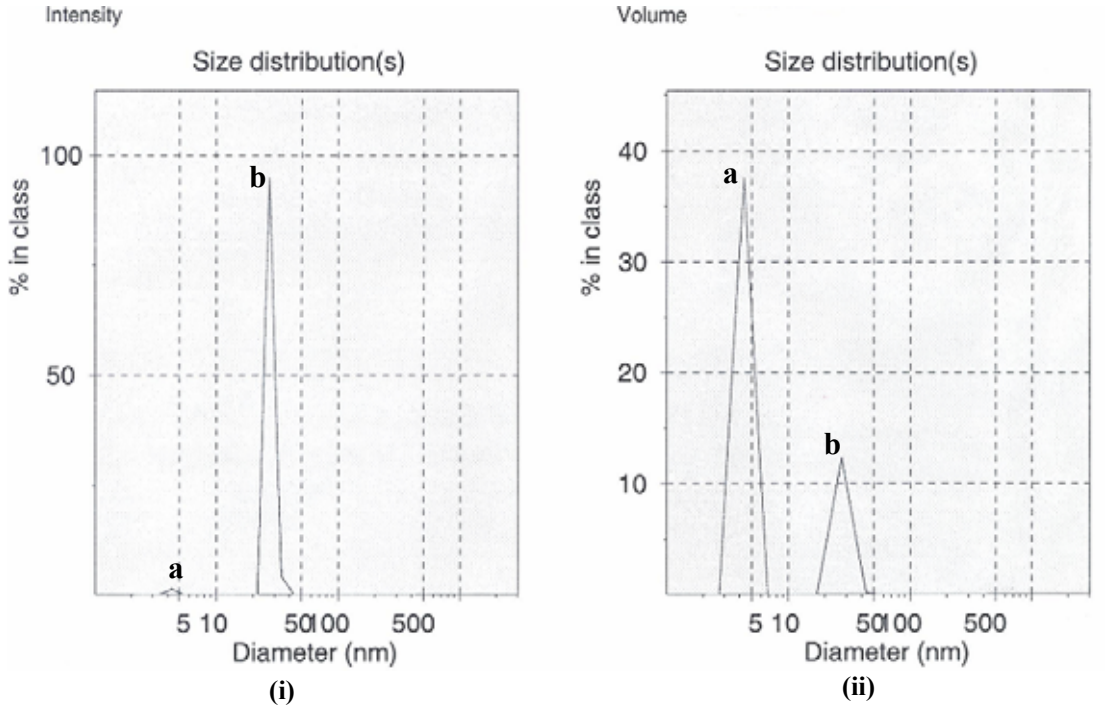

Figure 3.19: Size distribution of Au(0) (**20b**) nanoparticles generated in $[Bu_4P][hexylPO_2H]$ from $(CH_2)_4SAuCl$ in Intensity and in Volume

3.2.4 Infrared spectra of CO chemisorbed on Rh(0) and Ir(0) colloids generated in ionic liquids

3.2.4.1 IR spectra of CO chemisorbed on Rh(0) in ionic liquids

Initial IR spectral studies of CO adsorbed on Rh colloids

In the present study, CO was used as an IR surface probe to determine if stable colloidal suspensions generated from H_2 reduction of the Rh and Ir salts dissolved in ionic liquids, actually contained Rh and Ir metal. If elemental metal were present, the absorption band of CO (CO = ^{12}CO, unless otherwise stated) due to chemisorption on the metal surface would be easily detected by infrared spectroscopy as discussed earlier. The assignment of the spectral features for chemisorbed CO on Rh has been widely studied in the literature, and was discussed in Section 3.1.3. Although infrared spectra of CO adsorbed on colloidal rhodium have been reported earlier [95], to our knowledge, no reports are available on infrared spectra of CO adsorbed on colloidal rhodium generated in ionic liquids. Figure 3.20 shows IR spectra of (**a**) H_2 then CO treated $RhCl_3 \cdot xH_2O$ in $[Bu_4P][(TMP)_2PO_2]$ ionic liquid. This spectrum shows a band at 1952 cm^{-1} which could be due to CO bridge-bonded to Rh(0). A peak at 2064 cm^{-1} is due to a CO complex with the starting unreduced Rh salt or reduced to Rh(I) from Rh(III) (see later discussion). However, to confirm that this 1952 cm^{-1} peak was not due to an ionic liquid-associated peak, an IR spectrum of the dried $[Bu_4P][(TMP)_2PO_2]$ ionic liquid was recorded and is displayed in Figure 3.20 (**b**). No 1952 cm^{-1} peak was observed in Figure 3.20 (**b**) which confirms that the 1952 cm^{-1} peak in Figure 3.20 (**a**) is due to a $\nu(CO)_{ads}$ peak.

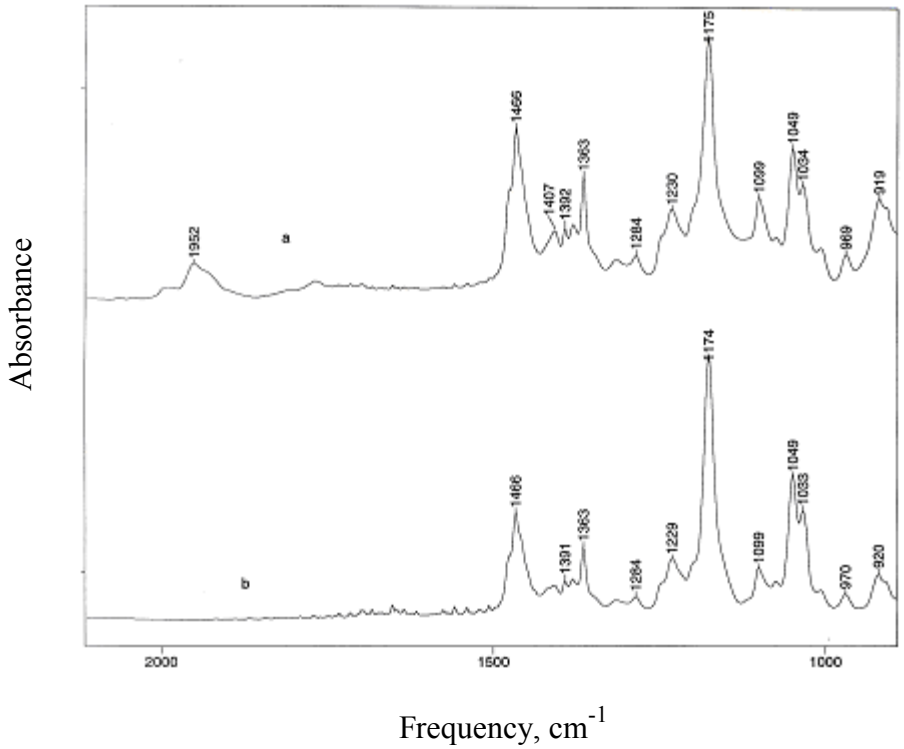

Figure 3.20: IR spectra of rhodium-CO adsorbed in $[Bu_4P][(TMP)_2PO_2]$ **23a** (a: $RhCl_3 \cdot xH_2O$ treated with H_2 and CO in dried IL; b: dried IL)

^{13}CO study to confirm adsorption peak

Further proof that the band was from a surface-adsorbed Rh(0)-carbonyl was obtained when ^{13}CO was used instead of ^{12}CO during CO treatment. Figure 3.21 shows IR spectra of ^{12}CO and ^{13}CO absorption on colloidal metal Rh(0). The IR adsorption bands of ^{13}CO spectra move to a lower frequency in contrast to ^{12}CO spectra, i.e. from 2064 shifts to 2014 cm^{-1}, 1982 to 1935 cm^{-1} and 1897 to 1853 cm^{-1} respectively. The isotopic $^{12}CO/^{13}CO$ frequency ratios are 1.025, 1.024 and 1.024 which fell in the range 1.026-1.022 [110]. This proves that the shift is due to isotopic-related factors; so that the peak is due to -C≡O stretching.

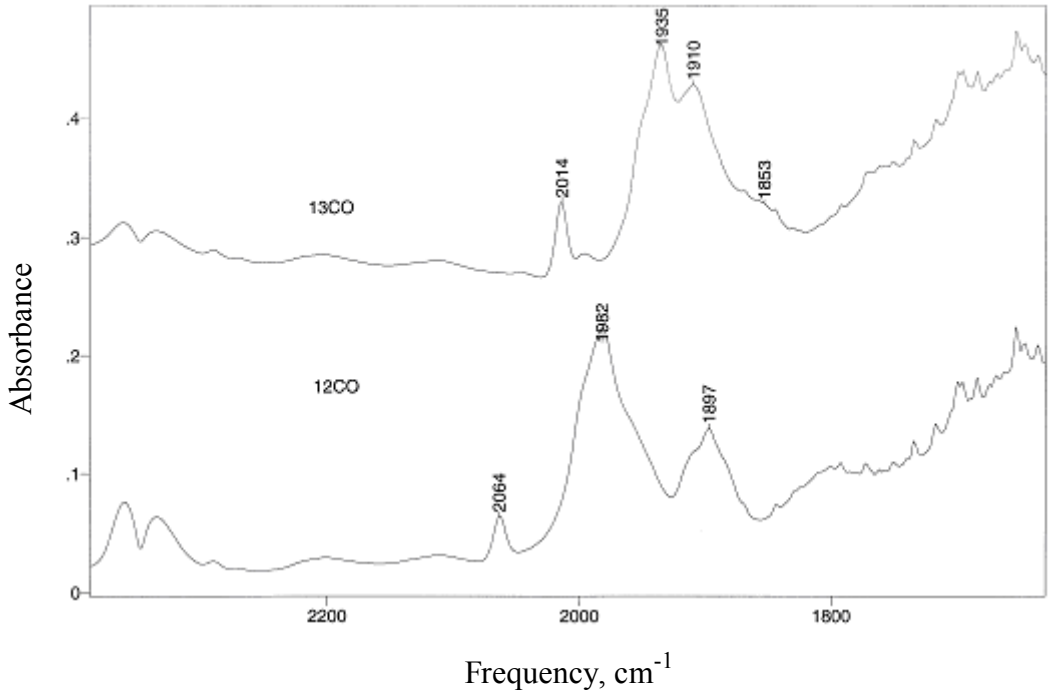

Figure 3.21: IR spectra of Rh(0) **23a** adsorbed ^{12}CO and ^{13}CO in $[Bu_4P][(TMP)_2PO_2]$

Effect of temperature on CO adsorption spectra on colloidal Rh(0) in $[Bu_4P][(TMP)_2PO_2]$

Figure 3.22 shows infrared spectra of Rh(0) metal treated with CO at different temperatures. These spectra show that the IR absorption bands vary with temperature.

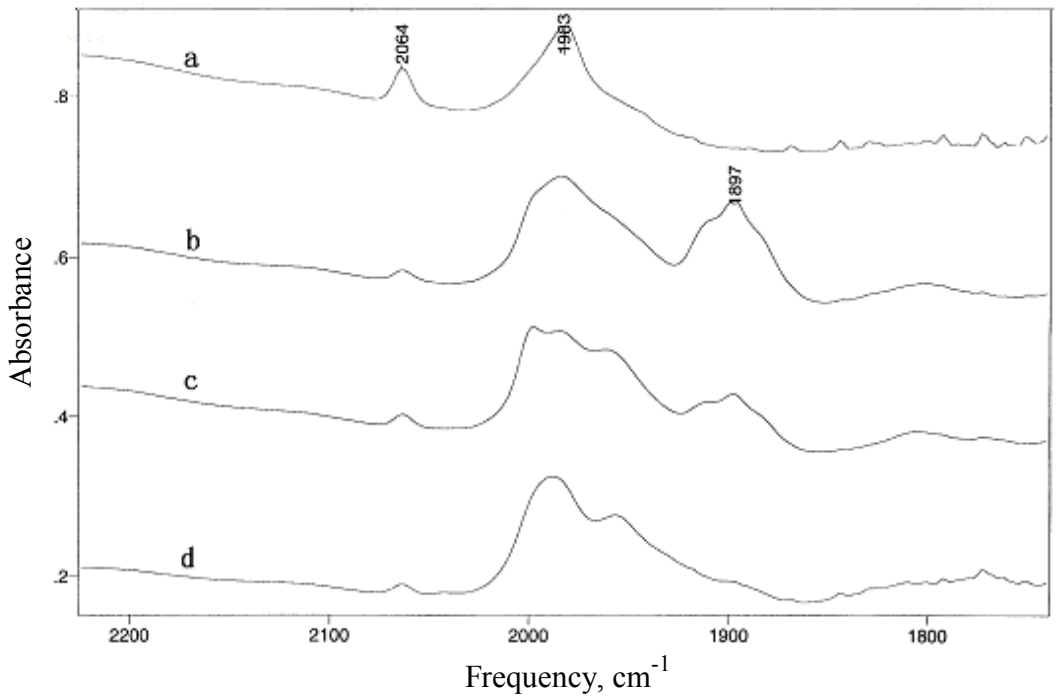

Figure 3.22: Rh(0) nanoparticles formed by H_2 reduction, followed by chemisorption of CO in $[Bu_4P][(TMP)_2PO_2]$ at different temperatures, (a): 17 °C; (b): 40 °C; (c): 75 °C; (d): 120 °C

Figure 3.22, shows a peak at 2064 cm^{-1} due to incompletely reduced starting material $RhCl_3 \cdot xH_2O$. It is relatively lower in intensity at higher temperatures due to more complete reaction with CO. There are complex changes to the 2-fold bridge-bond (1983 cm^{-1} peak) CO adsorption species as temperature increases. The peak gets broader and more complex due to increased heterogeneous character of Rh surface at higher temperature (may be caused by colloid aggregation as temperature increases). At 40 °C and 75 °C a peak at 1897 cm^{-1} is observed due to 3-fold bridge-bond CO, but this disappears at the highest temperature.

Variability of CO adsorption spectra and effect of different ionic liquids

Even when repeating the same reaction conditions, the IR spectra for CO adsorbed on Rh are not exactly the same from sample to sample (see Figure 3.23). The strong band which is assigned around 1982 cm^{-1} and another weak band at around 2065 cm^{-1} have not changed position, but have slightly different band shapes. The IR spectrum of CO chemisorbed colloidal on Rh(0) generated in a

different ionic liquid, ie, $[Bu_4P][(octyl)_2PO_2]$ has also been recorded (Figure 3.24). Figure 3.24 shows similarities to Figure 3.23, but has different peak shapes.

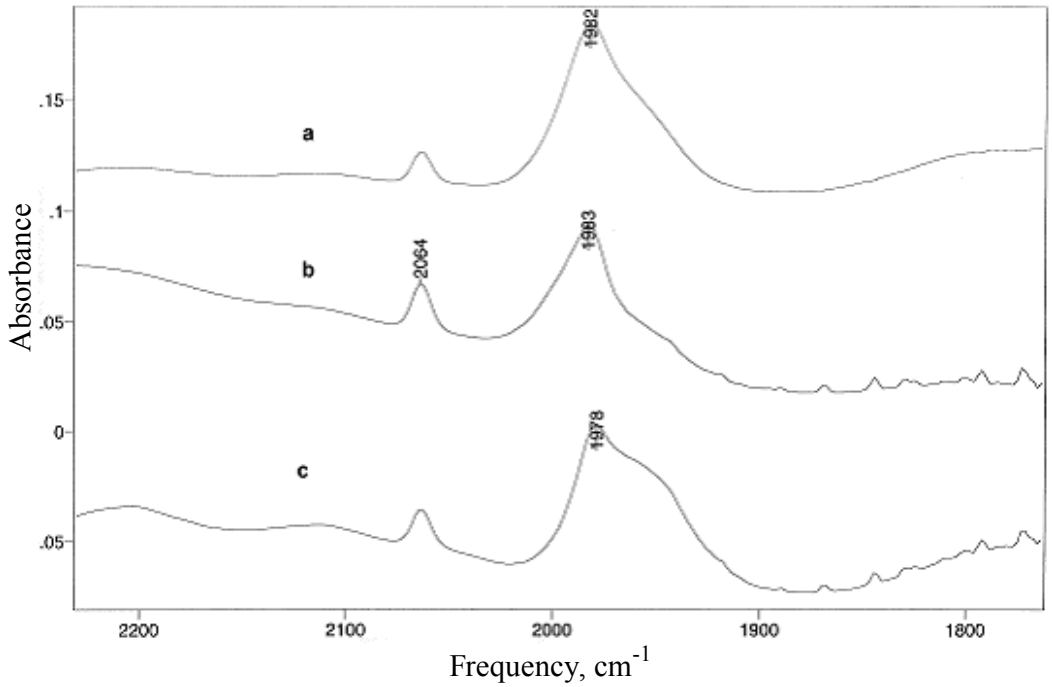

Figure 3.23: The IR spectra of rhodium(0) chemisorbed CO at room temperature in $[Bu_4P][(TMP)_2PO_2]$, (a), (b) and (c) are 3 replicates

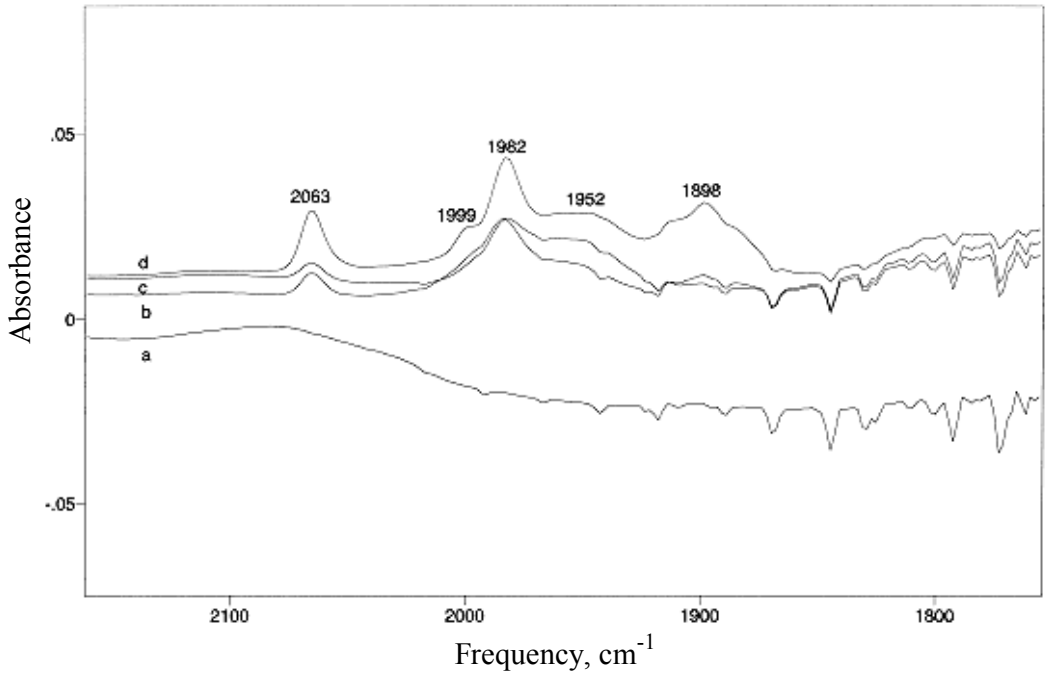

Figure 3.24: The IR spectra of (a): $[Bu_4P][(octyl)_2PO_2]$ reacted with CO, but with no Rh salt present and (b), (c) and (d) (3 replicates): CO chemisorbed on colloidal rhodium at room temperature generated by H_2 reduction of $RhCl_3 \cdot xH_2O$ in $[Bu_4P][(octyl)_2PO_2]$

IR spectrum of starting material, $RhCl_3 \cdot xH_2O$, reacted with CO

To further understand the CO peaks observed in the IR spectrum, a study was done on the Rh salt. Figure 3.25(**a**) shows the spectrum observed for CO adsorbed on colloidal Rh generated by H_2-treatment of $RhCl_3 \cdot xH_2O$ in $[Bu_4P][(TMP)_2PO_2]$. However, if CO treatment is carried out on the $RhCl_3 \cdot xH_2O$ in $[Bu_4P][(TMP)_2PO_2]$ without prior H_2 treatment, a different CO spectrum results (see Figure 3.25(**b**)). Narrow CO-peaks are seen at 2064 and 1981 cm^{-1}. These indicate CO species from a discrete compound. This species also appears to be present in the CO adsorption spectra in Figure 3.25(**a**). This implies H_2-treatment does not fully reduce the $RhCl_3 \cdot xH_2O$ and that the 2064 and 1981 cm^{-1} peaks could be complexes of a partially reduced Rh(I) complex.

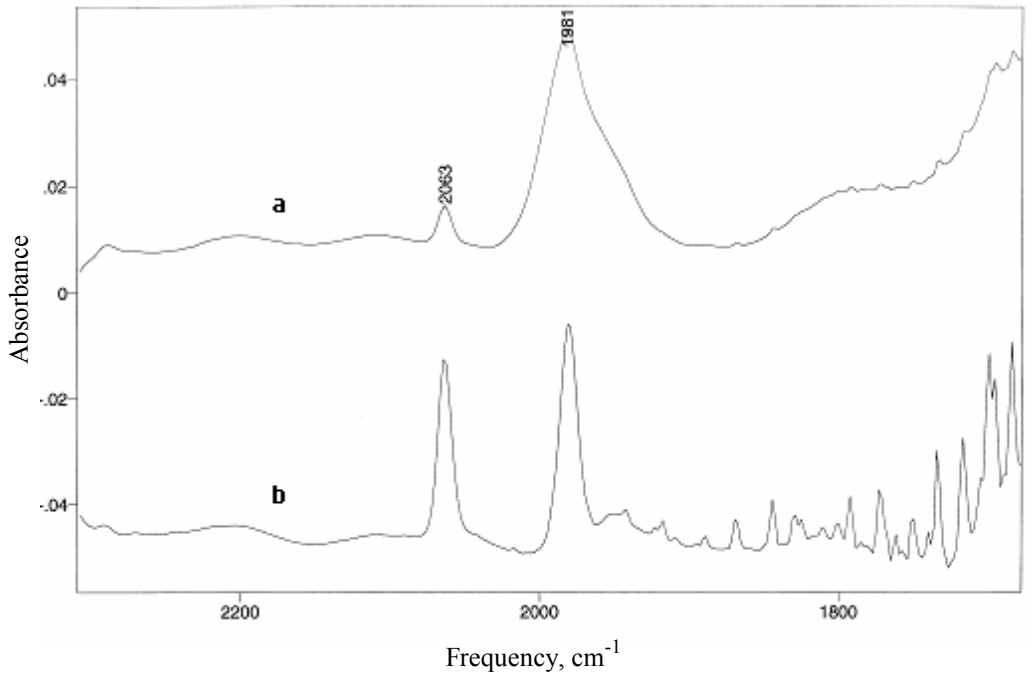

Figure 3.25: The IR spectra of $RhCl_3 \cdot xH_2O$ with (a) and without H_2 treatment (b), in $[Bu_4P][(TMP)_2PO_2]$, then the colloid react with CO

For instance, previous workers have reported the IR spectrum of rhodium carbonyl chloride, $Rh_2(CO)_4Cl_2$ [91]. In their research, IR spectrum of this complex in CCl_4 solution shows four bands. They described the strongest bands at 2033, 2088 cm^{-1} and the other two bands at 2002 and 2104 cm^{-1} were symmetrical and antisymmetrical CO stretching fundamentals [91]. Mink, J. *et al*. [111]

studied $RhCl_3$/Cab-O-Sil treated with CO, and exhibited four characteristic CO bands in FT-IR spectra. Strong bands at 2078-2083 cm^{-1} and 2003-2010 cm^{-1} were presumed to be a gem-dicarbonyl Rh(I) complex, $Rh(CO)_2Cl_xL_y$ (x+y = 6, L = OH^{-1} or H_2O)

In this case, the starting material ($RhCl_3 \cdot xH_2O$) formed carbonylated rhodium chloride could be not exactly same as $Rh_2(CO)_4Cl_2$. Figure 3.25 (**b**) CO stretching band at 2063 cm^{-1} probably is a $Rh^{n+}(CO)_x$ species with a bridging CO and a linear CO, the other band at 1981 cm^{-1} is observed due to bridge-bonded CO stretching, alternatively, two bands (2063 cm^{-1}, 1981 cm^{-1}) probably are gem-dicarbonyl of Rh(I) complex, $Rh(CO)_2Cl_xL_y$ [111].

Conclusion

The features in the IR CO adsorption at 1983 cm^{-1} and 1897 cm^{-1} could be assigned as two-fold-bridged and three-fold-bridged CO adsorption on Rh(0) respectively [83]. The features at 2063 cm^{-1} and part of the bridge-bond peak at 1981 cm^{-1} are due to CO reacting with a partially reduced Rh metal centre.

Clearly, the character of the Rh surface varies with temperatures and times with CO treatment. Spectra of CO adsorbed on Rh(0) in $[Bu_4P][(TMP)_2PO_2]$ are more reproducible than in $[Bu_4P][(octyl)_2PO_2]$ from Figures 3.23 and 3.24. Spectra of Rh(0) metal are more variable in $[Bu_4P][(TMP)_2PO_2]$. Therefore, these IR spectra confirm that Rh(0) metal (nanoparticles) exist in the black reaction mixtures after H_2 reduction.

3.2.4.2 IR spectra of CO adsorbed on colloidal Ir(0) in $[Bu_4P][(TMP)_2PO_2]$

Figure 3.26 and Figure 3.27 show the IR spectra of chemisorbed CO on Ir(0) at different temperatures (**a, b** and **c**) and of CO reacted with $[Ir(COD)Cl]_2$ at room temperature in $[Bu_4P][(TMP)_2PO_2]$. The important feature in Figure 3.26 spectra **a**, **b**, and **c** was the strong band at *ca*. 1988 cm^{-1} [96] [89] which had a frequency independent of temperature. Two weak bands appearing at *ca*. 1908 and

2047 cm^{-1} also do not change position with increasing temperature. However a weak band appears at 1892 cm^{-1} when CO treatment is done at 50 °C and 80 °C. The spectrum shown in Figure 3.27 does not indicate that Ir(0) is present or has formed because the peaks are narrower and more well defined suggesting a molecular species. This is because the sample had not been previously reduced to Ir(0) using H_2 gas as was done in Figure 3.26 **a**, **b** and **c**.

In spectra **a**, **b**, and **c** (Figure 3.26) the band at 1988 cm^{-1} is mostly due to 2-fold bridged [83] [84] adsorbed CO on Ir(0) metal. Its broadness shows how heterogeneous the Ir metal surface is. The band at 1908-1890 cm^{-1} can be assigned to a 3-fold bridged [83] adsorbed CO species on Ir(0). The band around 2047 cm^{-1} is most likely due to incompletely reduced starting material reacted with CO (compare with Figure 3.27).

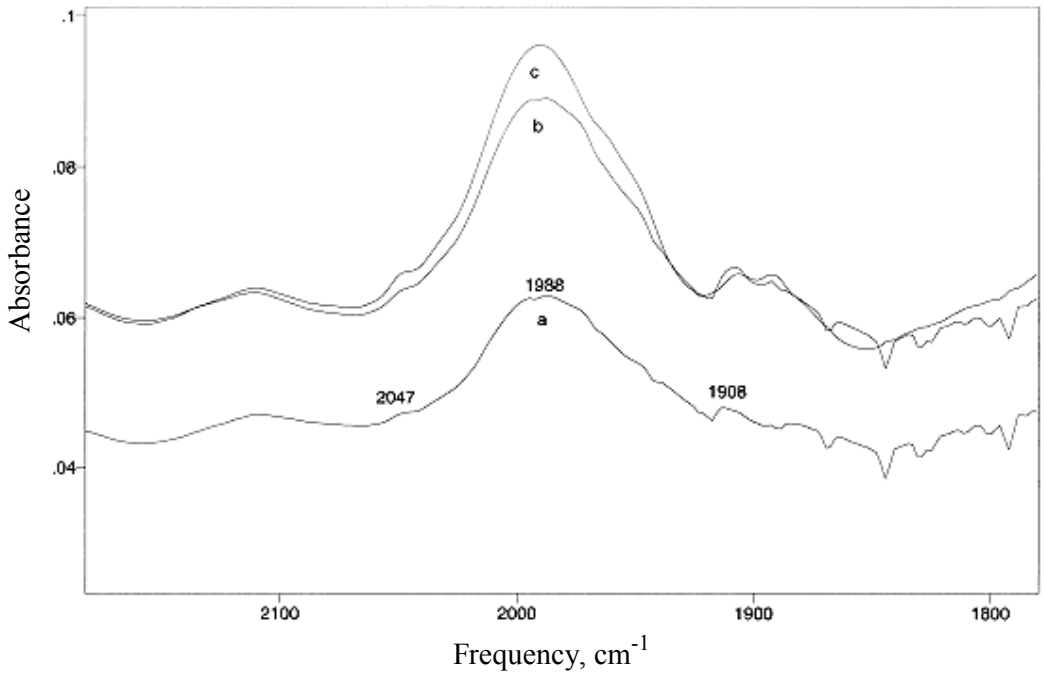

Figure 3.26: The IR spectrum of CO-treated Ir(0) nanoparticles generated by H_2 reduction of $[Ir(COD)Cl]_2$ in $[Bu_4P][(TMP)_2PO_2]$. Spectra (a), (b), and (c) represent the temperature (at room temperature, 50 °C, 80 °C) at which CO treatment was carried out in $[Bu_4P][(TMP)_2PO_2]$

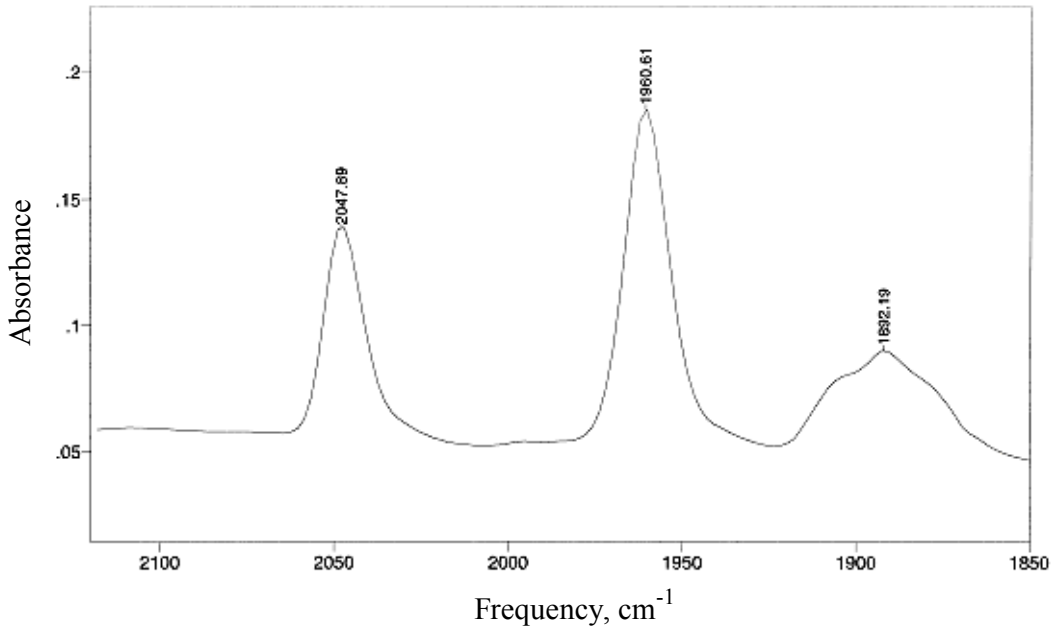

Figure 3.27: IR spectrum of CO-treated $[Ir(COD)Cl]_2$ in $[Bu_4P][(TMP)_2PO_2]$ at room temperature before any treatment with H_2

3.2.5 SEM and TEM analysis

Au metal compounds (**20a**, **20b**, **20c**, **21a**, **21b**, and **21c**) and Ir metal compound (**22a**) were studied by TEM. The SEM micrograph of the Au and Ir metal nanoparticles samples shown in Figure 3.28, verified that Au(0) nanoparticles were formed with a spherical shape. The SEM micrograph also indicated that the average particle size was found to be around 25-50 nm which are bigger than that dispersed in ionic liquid, such as **20b** was around 5 nm by UV-Visible spectrometer. It proved aggregation of these nanoparticles after the ionic liquid was removed. Aggregation also occurred after washing and centrifuging more times for **21b** and **22a**. Figure 3.28 **d** (left), the particles were so small that their size could not be estimated by SEM.

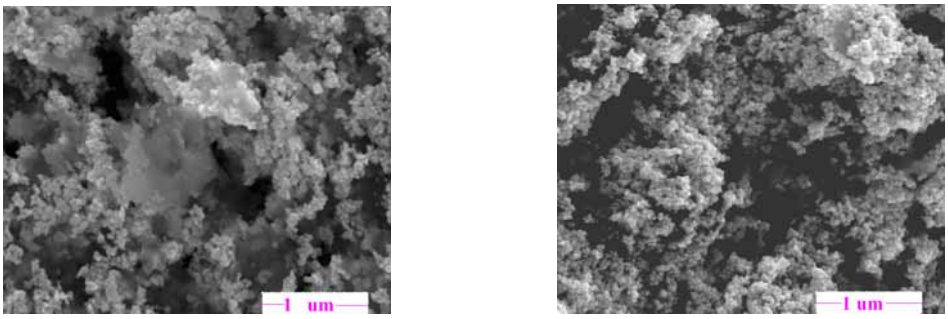

a: **21a** Au(0) produced from $[Me_4N][AuCl_4]$ in $[Bu_4P][(TMP)_2PO_2]$

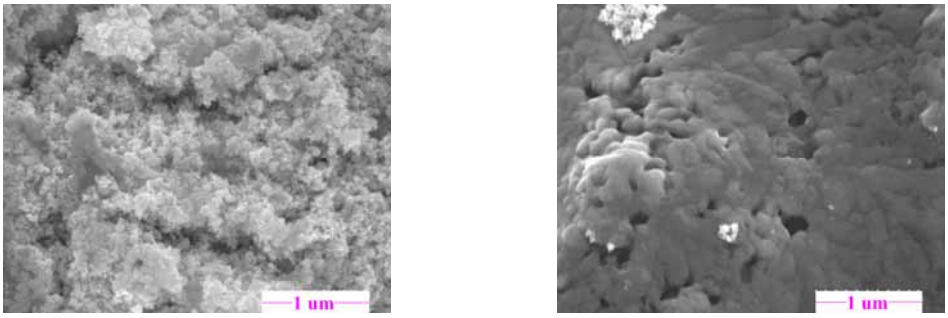

b: **21b** Au(0) produced from $[Me_4N][AuCl_4]$ in $[Bu_4P][(octyl)_2PO_2]$

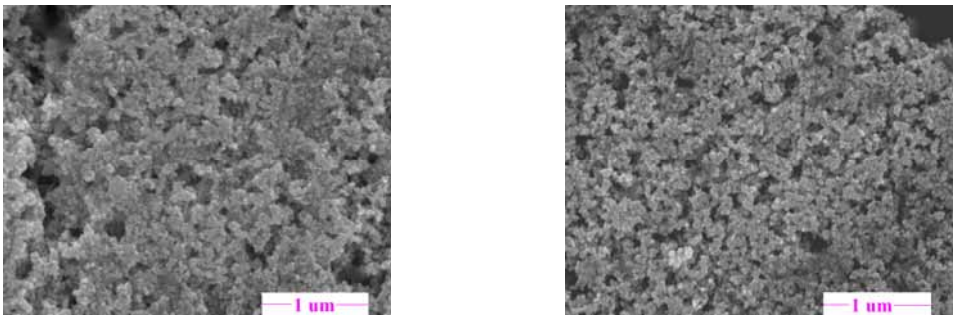

c: **21c** Au(0) produced from $[Me_4N][AuCl_4]$ in $[Bu_4P][hexylPO_2H]$

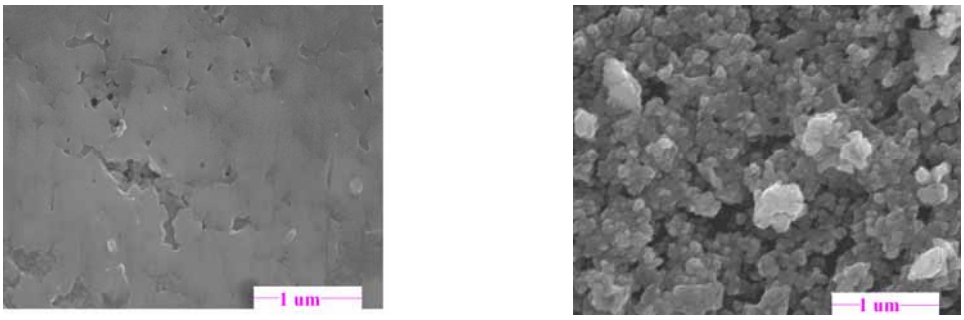

d: **22a** Ir(0) produced from $[Ir(COD)Cl]_2$ in $[Et_3NH][(TMP)_2PO_2]$

Figure 3.28: SEM images of the gold(0) and iridium(0) particles which were formed in different ionic liquids, for right side is left side sample after an additional washing with a solvent

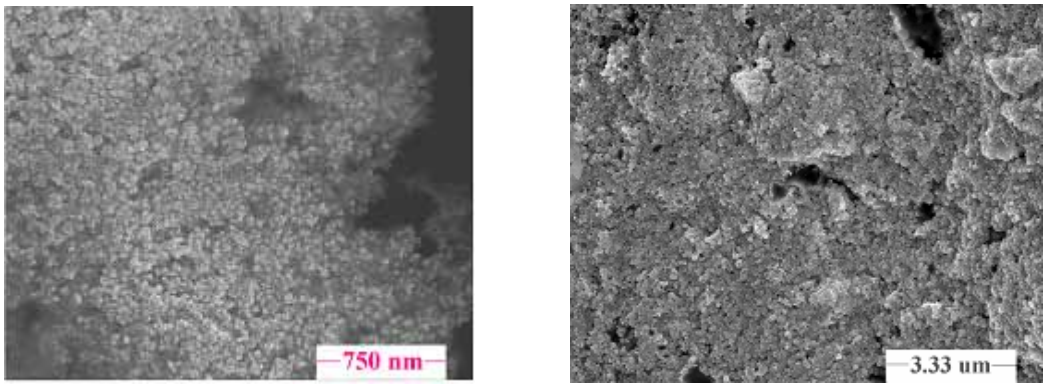

Figure 3.29: SEM image of the Au(0) nanoparticles **20a** (left) and **20c** (right) which were synthesised in $[Et_3NH][hexylPO_2H]$ and $[Bu_4P][(octyl)_2PO_2]$ from $(CH_2)_4SAuCl$ respectively

Figure 3.29 showed SEM of the fresh Au(0) nanoparticles samples **20a** generated in $[Et_3NH][hexylPO_2H]$ and **20c** generated in $[Bu_4P][(octyl)_2PO_2]$ from $(CH_2)_4SAuCl$ respectively when the ionic liquid was removed. The size of the particles **20a** estimated by less than 25 nm was smaller than **20c**.

Transmission electron microscopy (TEM) is a very powerful tool for analyzing the structure and size of the nanoparticles. Au(0) nanoparticles **21b** have been tested by TEM in different conditions. Figure 3.30 (**a**) shows **21b** tested in $[Bu_4P][(octyl)_2PO_2]$. The ionic liquid is quite opaque to electrons, so it could only be seen the edges of the droplet, where the film was thinnest. Clusters of particles were easy to spot and were all reasonably large. Figure 3.30 (**b**) shows **21b** tested in $[Bu_4P][(octyl)_2PO_2]$ dispersed in dichloroethane. Dichloroethane seems to have broken up the particle aggregates, so some individual particles and small clumps, as well as the aggregates were observed. Gold powder particles **21b** were redispersed in acetone and their TEM image is shown in Figure 3.30 (**c**). The average size of these particles is around 25 nm which is in good agreement with the result from SEM (Figure 3.28 (**b**)). In all three images, amorphous aggregations were observed in different extent. The samples were analysed by TEM which showed aggregation, possibly resulting from the samples being old (nearly one month after preparation).

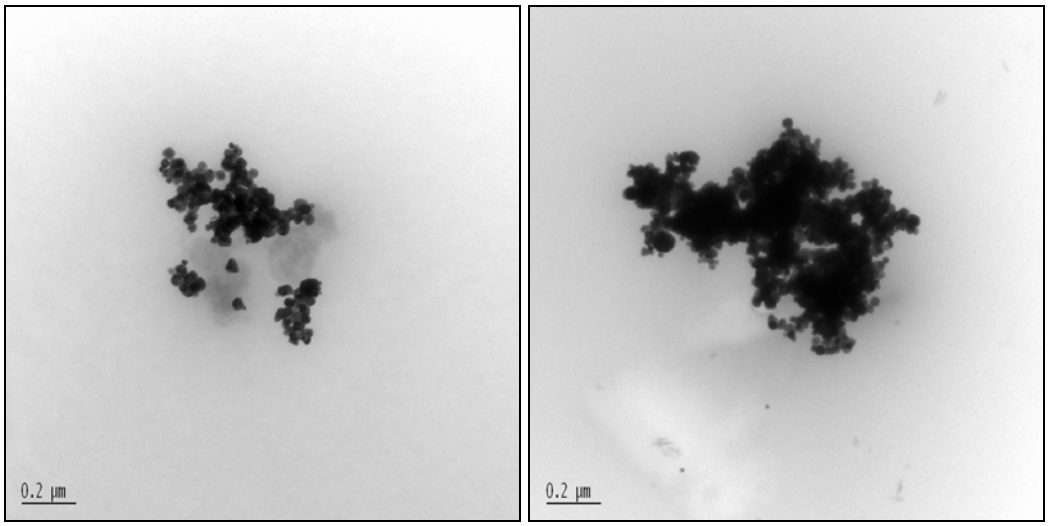

(a) (b)

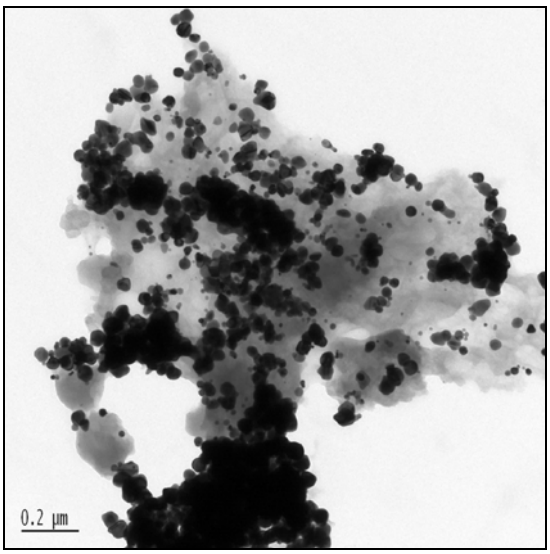

(c)

Figure 3.30: TEM images of Au(0) nanoparticles **21b** produced from $[Me_4N][AuCl_4]$ in $[Bu_4P][(octyl)_2PO_2]$. (a): in $[Bu_4P][(octyl)_2PO_2]$; (b): in $[Bu_4P][(octyl)_2PO_2]$ and dichloroethane; and (c): solid **21b** redispersed in acetone

3.2.6 Conclusions

The results presented here are preliminary outcomes for one of these phosphinate-based ionic liquids applications. Au(0), Ir(0) and Rh(0) nanoparticles were prepared through reducing $[Me_4N][AuCl_4]$, $[Ir(COD)Cl]_2$ and $RhCl_3 \cdot xH_2O$

in phosphinate-based ionic liquids. In general, these ionic liquids are good media for the formation of nanoparticles and prevent the aggregation of nanoparticles. The mechanism is not yet known.

Au(0) nanoparticles **20**, in $[Bu_4P][hexylPO_2H]$ are very stable, confirmed by UV-Visible spectroscopy and Zetasizer measurements. However, these particles quickly aggregate from black to gold yellow when the ionic liquid was removed by centrifugation. The powder nanoparticles of Au(0), **21,** which were synthesised in $[Bu_4P][(octyl)_2PO_2]$ or $[Bu_4P][(TMP)_2PO_2]$ or $[Bu_4P][hexylPO_2H]$ were tested by SEM and gradually, aggregation also was observed when the ionic liquid was removed.

The powder of the Ir(0), **22a**, nanoparticles formed bulk metals after multifold washing with solvent, confirmed by SEM. The size of the nanoclusters of Rh(0), **23**, and Ir(0), **22c** and **22b**, formed in $[Bu_4P][(octyl)_2PO_2]$ or $[Bu_4P][(TMP)_2PO_2]$, were around 2 nm, proved by Zetasizer and IR spectra measurements of CO chemisorbed on the Rh(0) and Ir(0) nanoparticles

Generally, the size of these synthesised Au(0), Ir(0) and Rh(0) particles were smaller within than without the phosphinate-based ionic liquids. The particle size of Au(0), Ir(0) and Rh(0) in ionic liquid can be less than 10 nm. Once ionic liquid is removed, the size of these particles can be around 25-50 nm or more.

The use of these transition metal nanoparticles in phosphinate-based ionic liquids in catalytic organic synthesis reactions is beyond this work, but is also one of the important potential applications of these ionic liquids. It would be interesting for this nanocatalyst performance in the new media. The investigation of CO chemisorption on transition metal nanoparticles such as Rh(0), Ir(0) in ionic liquids appears not to have been previously studied.

3.3 Experimental

3.3.1 Materials

Iridium(III) chloride hydrochloride hydrate ($IrCl_3 \cdot HCl \cdot nH_2O$) and 1,5-cyclooctadiene (99%) (COD) was purchased from Aldrich Chem. Co. $[Ir(COD)Cl]_2$ was prepared by the literature procedure [112]. Tetrahydrothiophene gold(I) chloride ($(CH_2)_4SAuCl$) and rhodium(III) chloride hydrate ($RhCl_3 \cdot xH_2O$) were provided by Brian Nicholson and Bill Henderson respectively. Tetramethylammonium tetrachloroaurate ($[Me_4N][AuCl_4]$) was synthesised by reaction of tetrachloroauric acid ($HAuCl_4$) with tetramethylammonium chloride (Me_4NCl) in water.

3.3.2 Instrumentation

UV-Visible absorption spectra were recorded on a Cary 100 Scan UV-Visible spectrophotometer. The C, H, and N analyses were performed by the Microanalytical Laboratory of the University of Otago. Particle size distributions were recorded on the Malvern Zetasizer 3000HS. The sample, two drops of reaction mixture reduced from $(CH_2)_4SAuCl$ in $[Bu_4P][hexylPO_2H]$ were diluted with 5 mL $[Bu_4P][hexylPO_2H]$ in a (1 × 1 cm) plastic cuvette, was tested by Zetasizer. This instrument allows measurement of particle sizes in the range 2 to 3000 nm.

Infrared spectra were obtained from 2500 cm^{-1} – 1700 cm^{-1} using a BIO-RAD DIGILAB DIVISION FTS-40 infrared spectrometer. The reduced Rh/Ir, which was from $RhCl_3 \cdot xH_2O$ and $[Ir(COD)Cl]_2$ respectively by H_2, in ionic liquid was studied in a PressLok infrared cell having CaF_2 windows.

Scanning electron microscopy was performed on a Hitachi S-4000 Scanning Electron Microscope. Powder nanoparticles were attached onto a stub

through double sized adhesive tape. The stub was fixed into sample holder and placed in the vacuum chamber of the instrument. Transmission electron microscopy (TEM) images were done by Adrian Turner of Biological Sciences School in the University of Auckland. Three kinds of samples were tested. One was directly tested the reaction mixture reduced from $[Me_4N][AuCl_4]$ by H_2 in $[Bu_4P][(octyl)_2PO_2]$, the other was tested the reaction mixture dispersed in dichloroethane, the last was tested the Au(0) powder which produced the reaction mixture was removed ionic liquid, redispersed in acetone.

^{31}P and ^{1}H NMR spectra were recorded on a Bruker Avance 300 spectrometer. Solvents were assigned the following chemical shift values with respect to $SiMe_4$: $CDCl_3$, 7.26 (^{1}H), 77.06 (^{13}C); d6-DMSO, 2.6 (^{1}H), 39.5 (^{13}C); D_2O, 3.5 (MeOH, ^{1}H), 49.3 (MeOH, ^{13}H). ^{31}P chemical shift assignment was with respect to a simple external reference of 85% phosphoric acid. The spectrometer was operated at 75.47 MHz for ^{13}C, 300.13 MHz for ^{1}H and 121.51 MHz for ^{31}P.

3.3.3 Synthesis of RPO_3H_2

A solution of hexylphosphinic acid ($C_6H_{13}PO_2H_2$) in isopropanol under a SO_2(g) atmosphere was stirred with refluxing for about 45 minutes (see Section 3.2.1.1). The $C_6H_{13}PO_3H_2$ was easily separated from the by-product of yellow powder of sulfur by filtration. The colourless oily liquid was obtained after removing the solvent.

3.3.4 Synthesis of nanoparticles

3.3.4.1 Synthesis of Au(0) from $(CH_2)_4SAuCl$ 20

Synthesis of Au(0) from $(CH_2)_4SAuCl$ in $[Et_3NH][hexylPO_2H]$ 20a

A white powder of tetrahydrothiophene gold(I) chloride ($(CH_2)_4SAuCl$) (29 mg, 0.92 mmol) was directly dissolved in $[Et_3NH][hexylPO_2H]$ **16** (2.7 g), and then stirred. The mixture changed from white to pink to purple to black in 5

minutes. Au(0) particles were isolated by centrifugation for 5 minutes and washed with methanol (3 × 1 mL). This sample was prepared for SEM.

Synthesis of Au(0) from $(CH_2)_4SAuCl$ in $[Bu_4P][hexylPO_2H]$ 20b

A white powder of tetrahydrothiophene gold(I) chloride ($(CH_2)_4SAuCl$) (6 mg, 0.02 mmol) was directly dissolved in $[Bu_4P][hexylPO_2H]$ **7** (1.0 g), and stirred; the mixture turned to a brown-black solution in 5 minutes. Two drops of this reaction mixture was diluted with 2 mL $[Bu_4P][hexylPO_2H]$, and the UV-Visible spectrum recorded; and two droplets of this reaction mixture were diluted with 5 mL $[Bu_4P][hexylPO_2H]$, and size distribution graph was recorded by Zetasizer.

Synthesis of Au(0) from $(CH_2)_4SAuCl$ in $[Bu_4P][(octyl)_2PO_2]$ 20c

The same procedure for **20a** was used, except $[Bu_4P][(octyl)_2PO_2]$ **11** (1.24 g) instead of $[Et_3NH][hexylPO_2H]$ **16** was used, to give a black mixture in 5 minutes at room temperature. Au(0) particles were isolated by centrifugation (3000 rpm) for 30 minutes and washed with acetone (3 × 15 mL). This sample was prepared for SEM. Additionally, two drops of the reaction mixture was diluted by 2 mL $[Bu_4P][(octyl)_2PO_2]$, and the UV-Visible spectrum recorded.

3.3.4.2 Synthesis of Au(0) from $[Me_4N][AuCl_4]$ 21 in different ionic liquids

Synthesis of Au(0) from $[Me_4N][AuCl_4]$ in $[Bu_4P][(TMP)_2PO_2]$ 21a

A yellow solution of tetramethylammonium tetrachloroaurate ($[Me_4N][AuCl_4]$) (44 mg, 0.10 mmol) in $[Bu_4P][(TMP)_2PO_2]$ (2.0 g) was obtained after stirring for approximately 2 hours at room temperature, and then reacted with hydrogen gas (1 bar) at 80-87 °C. A black "solution" was given under stirring for 15 minutes. The stabilized particles could be purified by centrifugation (3000 rpm) for 5 minutes to remove excess unbound ionic liquid and washed with

methanol (6 × 10 mL) and dried under vacuum. The purified powder of Au was analysed by SEM.

Synthesis of Au(0) from [Me_4N][$AuCl_4$] in [Bu_4P][(octyl)$_2PO_2$] 21b

The same procedure was used for **21a**, [Bu_4P][(octyl)$_2PO_2$] (1.2 g) instead of [Bu_4P][(TMP)$_2PO_2$], and the solution was kept at 70-75 °C with hydrogen (1 bar). The black purified powder of Au was prepared for SEM and or redispersed into acetone or dichloromethane for TEM. In addition, a droplet of the reaction mixture was directly tested by TEM, and reaction mixture dispersed in dichloroethane and then was tested by TEM.

Synthesis of Au(0) from [Me_4N][$AuCl_4$] in [Bu_4P][hexylPO_2H] 21c

The same procedure was used for **21a**, [Bu_4P][(hexylPO_2H) (1.2 g)] instead of [Bu_4P][(TMP)$_2PO_2$], and the solution was kept at 55-75 °C with hydrogen (1 bar). The black purified powder of Au was prepared for SEM.

3.3.4.3 Synthesis of Ir(0) from [Ir(COD)Cl]$_2$ 22 in different ionic liquids

Synthesis of Ir(0) from [Ir(COD)Cl]$_2$ in [Et_3NH][(TMP)$_2PO_2$] 22a

A brown-yellow solution of [Ir(COD)Cl]$_2$ (16 mg, 0.05 mmol) in dichloromethane (3 mL) was added to [Et_3NH][(TMP)$_2PO_2$] **13** (1.5 g) and stirred at room temperature for 15 minutes. The CH_2Cl_2 was then removed under rotary evaporation (45 °C) for 10 minutes and then on a vacuum line for 1.5 hours. The system was kept at 70-75 °C and hydrogen (1 bar) was admitted to the system. After stirring for 15 minutes, a black "solution" was obtained. Ir(0) particles were isolated by centrifugation (3000 rpm) for 5 minutes and washed with acetone (3 × 15 mL) and dichloromethane (3 × 15 mL) and dried under vacuum. The sample obtained was prepared for SEM.

Synthesis of Ir(0) from [Ir(COD)Cl]$_2$ in [Bu$_4$P][(TMP)$_2$PO$_2$] 22b

The same procedure for **22a** was used, using compound **8** (1.3 g) instead of compound **13**. After H_2 reducing, the sample was bubbled through by CO at different temperature for 10 minutes and the infrared spectrum recorded.

Synthesis of Ir(0) from [Ir(COD)Cl]$_2$ in [Bu$_4$P][(octyl)$_2$PO$_2$] 22c

The same procedure for **22a** was used, using compound **11** (1.3 g) instead of compound **13**. After H_2 reducing, the sample was bubbled through by CO at different temperature for 10 minutes and the infrared spectrum recorded.

3.3.4.4 Synthesis of Rh(0) from $RhCl_3 \cdot xH_2O$ 23 in different ionic liquids

Synthesis of Rh(0) from RhCl$_3 \cdot$ xH$_2$O in [Bu$_4$P][(TMP)$_2$PO$_2$] 23a

An cloudy red mixture of $RhCl_3 \cdot xH_2O$ (35.6 mg) in 8 mL in acetone was added to $[Bu_4P][(TMP)_2PO_2]$ **8** (1.54 g) to give a clear brown-red solution and stirred at room temperature for 15 minutes. The acetone was then removed under rotary evaporation (40 °C) for 30 minutes and then on a vacuum line for 1.5 hr. The system was kept at 75-85 °C and hydrogen (1 atm) was applied to the system. After stirring for 20 minutes, a black "solution" was obtained. CO was bubbled through the sample at different temperatures for 10 minutes and the infrared spectrum recorded. ^{13}CO was also employed to bubble the sample at room temperature for 5 minutes and infrared spectrum recorded. The $RhCl_3 \cdot xH_2O$ in $[Bu_4P][(TMP)_2PO_2]$ **8** before and after reaction with H_2, and after H_2 reduction then reaction with CO were tested by UV-Visible spectra using acetone to dilute.

Synthesis of Rh (0) from $RhCl_3 \cdot xH_2O$ in $[Bu_4P][(octyl)_2PO_2]$ 23b

$RhCl_3 \cdot xH_2O$ (38.8 mg) was used and the same procedure for **23a** was employed, except dichloromethane and $[Bu_4P][(octyl)_2PO_2]$ (1.74 g) instead of acetone and $[Bu_4P][(TMP)_2PO_2]$ respectively. After the solution reacting with H_2, the sample was bubbled by CO and infrared spectrum recorded.

3.4 References

[1] (a) Welton, T. *Coord. Chem. Rev*. **2004**, *248,* 2459-2477.
(b) Lee, S. *Chem. Commun*. **2006**, 1049-1063.

[2] (a) Lu, J.; Dreisinger, D. in *Ionic Liquids as Green Solvents Progress and Prospects* Rogers R. D., Seddon K.R., Ed., American Chemical Society, Washington, DC, 2003, pp 495-509.
(b) AlNashef, I. M.; Matthews, M. A.; Weidner, J. W. in *Ionic Liquids as Green Solvents Progress and Prospects* Rogers R. D., Seddon K. R., Ed., American Chemical Society, Washington, DC, 2003, pp 509-525.

[3] Oxley, J. D.; Prozorov, T.; Suslick, K. S. *J. Am. Chem. Soc*. **2003**, *125*, 11138-11139.

[4] Suarez, P. A. Z.; Dullius, J. E. L.; Einloft, S.; de Souza, R. F.; Dupont, J. *Polyhedron* **1996**, *15*, 1217-1219.

[5] Chauvin, Y.; Muβmann, L.; Olivier, H. *Angew. Chem. Int. Ed. Engl*. **1995**, *34*, 2698-2700.

[6] Scheeren, C. W.; Machado, G.; Dupont, J.; Fichtner, P. F. P.; Teixeira, S. R. *Inorg. Chem*. **2003**, *42*, 4738-4742.

[7] Dupont, J.; Fonseca, G. S.; Umpierre, A. P.; Fichtner, P. F. P.; Teixeira, S. R. *J. Am. Chem. Soc.* **2002**, *124*, 4228-4229.

[8] Huang, J.; Jiang, T.; Han, B.; Gao, H.; Chang, Y.; Zhao, G.; Wu, W. *Chem. Commun*. **2003**, 1654-1655.

[9] Suarez, P. A. Z.; Dullius, J. E. L.; Einloft, S.; de Souza, R. F.; Dupont, J. *Inorg. Chim. Acta* **1997**, *255*, 207-209.

[10] Steines, S.; Wasserscheid, P.; Drieβen-Hőlscher, B. *J. Prakt. Chem*. **2000,** *342*, 348-354.

[11] Monteiro, A. L.; Zinn, F. K.; de Sousz, R. F.; Dupont, J. *Tetrahedron: Asymmetry* **1997**, 8, 177-179.

[12] Berger, A.; de Sousz, R. F.; Delgade, M. R.; Dupont, J. *Tetrahedron: Asymmetry* **2001**, *12*, 1825-1828.

[13] Song, C. E.; Roh, E. J. *Chem. Commun*. **2000**, 837-838.

[14] Song, C. E.; Oh, C. R.; Roh, E. J.; Choo, D. J. *Chem. Commun*. **2000**,

1743-1744.

[15] Owens, G. S.; Abu-Omar, M. M. *Chem. Commun*. **2000**, 1165-1166.

[16] Parshall, G. W. *J. Am. Chem. Soc*. **1972**, *94*, 8716-8719.

[17] Wasserscheid, P.; Waffenschmidt, H. *J. Mol. Cata*l. *A: Chem*. **2000**, *164*, 61-67.

[18] Karodia, N.; Guise, S.; Newlands, C.; Andersen, J. A. *Chem. Commun*. **1998**, 2341-2342.

[19] Chauvin, Y.; Muβmann, L.; Olivier, H. *Angew. Chem.* **1995**, *107*, 2941-2943.

[20] Zim, D.; de Souza, R. F.; Dupont, J.; Monteiro, A. L. *Tetrahedron Lett.* **1998**, *39*, 7071-7074.

[21] Kaufmann, D. E.; Nouroozian, M.; Henze, H. *Synlett* **1996**, *11,* 1091-1092.

[22] (a) Herrmann, W. A.; Böhm, V. P. W. *J. Organomet. Chem*. **1999**, *572*, 141-145.

(b) Böhm, V. P. W.; Herrmann, W. A. *Chem. Eur. J.* **2000**, *6,* 1017-1025.

[23] Carmichael, A. J.; Earle, M. J.; Holbrey, J. D.; McCormac, P. B.; Seddon, K. R. *Org. Lett.* **1999**, *1*, 997-1000.

[24] Hagiwara, H.; Shimizu, Y.; Hoshi, T.; Suzuki, T.; Ando, M.; Ohkubo, K.; Yokoyama, C. *Tetrahedron Lett.* **2001**, *42*, 4349-4351.

[25] Dullius, J. E. L.; Suarez, P. A. Z.; Einloft, S.; de Souza, R. F.; Dupont, J. *Organometallics* **1998**, *17*, 815-819.

[26] Einloft, S.; Dietrich, F. K.; de Souza, R. F.; Dupont, J. *Polyhedron* **1996**, *15*, 3257-3259.

[27] Simon, L. C.; Dupont, J.; de Souza, R. F. *Appl. Catal. A* **1998**, *175*, 215-220.

[28] Magna, L.; Chauvin, Y.; Niccolai, G. P.; Basset, J. M. *Organometallics* **2003**, *22*, 4418-4425.

[29] Chen, W.; Xu, L.; Chatterton, C.; Xiao, J. *Chem. Commun.* **1999**, 1247-1248.

[30] de Bellefon, C.; Pollet, E.; Grenouillet, P. *J. Mol. Catal. A: Chem.* **1999**, *145*, 121-126.

[31] (a) Pardy, R. B. A.; Tkatschenko, I. *J. Chem. Soc. Chem. Commun.* **1981**, 49-50.

(b) Ascenso, J. R.; Carrondo, M. A. A. F. de C.T.; Dias, A. R.; Gomes, P. T.; Piedade, M. F. M.; Romao, C. C.; Revillon A.; Tkatchenko, I. *Polyhedron* **1989**, *8*, 2449-2457.

(c) Grenouillet, P.; Neibecker, D.; Tkatschenko, I. *J. Organomet. Chem.*

1983, *243*, 213-222.

[32] Chauvin, Y.; Olivier, H.; Wyrvalski, C. N.; Simon, L. C.; de Souza, R. F. *J. Catal.* **1997**, *165*, 275-278.

[33] Olivier, H. *J. Mol. Catal. A: Chem*. **1999**, *146*, 285-289.

[34] Roucoux, A.; Schulz, J.; Patin, H. *Chem. Rev*. **2002**, *102*, 3757-3778.

[35] Widegren, J. A.; Finke, R. G. *J. Mol. Catal. A: Chem*. **2003,** *191*, 187-207.

[36] Fonseca, G. S.; Umpierre, A. P.; Fichtner, P. F. P.; Teixeira, S. R.; Dupont, J. *Chem. Eur. J*. **2003**, *9*, 3263-3269.

[37] Mu, X.; Meng, J.; Li, Z.; Kou, Y. *J. Am. Chem. Soc.* **2005**, *127*, 9694-9696.

[38] Cassol, C. C.; Umpierre, A. P.; Machado, G.; Wolke, S. I.; Dupont, J. *J. Am. Chem. Soc*. **2005,** *127*, 3298-3299.

[39] (a) Aiken III, J. D.; Finke, R. G. *J. Mol. Catal. A*: *Chem.* **1999**, *145*, 1-44. (b) Bonnemann, H.; Richards, R. M. *Eur. J. Inorg. Chem.* **2001**, 2455-2480.

[40] Ramachandra Rao, C. N.; Kulkarni, G. U.; John Thomas, P.; Edwards, P. P. *Chem. Soc. Rev*. **2000**, *29*, 27-35.

[41] Murray, C. B.; Kagan, C. R.; Bawendi, M. G. *Annu. Rev. Mater Sci***. 2000**, *30*, 545-610.

[42] Simon, U.; Schon, G.; Schmid, G. *Angew. Chem., Int. Ed. Eng*. **1993**, *32*, 250-254.

[43] Schön, G.; Simon, U. *Colloid Polym. Sci*. **1995**, *273*, 202-218.

[44] Elghanian, R.; Storhoff, J. J.; Mucic, R. C.; Letsinger, R. L.; Mirkin, C. A. *Science* **1997**, *277*, 1078-1081.

[45] Colvin, V. L.; Schlamp, M. C.; Alivisatos, A. P. *Nature* **1994**, *370*, 354-357.

[46] Panatarotto, D.; Partidos, C. D.; Hoebeke, J.; Brown, F.; Kramer, E.; Briand, J. P.; Muller, S.; Prato, M.; Bianco, A. *Chemistry & Biology* **2003**, *10*, 961-966.

[47] Sonti, S. V.; Bose, A. *J. Colloid Interface Sci*. **1995**, *170*, 575-585.

[48] Reetz, M. T.; Winter, M.; Dumpich, G.; Lohau, J.; Friedrichowski, S. *J. Am. Chem. Soc.* **1997**, *119*, 4539-4540.

[49] Vossmeyer, T.; DeIonno, E.; Heath, J. R. *Angew. Chem., Int. Ed. Engl*. **1997**, *36*, 1080-1083.

[50] http://www.pcimag.com/CDA/Archives/0a3006395c6a7010VgnVCM100000f932a8c0 (18/02/2006).

[51] Olivier-Bourbigou, H. *Actualite Chimique* **2002**, *5-6*, 86-90.

[52] Bradley, J. S. In *Clusters and Colloids, From Theory to Applications;* Schmid, G., Ed.; VCH: Weinheim, Germany, 1994; pp 459-544.

[53] Toshima, N.; Yonezawa, T. *New J. Chem.* **1998**, *22*, 1179-1201.

[54] Schmid, G.; Pfeil, R.; Boese, R.; Bandermann, F.; Meyer, S.; Calis, G. H. M.; Van der Velden, J. A. W. *Chem. Ber.* **1981**, *114*, 3634-3642.

[55] Schmid, G. *Struct. Bonding* **1985**, *62*, 51-85.

[56] (a) Schmid, G. *Polyhedron* **1988**, *7*, 2321-2329.
(b) de Jongh, L. J.; Albino, J.; de Aguiar, O.; Brom, H. B.; Longoni, G.; van Ruitenbeek, J. M.; Schmid, G.; Smit, H. H. A.; van Staveren, M. P. J.; Thiel, R. C. *Z. Phys. D: At., Mol. Clusters* 1989, *12*, 445-450.

[57] Vargaftik, M. N.; Zagorodnikov, V. P.; Stolarov, I. P.; Moiseev, I. I.; Kochubey, D. I.; Likholobov, V. A.; Chuvilin, A. L.; Zamaraev, K. I. *J. Mol. Catal.* **1989**, *53*, 315-348.

[58] Vargaftik, M. N.; Zagorodnikov, V. P.; Stolyarov, I. P.; Moiseev, I. I.; Likholobov, V. A.; Kochubey, D. I.; Chuvilin, A. L.; Zaikovsky, V. I.; Zamaraev, K. I.; Timofeeva, G. I. *J. Chem. Soc., Chem. Commun.* **1985**, 937-939.

[59] Bönnemann, H.; Braun, G.; Brijoux, W.; Brinkmann, R.; Schulze Tilling, A.; Seevogel, K.; Siepen, K. *J. Organomet. Chem.* **1996**, *520***,** 143-162.

[60] Bönnemann, H.; Brijoux, W.; Brinkmann, R.; Dinjus, E.; Jouβen, T.; Korall, B. *Angew. Chem., Int. Ed. Engl.* **1991**, *30*, 1312-1314.

[61] Bönnemann, H.; Brijoux, W.; Brinkmann, R.; Dinjus, E.; Fretzen, R.; Jouben, T.; Korall, B. *J. Mol. Catal.* **1992**, *74*, 323-333.

[62] Bönnemann, H.; Brijoux, W.; Brinkmann, R.; Fretzen, R.; Joussen, T.; Köppler, R.; Korall, B.; Neiteler P.; Richter. J. *J. Mol. Catal*. **1994**, *86*, 129-177.

[63] Bönnemann, H.; Brinkmann, R.; Neiteler, P. *Appl. Organomet. Chem*. **1994**, *8*, 361-378.

[64] Bönnemann, H.; W. Brijoux, In *Active Metals: Preparation, Characterization, Applications*; Fürstner, A. Ed.; VCH, New York, 1996; pp. 339-379.

[65] Bönnemann, H.; Brinkmann, R.; Kőppler, R.; Neiteler, P. Richter. J. *Adv. Mater*. **1992**, *4*, 804-806.

[66] Reetz, M. T.; Helbig, W. *J. Am. Chem. Soc.* **1994**, *116*, 7401-7402.

[67] Lin, Y.; Finke, R. G. *Inorg. Chem.* 1**994**, *33*, 4891-4910.

[68] Lin, Y. Finke, R. G. *J. Am. Chem. Soc.* **1994,** *116,* 8335-8353.

[69] Aiken III, J. D.; Lin, Y. Finke, R. G. *J. Mol. Catal. A: Chem*. **1996**, *114*, 29-51.

[70] Moreno-Manas, M.; Pleixats, R. *Acc. Chem. Res*. **2003**, *36*, 638-643.

[71] Labib, M. E. *Colloids Surf.* **1988**, *29*, 293-340.

[72] Cole, D. H.; Shull, K. R.; Baldo, P.; Rehn, L. *Macromolecules* **1999**, *32*, 771-779.

[73] Aiken III, J. D.; Lin, Y.; Finke, R. G. *J. Mol. Catal. A: Chem.* **1996**, *114*, 29-51.

[74] Lin, Y.; Finke, R. G. *J. Am. Chem. Soc.* **1994**, *116*, 8335-8353.

[75] Schmid, G.; Pfeil, R.; Boese, R.; Bandermann, F.; Meyer, S.; Calis, G. H. M.; Van Der Velden, J. W. A. *Chem. Ber.* **1981**, *114*, 3634-3642.

[76] Amiens, C.; De Caro, D.; Chaudret, B.; Bradley, J. S.; Mazel, R.; Roucau, C. *J. Am. Chem. Soc.* **1993**, *115*, 11638-11639.

[77] Duteil, A.; Schmid, G.; Meyer-Zaika, W. *J. Chem. Soc., Chem. Commun.* **1995**, 31-32.

[78] Dassenoy, F.; Philippot, K.; Ould Ely, T.; Amiens, C.; Lecante, P.; Snoeck, E.; Mosset, A.; Casanove, M. J.; Chaudret, B. *New J. Chem.* **1998**, *22*, 703-712

[79] Chen, S.; Kimura, K. *J. Phys. Chem. B* **2001**, *105*, 5397-5403.

[80] Schmid, G.; Maihack, V.; Lantermann, F.; Peschel, S. *J. Chem. Soc., Dalton Trans.* **1996**, 589-595.

[81] Schmid, G.; Emde, S.; Maihack, V.; Meyer-Zaika, W.; Peschel, S. *J. Mol. Catal. A: Chem.* **1996**, *107*, 95-104.

[82] Rodriguez, A.; Amiens, C.; Chaudret, B.; Casanove, M. J.; Lecante, P.; Bradley, J. S. *Chem. Mater.* **1996**, *8*, 1978-1986.

[83] Sheppard, N.; Nguyen, T. T. In *Advances* in *Infrared and Raman Spectroscopy*, Clark, R. J. H.; Hester, R. E.; Eds; Wiley Heyden, London, 1978; Vol. 5, pp 68-148.

[84] Eischens, R. P; Pliskin, W. A., Francis, S. A. *J. Chem. Ph*ys. **1954**, *22*, 1786-1787.

[85] Queau, R.; Poilblanc, R. *J. Catal.* **1972**, *27*, 200-206.

[86] Garland, C. W.; Lord, R, C.; Troiano, P. F. *J. Phys. Chem.* **1965,** *69*, 1188-

1195.

[87] Eckstrom, H. C.; Possley, G. G.; Hannum, S. E.; Smith, W. H. *J. Chem. Phys*. **1970**, *52*, 5435-5441.

[88] Hayward, D. O. In *Chemisorption and Reactions on metallic Films*; Anderson, J. R., Ed; Academic Press: London, 1971; pp 225-326.

[89] Harrod, J. F.; Roberts, R. W.; Rissmann, E. F. *J. Phys. Chem.* **1967**, *71*, 343-352.

[90] Wojtczak, J.; Queau, R.; Poilblanc, R. *J. Catal.* **1975**, *37*, 391-395.

[91] Yang, A. C.; Garland, C. W. *J. Phys. Chem*. **1957**, *61*, 1504-1512.

[92] Wells, M. G.; Cant, N. W.; Greenler, R. G. *Surf. Sci*. **1977**, *67*, 541-554.

[93] Guerra, C. R.; Schulman, J. H. *Surf. Sci*. **1967**, *7*, 229-249.

[94] Cavanagh, R. R.; Yates, Jr. J. T. *J. Chem. Phys*. **1981**, *74*, 4150-4155.

[95] Mucalo, M. R.; Cooney, R. P. *Chem. Mater*. **1991**, *3*, 1081-1087.

[96] Baker, F. S.; Bradshaw, A. M.; Pritchard, J.; Sykes, K. W. *Surf. Sci.* **1968**, *12*, 426-436.

[97] Lynds, L. *Spectrochim. Acta* **1964**, *20*, 1369-1372.

[98] Griffin, C. E.; Wells, H. *J. Org. Chem*. **1959**, *24*, 2049-2051.

[99] Griffin, C. E. *J. Org. Chem.* **1960**, *25*, 665-666.

[100] Su, B. M.; Zhang, S.; Zhang.; Z. C. *J. Phys. Chem. B* **2004**, *108*, 19510-19517.

[101] Hittle, L. H. In *Chemisorption and Reactions on Metallic Films*; Anderson, J. R., Ed; Academic Press: London, 1971; pp 490-531.

[102] Ohno, K.; Koh, K.; Tsujii, Y.; Fukuda, T. *Macromolecules* **2002**, *35*, 8989-8993.

[103] Itoh, H.; Naka, K.; Chujo, Y. *J. Am. Chem. Soc*. **2004**, *126*, 3026-3027.

[104] Weare, W. W.; Reed, S. M.; Warner, M. G.; Hutchison, J. E. *J. Am. Chem. Soc*. **2000**, *122*, 12890-12891.

[105] Yao, H.; Momozawa, O.; Hamatani, T.; Kimura, K. *Chem. Mater*. **2001**, *13*, 4692-4697.

[106] Alvarez, M. M.; Khoury, J. T.; Schaaff, T. G.; Shafigullin, M. N.; Vezmar, I.; Whetten, R. L. *J. Phys. Chem*. *B* **1997**, *101*, 3706-3712.

[107] Creighton, J. A.; Eadon, D. G. *J. Chem. Soc. Faraday Trans*. **1991**, *87*, 3881-3891.

[108] Ohde, M.; Ohde, H.; Wai, C. M. *Chem. Commun*. **2002***,* 2388-2389.

[109] Washington, C. *Particle Size Analysis In Pharmaceutics and other Industries theory and practice*; Ellis Horwood Ltd: Chichester, UK, 1992.

[110] Zhou, M.; Andrews, L. *J. Am. Chem. Soc*. **1999**, *121*, 9171-9175.

[111] Bódis, J.; Zsakó, J.; Németh, C.; Mink, J. *Vib. Spectrosc.* 1995, *9*, 197-202.

[112] Herde, J. L.; Lambert, J. C.; Senoff, C. V. in *Inorganic Syntheses* (Volume XV) Parshall, G. W., Ed.; Mcgraw-Hill Book Company, New York, 1974, pp 19-20.